Fall 12-20-2019

Genetic analysis of a novel FtsK homolog, HfkA, in Streptomyces coelicolor development-associated chromosome segregation

Sumedha Sethi

GENETIC ANALYSIS OF A NOVEL FTSK HOMOLOG, HFKA, IN *STREPTOMYCES COELICOLOR* DEVELOPMENT-ASSOCIATED CHROMOSOME SEGREGATION

A Dissertation

Submitted to Bayer School of Natural and Environmental Sciences

Duquesne University

In partial fulfillment of the requirements for

the degree of Doctor of Philosophy

By

Sumedha Sethi

December 2019

GENETIC ANALYSIS OF A NOVEL FTSK HOMOLOG, HFKA, IN *STREPTOMYCES COELICOLOR* DEVELOPMENT-ASSOCIATED CHROMOSOME SEGREGATION

By

Sumedha Sethi

Approved June 26th, 2019

Joseph McCormick, Ph.D. Professor of Biological Sciences (Committee Chair)	Jana Patton-Vogt, Ph.D. Professor of Biological Sciences (Committee Member)
Nancy Trun, Ph.D. Associate Professor of Biological Sciences (Committee Member)	Valerie Oke, Ph.D. Senior Lecturer of Biological Sciences University of Pittsburgh (Committee Member)
Philip Reeder, Ph.D. Dean, Bayer School of Natural and Environmental Sciences Professor of Biological Sciences	Joseph McCormick, Ph.D. Chair, Department of Biological Sciences Professor of Biological Sciences

ABSTRACT

GENETIC ANALYSIS OF A NOVEL FTSK HOMOLOG, HFKA, IN *STREPTOMYCES COELICOLOR* DEVELOPMENT-ASSOCIATED CHROMOSOME SEGREGATION

By

Sumedha Sethi

December 2019

Dissertation supervised by Dr. Joseph R. McCormick

A quintessential phenomenon occurring during prokaryotic development is accurate segregation of the replicated genomes into the daughter cells. Key energy-dependent processes like chromosome condensation and subcellular partitioning of the genomes are driven by conserved proteins like SMC, ParB, FtsK. During its complex developmental cycle, *Streptomyces coelicolor* segregates its genomes into chains of unicellular spores when its multigenomic syncytial aerial hyphae undergo division.

A novel *ftsK*-like gene, *hfkA* (Homolog of FtsK protein A), was examined for function and localization during development-associated chromosome segregation. Individual deletions did not affect segregation, but a Δ*hfkA* Δ*ftsK* mutant exhibited 8% anucleate spores, suggesting that HfkA and FtsK are redundant in function. To understand the combined effect of existing deletions, a series of mutant strains of *hfkA*,

ftsK, *smc* and *parB* were isolated and analyzed. The triple mutants Δ*hfkA* Δ*ftsK* Δ*smc* and Δ*hfkA* Δ*ftsK* Δ*parB* indicated an additive property of the segregation defects of Δ*hfkA* Δ*ftsK* with the Δ*smc* and Δ*parB* mutants, respectively. Finally, a viable quadruple *hfkA ftsK smc parB* strain was isolated with 20% anucleate spores, and showed no noticeable increase in its segregation phenotype from the double mutant Δ*parB* Δ*smc* (18.8%). This indicated that a complete deletion of *hfkA* and *ftsK* has no effect, whereas the loss of *parB* and *smc* causes the highest percentage of anucleate spores.

To collect additional data, a previously published *ftsK'* truncated allele was tested. A *ftsK' smc parB* triple mutant (10%) was used to isolate a *hfkA ftsK' smc parB* quadruple mutant (14%). This strain did not have a severe phenotype compared to Δ*ftsK'* Δ*smc* Δ*parB*. It was lower in segregation defect than the quadruple mutant containing a complete deletion of *ftsK*, disproving that it was *hfkA*$^{+}$ that was the reason *ftsK'* had a lowering effect. It was concluded that *ftsK'* and *hfkA* could be mitigating some of the segregation defect caused by the loss of *parB smc*.

Some FtsK/SpoIIIE-like proteins (Sco5734) have been characterized as type VII secretion system proteins in bacteria. Bioinformatics analysis suggests that HfkA could be a putative type VII membrane ATPase motor protein, which directly or indirectly affects segregation.

DEDICATION

This dissertation is dedicated to my parents Mrs. Ranjana and Dr. Satynder Kumar Sethi, who raised me to be a kind and compassionate human being, and to move forward in life by lifting others up. Thank you for fostering pride, passion, and a fierce sense of independence in my heart for everything I endeavor and believe in. I am truly grateful for all the sacrifices you made so that I could have the best chance in life. Thank you for constantly worrying about me from thousands of miles away, and sharing every moment of happiness and despair. Without your love, prayers, and support during the good and the tough times, I would not have been able to persevere through this journey, let alone show up every day with a smile. This is not just mine, but our success.

ACKNOWLEDGEMENT

I would like to thank my dissertation committee for supervising this project. My advisor, Dr. Joseph McCormick for welcoming me into his lab, and guiding me to complete this project every step of the way. Thank you Joe for everything, I have learned a lot from you! Thanks to Dr. Jana Patton-Vogt and Dr. Nancy Trun for their constant feedback and encouragement, and for being wonderful teaching supervisors. And to Dr. Valerie Oke for her critical input and direction for this project throughout these years.

I want to thank the entire department of Biological Sciences, and the Bayer school for their help and support, all through my tenure, whenever I have needed it. Especially Dr. Philip Palmer, Dr. Alan Seadler, Dr. Mike Seaman, Dr. Phil Auron, Heather, Pam, Judy, Terri, Lalitha, Jason, and Kim. Anytime I knocked on a door, help was given.

I would like to thank all the past and present McCormick lab members, especially Allen and Metis for being the best peer mentors and amazing friends! Metis, I couldn't have done it without you constantly cheering me on as a dear friend and a big sister till the very end. Thanks to Stuart, Joe, Ning, and Jeevitha for their constant help and support! I will miss you all very much!

I want to thank my peers Jess and Kate for always making me cool, and to Chris, Jackie, Amanda, and Sarah for making me laugh, listening to me cry and celebrating all my special moments! My dear friends Sanket, Harsha, Dhruv, Rishabh, Narthana, and Swagatika, thank you always for being there for me, you have a special place in my heart.

I have been very fortunate to make some lifelong friends, who support you from wherever they are. Special thanks to my dearest friends Rathna and Maryam for being my

friend, family, counselor, and mentor anytime I have needed. Thank you Anupama, Hamza, Chirag, Debroop, and Divya for being my pillars of humor and support.

I am deeply grateful to Dr. Laura Kessler for being a reassuring anchor, and for her encouragement amidst all the difficult days. I can never thank you enough for picking me up and helping me overcome many obstacles. A big shout out to my dear friend and health coach Chris Densel, for teaching me how to maintain a healthy lifestyle.

I would be nothing if not for my family cheering me on and supporting me from afar. My brother Sudhanshu for not letting me feel like I was alone, my sister Samriti and brother-in-law Puneet for always having faith in me, and to my little nephew Krishiv for being my ray of sunshine. Special thanks to my uncle Surinder and aunt Veena, who always wanted me to be the very best I could be. I want to remember my late grandparents for passionately believing in the pursuit of higher education and hard work.

I want to thank my new Agarwal family, especially my in-laws Bandana and Vinay, for heartily supporting and encouraging me in my scholarly pursuits. Thanks for always being my cheerleaders!

Last but not the least, I want to thank my husband, Vikrant, without whom crossing the last leg of this degree wouldn't have been possible. Words cannot describe what your love and support have meant to me since I have known you. You are the most kind, understanding and wonderful partner anyone can imagine. Thank you for not only selflessly supporting me while I fulfilled my dream, but for being by my side, every step of the way, and pausing everything you wanted for yourself and for us for the last 2 years. You have my eternal gratitude for never ever doubting that I could get here. I love you. We can finally begin our lives together. It has been a long road, but we made it!

ATTRIBUTIONS

Dr. Rebekah Dedrick constructed the strains RMD1, RMD6, and the complementation plasmid pRMD6.

Dr. Dagmara Jakimowicz donated the mutant strains J2537, J3305, complementation plasmid pIJ6539, and two-hybrid plasmids expressing fusion proteins for ParA and ParJ.

Drs. Hans Wildschutte and Joseph McCormick isolated the mutant strain HJ2, and the complementation plasmid pHW35.

TABLE OF CONTENTS

LIST OF TABLES

Page

LIST OF FIGURES

Page

Chapter 1: Introduction and Literature Review

Prokaryotic cell biology and differentiation

The fundamentals of bacterial cell biology have been of interest to investigators for many years. Typical bacterial cells exist in different shapes and sizes, like spheres, rods, or spirals, each containing a single chromosome complex called a nucleoid (Brown et al., 2011). Depending on environmental and topological factors, several bacteria exhibit specific behaviors like branching, colonization, sporulation or differentiation (Jiang et al., 2015). These highly conserved phenomenon and internal architectures are dependent on the coordination of several regulatory mechanisms (Thanbichler, 2009).

Bacterial cells contain a complex cell wall made of peptidoglycan which maintains its shape against turgor pressure. In addition to harboring key anchored proteins and lipids, which are crucial to its life cycle, the cell wall plays a role in facilitating several cellular processes (Vollmer et al., 2008; Strahl & Errington, 2017). The growth of a bacterial cell involves controlled growth of its peptidoglycan cell wall spatiotemporally in an organized fashion, synchronously synthesizing new internal cell materials for division into daughter cells. The bacterial cell wall plays a central role in facilitating cell morphogenesis by operating as a scaffold for protein interactions across lipid membranes in gram positive bacteria (Brown et al., 2011; Strahl & Errington, 2017). The growth and development of bacteria during its life cycle is a highly coordinated process generally misjudged for being random and arbitrary due to its simplistic structure. It can be observed that typical bacterial growth involves organization of spatial and temporal orientation of cellular processes like peptidoglycan synthesis. This occurs at

specific zones within the cell during both polar and non-polar growth for most established prokaryotic model systems (Brown et al., 2011).

In addition to increasing size and mass, there are other cellular components which direct the salient features of advancement through the bacterial life cycle, which leads from cellular growth to cell division. Different groups of bacteria have different modes of cell division which are crucial to understanding this progression. A unicellular bacterium like *Escherichia coli* divides symmetrically after elongation of a single cell via binary fission into two equal-sized daughter cells (Donovan & Brankamp, 2014). However, in a multicellular filamentous bacterium like *Streptomyces coelicolor*, the growth and differentiation of the cell is developmentally controlled. A single aerial cell elongates to form a multinucleoid syncytial filament, which synchronously divides into a chain of spores (Flärdh & Buttner, 2009). This form of cell division, which leads to different morphology of the daughter cell, is known as development-associated cell division.

Prokaryotic development

Over the last few decades, the field of prokaryotic development has progressed from the basic understanding of bacterial cell division to identifying intricacies of life cycles for different model organisms. Investigation of several prokaryotic growth processes has illuminated previously unknown nuances of molecular mechanisms, and novel underlying proteins.

A simple way to understand these separate yet interwoven growth processes is to examine bacterial progression through the cell cycle. Successful completion of the bacterial life cycle and propagation revolves around faithful coordination of several complex and often poorly understood cellular processes like cell growth, chromosome

segregation, and cell division. Several prokaryotic models have been established to elucidate these multifaceted phenomena during prokaryotic development. Recent expansion and availability of advanced genetic and microscopy tools have enabled scientists to shed light on the elusive mechanisms of DNA movement during the cell cycle.

The original replicon model suggested that in *E. coli*, the replicated chromosomes tether to the cell membrane before spatially orienting and then passively separating as the daughter cell envelope is synthesized. It also proposed that the membrane-chromosome interactions drive the segregation of the genome in *E. coli* (Jacob & Brenner, 1963). For most bacterial species, the general sequence of events consists of a series of cellular processes. Cellular growth leads to increased cell size, replication of the genome, partitioning and segregation of the duplicated genome into the newly forming predivisional cells. This is followed by the final accurate cell division, which generates daughter cells to complete the cell cycle (Galli et al., 2017). To understand how these processes result in prokaryotic development in different bacterial species, it is essential to examine them individually and characterize the different proteins.

Chromosome replication dynamics and chromosomal architecture

Bacterial cells have specific structural features, which facilitate cellular processes. One of these crucial processes is replicating the genome, which is passed on to the daughter cells during division. It is commonly misconstrued that due to the lack of a membrane bound nucleus, bacterial chromosomes are randomly present in an unsystematic orientation in the cell. These bacterial chromosomes possess specific temporal and spatial properties, depending on their cellular shape, growth pattern and cell

division. Hence, bacterial chromosome architecture is known to be crucial to the rest of the cellular organization (Toro & Shapiro, 2010).

To pack the chromosome of a ~4 Mbp (*Bacillus*) or ~9 Mbp (*Streptomyces*) DNA molecule in a ~1 μm diameter cell is a challenging problem for cellular organization. This problem increases during replication since a cell needs to accommodate double the DNA content prior to segregation and division. Chromosome condensation in conjunction with topoisomerases helps condense and detangle this large DNA molecule in a specific cellular organization (Toro & Shapiro, 2010).

Even though high variability exists amongst bacterial chromatin structures, certain features are highly conserved. The origin of replication (*oriC*) and termination (*ter*) sequence loci are found in all the chromosomes specifically positioned across the cell along its axes. In *E. coli*, initially it was proposed that *oriC* was positioned at one pole, and *ter* at the other. It was later observed that the position of *oriC* changes from the beginning of the cell cycle, where it resides at mid-cell, to after replication where it moves to the longer axis during division. After division, both daughter cells have symmetric orientations of their respective *oriC* locus along mid-cell, similar to the mother cell (Wang et al., 2006; Toro & Shapiro, 2010). In *Bacillus subtilis*, due to the existence of a sporulation cycle, the chromosome dynamics are highly specific during the vegetative phase as well (Wu & Errington, 1994). During its vegetative growth, the chromosomal segments of a *B. subtilis* cell are aligned distinctively with the *oriC* locus near the pole, and the *ter* segments near the mid-cell. Based on FISH (Fluorescent In Situ Hybridization) studies, once replication progresses, the entire replisome migrates towards the mid-cell in an intermediate cell-cycle-dependent fashion (Jensen & Shapiro, 2009).

Other bacterial species like *Caulobacter crescentus* showed similar movement of *oriC* and *ter* from cell poles at the beginning of the cell cycle to mid-cell positions post replication (Viollier et al., 2004). Different proteins are responsible for these shifts of the chromosomal structure and anchoring near the cell pole. These proteins regulate these shifts by binding to specific *cis*-acting sites on the chromosome. Certain protein-protein interactions like RacA and DivIVA proteins in *B. subtilis,* and PopZ and ParB proteins in *C. crescentus,* interact with DNA at specific sites to assist in the dynamic altering of the chromosome orientation during the cell cycle (Ramamurthi & Losick, 2009; Toro et al., 2008) (Figure 1.1).

Understanding general chromosomal architecture sheds light on the roles of different proteins and mechanisms involved in processes like chromosome partitioning and segregation, which leads to successful cell division. Recent studies conducted via genome wide capturing, Hi-C and super resolution microscopy have identified chromosome interaction domains with specific cell proteins. This dynamic architecture led researchers to conclude that spatial organization of the chromosome forms an important link between DNA replication and cell division. This organization also facilitates highly regulated future chromosomal events, which are synchronized to ensure faithful cell division (Le & Laub, 2014; Hajduk et al., 2016).

Discovery of low-copy-number plasmids as a model for segregation

To understand successful progression through the cell cycle, it is essential to explore the various mechanisms employed by cells in passing their genomes to the daughter cells. Once the DNA is replicated, it needs to be partitioned and segregated for reliable inheritance during cell division. Based on historical studies, high-copy-number

plasmids are known to allocate randomly during division, and therefore do not require an elaborate segregation system. Low-copy-number plasmids on the other hand are unable to do so, and have therefore evolved specific mechanisms which enables them to be consistently passed on. These mechanisms can also be applied to current chromosomal portioning models proposing the role of Par (partitioning) proteins in segregating DNA molecules. (Mori et al., 1986; Bignell & Thomas, 2011). This led to the discovery of entire partitioning systems conserved within different species for both smaller DNA molecules like plasmids, and larger complex molecules like chromosomes.

For plasmids, these mechanisms involve positioning them so that division can separate each replicated plasmid copy to a daughter cell. The basic components of this system are the centromere-like *parS* sites on the DNA molecule which direct the segregation machinery. These sites bind to a site-specific DNA-binding protein or a centromere-binding protein (CBP). The other component is an ATPase or GTPase protein which powers plasmid movement. Several partitioning systems are based and characterized on this original model, and can be used to explore the specific mechanisms and proteins involved for different bacterial species.

The partitioning system

One of the major protein complexes, which causes partitioning of bacterial chromosomes during the cell cycle, is known as the *par* system. ParA is a Walker-type ATPase, which assists the assembly of ParB at specific centromere-like sites called *parS* sites on the chromosome (Figure 1.2). These *parS* sites reside near the origin of replication (*oriC*). This association forms a ParB-*parS* nucleoprotein complex, which spreads beyond the origin, aiding the *oriC* to move towards the poles and ensuring

accurate chromosome segregation (Gordon & Wright, 2000). Extensive studies on segregation proteins, in particular the ParAB homologs, have been conducted on various bacterial species like *S. coelicolor*, *B. subtilis*, *C. crescentus,* and some *Mycobacterium, Corynebacterium,* and *Pseudomonas* species. Based on various studies, different partitioning systems are characterized as:

Type I segregation system

This commonly found ParA-based system is present on the *parABS* locus on the chromosome, and is known as the ParABS system. It is driven by the motor protein ParA, which is a deviant Walker-type ATPase. ParA contains a Walker box, also known as the A-type motif which consists of a hydrophobic beta strand, and a P loop, where the glycine-rich residues are modified to lysine-rich residues (Walker et al., 1982). In addition to ParA, the adapter CBP ParB forms a nucleocomplex with centromere-like sites, *parS*. Regulated assembly of dimerized ParA protein is required to polymerize across the surface of the bacterial nucleoid to position the ParB-*parS* interaction. Eventually, ParA depolymerizes to finally pull the redistributed plasmids across the nucleoids equally (Salje et al., 2010).

Type II segregation system

This system is mainly characterized in *E. coli* plasmid RI by the protein complex ParM (the eukaryotic actin-like ATPase motor protein), ParR (the adapter CBP), and the *parC* locus (centromere sites) (Jensen et al., 1998; van den Ent et al., 2002). This ParMRC protein system works by oligomerization of the ParM filaments in an ATP-dependent manner, positioning the ParR-*parC* interactions. This polymerization event

pushes (unlike pulling in Type I) the replicated plasmids toward opposite cell poles, and depolymerization completes this process.

Type III segregation system and treadmilling

This system is characterized by the tubulin-like TubZ protein. TubZ is a NTPase motor protein for plasmid segregation in *B. subtilis*. This system uses a small DNA-binding adapter CBP, TubR, and a putative centromere region *tubC* to perform a similar DNA partitioning event (as in Type I and II segregation systems), by aiding the formation of the TubR-*tubC* nucleoprotein complex (Salje et al., 2010). An interesting finding was that unlike tubulin, TubZ behaves as a tubulin-like protein exhibiting actin-like "treadmilling" activity in *B. subtilis* and *E. coli*. It was identified and recognized by the formation of double-helical TubZ filaments. Treadmilling was initially observed in the tubulin-like cell division protein FtsZ, which self-organizes into a ring-like structure at the cytoplasmic membrane, and acts as a scaffold to recruit the cell division machinery proteins. This GTP hydrolysis-dependent ring structure was observed to be dynamic in nature. Treadmilling has been observed to guide cell wall synthesis, which leads to division. Similar characteristics were observed in TubZ directional dynamic oligomerization of its linear polymers and plasmid maintenance within the cells (Larsen et al., 2007; Monteiro et al., 2018; Ramirez-Diaz et al., 2018).

Chromosome Condensation

A key process in chromosome segregation prior to partitioning is condensation of the chromosomes, mainly led by a family of ATPases known as the Structural Maintenance of Chromosomes (SMC) complex or bacterial condensins. The ATPase domains are globular in structure, and are highly conserved throughout different domains

of life. Initially discovered as the MukB protein in *E. coli* by a Japanese group in 1989, a specific anucleate or "mukaku" phenotype was observed in *mukB* mutants (Hiraga et al., 1989). Since then SMC-like proteins have been an active area of study for cell and developmental biologists as an essential chromosome segregation protein. Later on, it was observed that *mukB* gene encoded a large 117 kDa SMC-like coiled-coil protein with a C-terminal hinge-like domain that formed dimers. It was found to be part of the *mukBEF* operon where MukE and MukF are necessary for MukB function (Yamanaka et al., 1996). This conserved protein is found in several other bacteria and is collectively known as the "SMC" protein. SMC (MukB) is the main condensation protein, and other accessory proteins form a part of its operon or exist separately on the chromosome.

These accessory proteins were identified as accessories to SMC-like proteins in *B. subtilis* and *C. crescentus* as Scp (Segregation and condensation proteins) proteins, ScpA and ScpB (also known as kleisin proteins). Analagous to MukE and MukF, these were later found to interact with each other, and also with the SMC (MukB) dimer in an ATP-dependent manner, which is involved in DNA restructuring activities (Strunnikov, 2006; Bürmann et al., 2013). Structurally, the N-terminal head domain of SMC is a typical ABC transporter ATPase, characterized by the presence of Walker A and Walker B signature motifs that contain ATP-binding (Walker A), and ATP hydrolysis (Walker B) sites. The consensus sequences encoding these motifs are conserved and identified in several bacterial species like *E. coli, B. subtilis, C. crescentus,* and *S. coelicolor*. ATP binding to a SMC monomer is required for dimerization, which stabilizes and activates both ATP binding sites. This dimer can then associate with its respective kleisin protein

and form a SMC-Kleisin O-shaped tetrapartite ring structure (Figure 1.3) (Lim & Oh, 2009; Bürmann et al., 2013; Nolivos & Sherratt, 2014).

It is proposed that the dimerization interface of SMC is crucial for interacting with DNA. This is achieved by loading the DNA molecule on the SMC tetrapartite ring structure, and causes DNA restructuring by compaction, intermolecular DNA bridging, and restraining of the DNA topology. It is also indicated that the head domains of this structure function like type II topoisomerases to separate DNA and prevent entanglement by entrapping different segments of the DNA molecule (Bürmann et al., 2013, Nolivos & Sherratt, 2014).

These DNA condensation processes lead to changes in chromosomal dynamics and architecture, which triggers subsequent cellular processes. Assembly of the parB-*parS* partitioning complex has been linked to targeting SMC dimers to *oriC* sequences on the chromosome to initiate binding. It is still not known if SMC positions these sites for loading and condensation or vice-versa (Shwarts & Shapiro, 2011). Several studies have noted various SMC localization patterns in bacterial cells. It has been observed to colocalize with *oriC* in *E. coli*, and with Spo0J (ParB) in *B. subtilis*. SMC localization is rarely observed to be dependent on ParB in *Streptococcus pneumoniae*, and is not associated with any chromosomal region in either *S. coelicolor* or *C. crescentus* (Sullivan et al., 2009; Dedrick et al., 2009; Schwartz & Shapiro, 2011; Badrinarayan et al., 2012).

These studies have led to a common biochemical mechanism, which requires SMC to form specific structures to interact with chromosomal DNA. Exactly how these interactions take place and continue at a tightly regulated pace, is still not well known.

DNA partitioning and condensation are energy dependent processes, which work in parallel with DNA motors like FtsK to ensure faithful DNA translocation and segregation. In order to understand translocation, it is crucial to explore it in different model bacteria.

DNA translocation by FtsK and FtsK-like proteins

The energy dependent movement of chromosomes, which leads to partitioning into the correct subcellular locations, uses DNA motors present in the cell. Highly conserved in various bacterial species, FtsK is a motor protein that conducts DNA translocation. These DNA translocases direct chromosome segregation and cell division in bacteria. FtsK was discovered as the Filamentous Temperature Sensitive mutation in gene K (*ftsK*) in *E.coli* by Begg et al. (1995). The mutation of the *ftsK* allele in *E. coli* was observed to be conditionally lethal and caused a block in late stage cell division, but did not affect chromosome replication (Begg et al., 1995).

FtsK belongs to the FtsK/SpoIIIE/Tra family, which are DNA translocases that drive the segregating DNA towards the correct side of the septum during vegetative septation, sporulation, and conjugation between cells (Massey et al., 2006; Barre, 2007). It is also known that proteins belonging to the FtsK/SpoIIIE family are also found as a part of type VII secretion systems found in bacteria like *Mycobacterium*. These membrane ATPases function as protein motors which assemble as rings to secrete protein (or potentially DNA) cargo (Unnikrishnan et al., 2017). To understand how orthologs of the FtsK-like proteins function in each of these processes, it is important to explore their roles in bacterial model species.

B. subtilis

In *Bacillus* species, FtsK is named Sporulation protein IIIE (SpoIIIE), and therefore homologous proteins are listed as FtsK/SpoIIIE-like proteins. SpoIIIE is an 87 kDa protein, required for the completion of chromosome segregation during asymmetric differentiation of a *Bacillus* sporogenic cell. Initial studies showed that a mutation in the *spoIIIE* gene did not affect growth and viability during vegetative cell division. However, during asymmetric cell division, in addition to defects in chromosome segregation during the formation of prespores, a *spoIIIE* mutation led to incomplete sporulation (Wu & Errington, 1994).

The following years showed that as differentiation occurs during asymmetric cell division in *Bacillus*, formation of the septum occurs near one of the cell poles, leading to two different cells, the smaller prespore and the mother cell. The two different cells segregate the replicated nucleoid in a specific fashion. The replicated nucleoid is bisected by the newly formed septum, and about 1/3rd of the genome is entrapped by the prespore, leaving 2/3rd of the chromosome trapped in the mother cell (Figure 1.4). This trapped portion of the nucleoid is then translocated by SpoIIIE into the prespore compartment through the septum via a plasmid conjugation-like mechanism. Later, it was shown using photobleaching and TIRF microscopy that the septal assembly of SpoIIIE led to a membrane fission event prior to translocation (Fleming et al., 2010). It was also observed that the trapped DNA in the mother cell is sequence and polarity specific. This chromosomal DNA needs SpoIIIE to be rescued as it contains a functional ATPase site DNA motor (Wu & Errington, 1997; 1998).

It was later found that even though SpoIIIE is not required for cell viability in *B. subtilis* during vegetative growth, it has another function during asymmetric cell division. In addition to chromosome partitioning and translocation, it subsequently localizes at the pole. It is involved in catalyzing an engulfment and fusion event, where membrane fusion of the edges of the forespore with the mother cell membrane releases the forespore into the mother cell cytosol (Sharp & Pogliano, 1999; 2003). It was also noted that the specificity of assembly and localization of SpoIIIE within the cell was negatively regulated by the MinCD protein complex. Deletion of *minCD* led to over-assembly of SpoIIIE in the mother cell, which in return reversed the direction of DNA translocation. This suggested that positional and orientation specificity of SpoIIIE assembly within the cell was crucial for accurate translocation events (Sharp & Pogliano, 2002).

Further investigation and protein localization assays led to the discovery of a second DNA translocase, SftA (previously characterized as YptT), a 107 kDa protein which assembles earlier in the cell than SpoIIIE. Although the C-terminal domain of SftA shared similarity to the ATP and DNA recognition domains of SpoIIIE, its N-terminal domain lacked transmembrane-spanning segments. It was noted that SftA translocates DNA away from the septum, whereas SpoIIIE translocates entrapped DNA through the septum after it has closed. Deletion of both these DNA translocases led to a severe vegetative segregation phenotype. This double mutant strain contained a 10^{-2} log decrease in growth, 0.3% anucleate cells and 12.5% abnormally shaped cells compared to the 0.1% anucleate and abnormal cells found in wild type cells (Kaimer et al., 2009). It was also determined that SpoIIIE and SftA work in a synergistic fashion with the

recombination complex proteins in the cell. They aid chromosome decatenation by correctly positioning the *dif* sites, and resolving the replicated chromosome dimers in the cell (Kaimer et al., 2011).

Recent *in vivo* single molecule tracking experiments of SpoIIIE and SftA also showed differences in the dynamic assembly of the two different translocases. It was demonstrated that about 1/3 of SftA molecules were cytosolic and behaved as a soluble protein, whereas, 2/3 of the molecules were stationary and bound to the membrane. Compared to that, SpoIIIE molecules diffuse throughout the cell membrane. This supports the hypothesis that SpoIIIE binds to membrane-anchored DNA in the cell first, and SpoIIIE recruits SftA (Najjar et al., 2018).

E. coli

FtsK was initially discovered in *E. coli* as the homolog of the previously characterized SpoIIIE-like protein in *B. subtilis* (Begg et al., 1995). FtsK has been well-studied in *E. coli* as the protein that links chromosome segregation and cell division. A much larger polypeptide than its *Bacillus* ortholog SpoIIIE, FtsK is 147 kDa with a N-terminal transmembrane anchor domain, followed by a particularly large middle linker domain and a conserved C-terminal ATPase and DNA recognition domain (Figure 1.5). The deletion of *ftsK* makes cell division temperature sensitive, and leads to a phenotype of long undivided cells and normal segregation in the original *ftsK44* mutant. Since *E. coli* does not undergo sporulation, the replicated chromosomes are segregated concurrently with septation during binary fission. Hence, DNA translocation through the septa does not occur. Therefore, FtsK is likely to be involved in the correction of mis-located DNA (Begg et al., 1995; Liu et al., 1998). However, in a truncated *ftsK* mutant of

E. coli, up to 20% of the cells in log phase contained asymmetric positioning of nucleoids, and 1% of anucleate cells compared to 0.03% anucleate cells in the wild type strain (Yu et al., 1998). Another potential role of FtsK was shown during septation via its involvement in peptidoglycan (cell wall) synthesis. This was observed when a *ftsK* deletion phenotype was suppressed by the deletion of another gene, *dacA*. *dacA* encodes the peptidoglycan-modifying $_{D}$-alanine:$_{D}$-alanine carboxypeptidase PBP5 during cell wall synthesis (Matsuhashi et al., 1979).

Recent work has illustrated that different domains of the FtsK protein play different roles in late stage chromosome segregation. It was found using a two-hybrid assay analysis that the membrane anchored N-terminal domain (~200 amino acids) is required for cell division as it interacts with other divisome proteins, and presumably functions to stabilize them during cytokinesis (Lallo et al., 2003). The cytosolic C-terminal domain of FtsK acts as a DNA translocase that aids in terminating the final step of replication by catalyzing decatenation of the sister chromosome dimer resolution. This occurs when FtsK localizes at mid-cell in a *dif*-site specific manner by activating the XerCD protein complex (Bisicchia et al., 2013). The directionality and orientation specificity of FtsK is achieved by its DNA recognizing sequences, which assists in bringing the *dif* loci together for decatenation (Badrinarayan et al., 2015).

Although the main function of FtsK is to translocate double-stranded DNA and segregate the replicated sister chromosomes, it has an additional function in viability, especially in the absence of the SMC-like MukBEF proteins. FtsK is also known to play a crucial role in cell shape and morphology in *E. coli* (Badrinarayan et al., 2015).

Due to the nature of replication in *E. coli*, which starts bidirectionally at *oriC* and proceeds until the *ter* region, *oriC* and *ter* sites are asymmetric. This causes the replichore (the halves of the chromosomes between the *oriC* and the *ter* region) to become unequal, and the sequences containing FtsK-binding motifs are asymmetrically positioned on each replicated chromosome arm. Based on the order of these sequences, the two sister chromosomes are decatenated and segregated with the help of FtsK. This is accomplished by re-orienting the chromosome within the dividing cell, and by translocating the chromosome in a direction-specific manner through the division plane (Lesterlin et al., 2008; Surovtsev & Wagner, 2018). Therefore, FtsK is one of the key proteins essential for efficient segregation and successful division, hence forming a bridge between these two phenomena.

S. coelicolor

FtsK has been investigated to play a role in the unique life cycle of *Streptomyces* species. A comparative genomics study of several *Streptomyces* species showed that the highly conserved gene *sco5750* in the *S. coelicolor* database was most likely to encode the putative DNA translocase of the FtsK/SpoIIIE family (Hsiao & Kirby, 2008). With 45% sequence identity over the C-terminal domain of the *E. coli* protein FtsK, the *S. coelicolor* homolog forms one of the key proteins in cell segregation and division machinery (Wang et al., 2007). FtsK is the most characterized FtsK/SpoIIIE-like protein for *S. coelicolor*. It is a 98 kDa protein, with a 929 amino acid polypeptide chain. In addition to *ftsK,* the genome of *S. coelicolor* notably contains four more *ftsK*-like genes.

Going through both vegetative and sporulation growth phases, different proteins are expressed at specific timepoints during the life cycle of *S. coelicolor*. Continuous

replication of the linear chromosome within the cell makes some of the aerial filaments syncytial. These multinucleoid filaments need to accurately partition and segregate the genomes between the closing septum of the daughter cells. During this time, it has been hypothesized that FtsK translocates and directs DNA movement by interacting with specific sequences present on the chromosome. However, there is no direct experimental evidence supporting this hypothesis (Flärdh & Buttner, 2009).

Different research groups independently observed that complete deletion of *ftsK* did not cause an overt phenotype as seen in *E. coli* and *B. subtilis.* This deletion caused no noticeable change in viability or sporulation, but caused very a mild chromosome segregation phenotype (Wang et al., 2007; Ausmees et al., 2007; Dedrick et al., 2009). The exact mechanisms involving segregation and translocation of this linear chromosome are still quite elusive. Before the discovery of the *ftsK* gene in the *Streptomyces* genome, several experiments were conducted hypothesizing the role of plasmid transfer or Tra proteins for accurate chromosome segregation (Petis & Cohen, 1996).

Studies have shown FtsK-mCherry and FtsK-EGFP to localize in the predivisional hypha of a dividing spore chain prior to septation. Another study investigated two unrelated proteins SffA and SmeA, where the cytosolic protein SffA worked in conjunction with a small membrane protein SmeA for proper chromosome segregation. The loss of these genes resulted in a very mild segregation defect. It was later hypothesized that these proteins most likely play a role in spore maturation as well (Ausmees et al., 2007).

Once the sporogenic *S. coelicolor* cells of the aerial mycelium phase start differentiating into spores, it leads to a cascade of coordinated events. This phase starts

by the development of a septum, which then forms the edge of each prespore compartment, and the concomitant process of chromosome segregation. Before septation, protein complexes (like the ParAB partitioning machinery) are also functional. The ParAB complex works to equally position copies of the replicated DNA to be translocated. It was proposed that ParA, a Walker-type ATPase, facilitates the binding of ParB to the *parS* sites on the uncondensed chromosomes. Although it has not been directly demonstrated, this positioning was hypothesized to trigger the assembly of the FtsK protein at the septum, which then translocates the DNA into its respective daughter cells, so that these prespore compartments containing the segregated genome can develop into spores (Figure 1.7). (Flärdh & Buttner, 2009).

Chromosome segregation is a complex and entangled process with several cellular phenomena occurring simultaneously, and is based on the developmental cycle of the organism. Therefore, this makes it necessary to understand this process in detail by exploring development-associated segregation in different prokaryotic species.

Development-associated segregation

As mentioned before, the term development in prokaryotic cell biology comes from the specific and unique life cycle stages of bacteria. During development, one form of cell differentiates and develops into another form in a highly regulated manner. The replicated genomes segregate into daughter cells concomitantly with condensation and partitioning in a highly coordinated and non-random fashion. This segregation faithfully passes on these genomes to the daughter cell followed by cell division, and is known as developmental-associated chromosome segregation. Throughout this developmental

stage, several specific regulatory and metabolic activities occur in the cells, and it is important to understand their significance in individual signature bacteria.

Models of prokaryotic DNA segregation

Many important discoveries about chromosome segregation in bacteria have been made in model organisms containing linear or circular genomes like *S. coelicolor*, *E. coli, B. subtilis, M. smegmatis* and *C. crescentus* (Gordon & Wright, 2000). In order to comprehensively grasp and appreciate the unique yet overlapping cellular processes in each of these bacteria, it is necessary to explore them individually.

E. coli

E. coli has been at the forefront of many discoveries made in the domain of prokaryotic cell biology. Being a rod-shaped unicellular bacterium with a circular chromosome, *E. coli* is well studied and has been used as a laboratory workhorse for decades. It has been shown that during the life cycle of *E. coli*, its different cellular processes are inter-linked (Reyes-Lamothe et al., 2012). Highly regulated DNA replication in the *E. coli* cell is immediately followed by cell division, during which the coordinated process of chromosome segregation occurs (Männik & Bailey, 2015). Chromosome segregation has always been somewhat obscure and elusive. *E. coli* lacks the Par system or SMC complex, but possesses an analogous MukBEF protein complex. This complex plays a role in separating the *oriC* upon replication, by binding DNA in clusters, promoting DNA condensation, and leads to decatenation by a site-specific recombinase Xer protein (Niki et al., 1991).

The large protein complex involved in swiftly transitioning the *E. coli* cell from replication to enter cell division is called the “divisome”. Over 36 divisome proteins have

been discovered and characterized, including cytoskeletal proteins, peptidoglycan synthases and hydrolases, and a DNA translocase. The 12 essential cell division proteins are named as Fts (Filamentous temperature sensitive) proteins, each of which has a distinct role (Lutkenhaus et al., 2012). Assembly of the divisome is a complex process which is completed in two separate stages. The first stage involves the tubulin-like FtsZ protein, which polymerizes with the help of an actin-like FtsA protein to form a ring-like structure. This ring formation is aided by its interaction with Zap proteins to form a "Z ring". Once assembled, the FtsZ protofilaments of this Z-ring undergo what is known as "treadmilling", where controlled peptidoglycan synthesis and cell division occurs concurrently in a GTP-dependent fashion, hence forming the septum to divide the cell (Monteiro et al., 2018). This marks the future division site at midcell, which ensures accurate segregation followed by cell division. The second stage consists of the recruitment of other Fts proteins (FtsK, FtsQ, FtsL, FtsB, FtsW, FtsI, and FtsN) to the Z-ring, during which FtsN binding activates the Z ring for septal peptidoglycan synthesis, which enlists other remodeling proteins for successful cell division (de Boer, 2010; Du & Lutkenhaus, 2017). In addition to divisome assembly and Z-ring activation, there are other critical processes that occur for faithful division. One of these processes is nucleoid occlusion (NO), which occurs to avoid constricting the cells where the nucleoid is present and prevents the chromosome from being guillotined. NO is a multi-step process shown to be mediated by two independent protein complexes. Specific interactions of the protein SlmA with the chromosome spatially positions the Z-ring, thereby avoiding the nucleoid from being structurally damaged (Cho et al., 2011).

Another system to ensure accurate cell division is the positioning of the Z-ring by the Min protein complex (MinC, MinD, and MinE). The MinCDE protein complex functions in an oscillating fashion from pole to pole, and interacts with the FtsZ monomers, so that the Z-rings are not formed at the polar ends of the cell. This defines the geometric position of the divisome at the midcell (Shen & Lutkenhaus, 2010).

In addition to the guidance by the divisome to segregate the genomes and facilitate division, the DNA translocase FtsK plays a crucial role in coupling these processes. FtsK directionally pumps the nucleoid DNA in an ATP-dependent manner during the final stages of the cell cycle. It functions to position the *dif* site on the chromosome, which directs where the chromosome dimers are resolved by the XerCED protein complex (Männik & Bailey, 2015). All these proteins coordinate in a highly efficient manner to direct concomitant replication, segregation and division.

B. subtilis

In sporulating bacteria, DNA replication is a tightly regulated process ensuring the scrupulous segregation of genetic material to the spores (Tzeng & Singer, 2005). In *B. subtilis*, sporulation occurs during the asymmetric cell division by differentiation of the vegetative cell as a developmental progression process (Errington et al., 2005). Chromosome partitioning proteins Soj (ParA) and Spo0J (ParB) collaborate for initiation of sporulation, and affect gene expression by interacting with *parS* sites flanking the *oriC* on the chromosome, hence forming a nucleoprotein complex *oriC*-Spo0J. This nucleoprotein interaction is crucial for SMC complex recruitment and activity. A Δ*smc* mutant in *B. subtilis* displayed a high segregation defect of 2.1% compared to 0.06% in wild type (Quisel & Grossman, 2000; Lee & Grossman 2006; Duan et al., 2016). As

sporulation approaches, this complex is directed towards the cell poles. This is where the DivIVA protein has already been recruited with the aid of an adapter protein RacA and the partitioning protein Soj. This recruitment of DivIVA tethers the *oriC* region to the cell pole. Only DNA flanking this *oriC* region is arranged near the protein complexes, so that the rest of the chromosome remains trapped in the mother cell compartment. Chromosomal movement from mother cell to prespore is driven by the motor protein SpoIIIE (FtsK) at the division septum.

C. crescentus

In another bacterium with a circular chromosome, *C. crescentus*, it has been shown that the chromosomal origins of replication localize in cells towards opposite poles. The replication terminus stays in the middle of the cell indicating a highly organized chromosome orientation within the bacterial cell (Niki et al., 2000). Similar to *E. coli* and *B. subtilis*, *Caulobacter* species have their chromosome aligned in a specific manner inside the cell with its *oriC* and *ter* regions localized at opposite poles. The segregation process takes place with the aid of several key proteins using the ParABS system. The general life cycle of *C. crescentus* produces two types of cells, one is the immobile stalk cell, and the other is the mobile swarmer cell (Goley et al., 2011). After replication, different systems and proteins work together to segregate the genomes. The partitioning system consists of two *parS* sites which are bound by a ParB (CBP) protein, and the function of the motor NTPase is performed by a polar organizer protein called PopZ, which aids the assembly of this *parS*-ParB nucleoprotein complex. There are a few more components identified in *C. crescentus* segregation machinery like MipZ (an FtsZ inhibitor), which coordinates segregation and cell division, along with a protein TipN

which is known to interact and positively regulate PopZ polymerization (Livny et al., 2007; Ptacin et al., 2010; Bergé & Viollier 2018).

The condensation protein SMC has also been identified in *C. crescentus*, and is an essential player in segregation. A complete *smc* deletion causes a conditional lethal temperature-sensitive phenotype. At the permissive temperature, a Δ*smc* mutant exhibited irregularly shaped nucleoids within the cells, and about 0.1% anucleate cells compared to smooth and almost no anucleate cells in the parent wild type strain. A Δ*smc* mutant also caused the *oriC* and *ter* regions to be mislocalized within the cells. SMC-EGFP was not observed to localize with the *oriC* within the cell. Although the exact condensation mechanism is still unclear, co-immunoprecipitation assays identified the conserved ScpA and ScpB proteins in association with SMC. It has been hypothesized that ScpA and ScpB work as accessory proteins with SMC to condense DNA (Jensen & Shapiro, 1999; Shwartz & Shapiro, 2011). To power the segregation process, the ATPase motor protein FtsK is also found in *C. crescentus*, and is known to play a role in mediating the link between segregation and division by translocating the DNA. The N-terminal domain of FtsK has been shown to be function in initiating and localizing the FtsZ ring. There is also evidence that the C-terminal domain of FtsK is required for viability and completion of cell division in *C. crescentus* by playing a role in chromosome partitioning (Wang et al., 2006; Du & Lutkenhaus, 2012).

Corynebacterium glutamicum

A high GC Gram-positive actinobacterium, *C. glutamicum* is a common model organism to study pathogenesis in a non-pathogenic system. It is heavily used in the food industry to produce monosodium glutamate (MSG). Like *B. subtilis, C. glutamicum*

contains a ParABS partitioning system. The *parA* (encoding NTPase) and *parB* (encoding CBP) genes are encoded in an operon, which has close proximity to the *oriC*, and therefore the three *parS* (centromere) sites. At these *parS* sites, the ParB protein binds to the DNA and forms the *parS*-ParB nucleoprotein complex. These complexes are localized near the cell poles via ParB-DivIVA interaction. *parA* and *parB* deletions cause severe phenotypes with defective growth patterns such as long multinucleate or anucleate cells. A Δ*parB* mutant caused 28% anucleate cells compared to none observed in wild type. (Donovan et al., 2012).

Other homologous accessory partitioning proteins have been identified in *C. glutamicum* like *pldP* (ParA-like division Protein), which is known to localize at the midcell and interacts with ParB (*in vitro*), but does not seem to have an overt effect on segregation. However, it was proposed that it plays a role in cell division as it is suspected to interact with FtsZ, which also assembles around the same time at midcell. Other segregation processes like condensation by SMC and DNA translocation by FtsK (putative protein identified) have not yet been researched in *C. glutamicum*. Several key proteins have been identified during cell division (cytokinesis). These proteins are involved in spatial dynamics of processes like regulation of the divisome, septum placement, and septum synthesis (Donovan et al., 2010; 2012; 2013; Böhm et al., 2019).

Mycobacterium smegmatis

Mycobacterium is a Gram-positive organism belonging to the phylum Actinobacteria. It has a unique cell cycle that leads to asymmetric division (like *C. glutamicum*) into daughter cells of different sizes and growth rates (Jakimowicz et al., 2007). Unlike other bacteria, it does not have a Min system required for FtsZ ring

assembly. They use the ParA and ParB complexes to effectively segregate the DNA after replication, and have the FtsK DNA translocation protein, which has not been well studied in this organism (Hett & Rubin 2008). Like other bacterial species, *M. smegmatis* possesses the ParABS system. Formation of the *parS*-ParB nucleoprotein complex is mediated by the ParA protein. It has also been shown that the ParB is required for SMC protein localization necessary for chromosome condensation in the cell (Trojanowski et al., 2015).

These proteins have overlapping roles in chromosome architecture and replication dynamics, all taking place at the midcell. Several FROS (Fluorescent Repressor-Operator Systems) experiments and time-lapse microscopy showed that *parB* and *smc* mutants had phenotypes which displayed an aberrant number of replisomes/cells. A Δ*smc* mutant only showed a slight segregation defect of 0.3%, and is suspected to play a minor role in replisome assembly, septum localization and chromosome segregation. However, the exact mechanism of action of these proteins is still unclear. It was also observed that changes in growth rates also affected segregation efficiency (Santi & Kinney, 2015). A Δ*parB* mutant exhibited a 10.3% segregation defect compared to 0.8% in wild type (Jakimowicz et al., 2007). Recent microfluidic time-lapse fluorescent microscopy suggested that due to the dynamic chemistry and interchange of proteins, ParB complexes are segregated asymmetrically in *M. smegmatis,* and are regulated by ParA. A similar pattern has been observed in *C. crescentus.* It was also noted that although ParA enriches ParB-DNA binding, it does not particularly impact the organization of *oriC* mediated by ParB (Ginda et al., 2017).

Introduction to *Streptomyces coelicolor* development-associated chromosome segregation

S. coelicolor is a Gram-positive soil bacterium belonging to the phylum Actinobacteria and is a well characterized species of the genus *Streptomyces*. Members of the family Streptomycetaceae are known to have a complex and unique life cycle, which has been of interest to scientists for many decades (Shrempf et al. 2008). When a dormant *Streptomyces* spore germinates, the growth of the vegetative hyphal filaments commences in a polarized fashion. During this time, DNA condensation is not frequently observed, and is not essential (Flärdh, 2003). In the vegetative phase, assembly of peptidoglycan occurs at the hyphal tips to direct polar growth. Polarized growth is mainly regulated by a protein called DivIVA. However, a tip-organizing center (TIPOC) has been identified, and it consists of intermediate filament-like proteins FilP and Scy, which drive tip extension and hyphal branching (Holmes et al., 2013). Further colony growth results in a branching network of hyphae, which resembles the vegetative mycelium of filamentous fungi. At this stage, certain regulatory signals, like nutrient deprivation and environmental factors, prompt the formation of aerial mycelium, which contains the continuously replicating genomes, and are syncytial (Flärdh & Buttner, 2009). These multigenomic and syncytial aerial hypha undergo synchronous cell division, during which the replicated genomes need to be condensed, partitioned and accurately translocated. These genomes are segregated into a chain of up to 100 unicellular compartments that eventually metamorphose into spores (Figure 1.6) (Flärdh & Buttner, 2009; McCormick & Flärdh, 2012).

The 8.7 Mb linear genome of *S. coelicolor* has been sequenced (Bentley et al., 2002) and has a high GC content. Despite its linear structure, the chromosome arms are believed to condense, and the ends come in close proximity to acquire a circular form of the chromosome with the aid of terminal protein complexes (TPs). These terminal proteins are also essential for the replication of linear plasmids and chromosomes in *Streptomyces.* It was observed that TP proteins are bound to long inverted repeats on the 5' ends of the telomeres, and interact to make the ends of the DNA form a circular structure (Anderson et al*.,* 1977; Yang & Losick, 2001; Bao & Cohen, 2001; Yang et al., 2002). Analysis of segregation in this organism is actively studied in several laboratories with respect to other cellular processes like replication and cell division.

Mechanisms pertaining to the chromosome segregation in *S. coelicolor* and its workings are still unclear. This involves many processes working in an intricate fashion like condensation, partitioning, and translocation of the chromosome. The advantage of studying *S. coelicolor* as a developmental model is that several segregation mutants are viable during the course of its unique life cycle (McCormick & Flärdh, 2012).

Several studies have been conducted to understand the current model of segregation in *S. coelicolor*. Like the previously described prokaryotic models, *S. coelicolor* also possesses the ParABS segregation system. About 24 *parS* sites are known to exist on the *S. coelicolor* chromosome near its origin of replication (*oriC*), which have been shown to bind to the ParB adaptor protein (Jakimowicz et al*.,* 2005). This interaction forming the *parS*-ParB complex is known to be facilitated by the assembly of the ParA ATPase protein both *in vitro* and *in vivo*. ParB-EGFP was observed to localize into evenly spaced foci along the pre-divisional aerial hyphae (Jakimowicz et

al., 2005). *parA* and *parB* deletions have severe effects on chromosome segregation, but not on the general growth of the cells on sporulating media. A *parA* mutant produced about ~24% anucleate spores, where as a *parB* mutant had a segregation defect of about ~15% anucleate spores, compared to 1% in wild type (Jakimowicz et al., 2005).

ParA and ParB are observed to be interdependent, where ATP-dependent ParA dimers polymerize in a helical filament assembly along the aerial hyphae to mediate the interaction of ParB proteins with the *parS* sites on the chromosome. ParB interaction is also known to increase the ATPase activity of ParA (Jakimowicz et al., 2007). Other ParA-interacting proteins, like ParJ, were also discovered via two-hybrid library screening. ParA-ParJ binding was further characterized by Surface Plasmon Resonance (SPR) analysis. ParJ was found to interact with ParA and assist in its polymerization and depolymerization. The other ParA-binding proteins have not been characterized (Ditkowski et al., 2010).

As far as DNA condensation is concerned, SMC is a key component of the *S. coelicolor* segregation machinery along with its associated proteins ScpA and ScpB. The deletion of *smc* caused ~7% anucleate spores, but did not have an effect on the general morphology and growth. Deletion of *scpAB* caused a novel phenotype, which appeared to have bilobed nucleoids post-septation, and therefore play a role in condensation, but not segregation (Dedrick et al., 2009). The phenotype observed in a *smc scpAB* mutant showed 17% bilobed nucleoids and 3% anucleate spores, suggesting the presence of additional rescue proteins to fulfill the DNA condensation functions within the cell. Some fluorescent protein fusion studies also suggest that SMC may be

playing an uncharacterized role in the localization of ParB in the cells (Kois et al., 2009; Dedrick et al., 2009).

In addition to DNA translocation during segregation, studies suggest that the FtsK protein in *S. coelicolor* may be involved in performing other functions in the cell. However, a Δ*ftsK* mutant has no phenotype. It has been speculated that FtsK may be involved in a nucleoid occlusion (preventing guillotine of inaccurately segregated chromosomes) type function, as a distinct NO system does not exist in *S. coelicolor*. FtsK is known to localize along the pre-divisional septa of the aerial hyphae (Wang et al., 2007; Ausmees et al., 2007; Dedrick et al., 2009). A viable *ftsK* truncated deletion, which contains only a part of the gene (encoding the three membrane spanning segments) in the cell, behaves differently by displaying a higher segregation phenotype than a complete deletion, and also exhibits some heterogeneity in colony formation (Dedrick et al., 2009).

Despite having evidence of important roles played by key segregation proteins, the true mechanism of chromosome segregation is still largely unknown. For example, the FtsK/SpoIIIE-like Sco5734 protein has been characterized as a type VII secretion system protein. It is hypothesized that the type VII secretion (T7S) system is involved in maintaining nucleoid shape (Roman et al., 2010). There seems to be more than one unknown compensatory rescue systems acting to segregate replicated genomes and keep the cell viable prior to division. Therefore, it is critical to understand that there are pieces of the puzzle which are still unknown, and it is essential to find and scrutinize different target proteins for the known segregation machinery as they may be the missing components of the segregation machinery.

The goal of my study was to explore the role of a novel uncharacterized FtsK-like protein, HfkA, and its role in chromosome segregation or as a T7S system protein in *S. coelicolor*. I have inspected the segregation phenotype of a *hfkA* mutant, and concluded that HfkA and FtsK are redundant in function. I also isolated a series of segregation mutants, which suggest that several key segregation protein-coding genes can be deleted together in *S. coelicolor*, and still have a viable phenotype. My work further describes the phylogenetic analysis of conserved FtsK and FtsK-like proteins. I also found novel interactions between FtsK and partitioning proteins ParA and ParJ in a bacterial two-hybrid assay (*in vivo*). This can be useful in the future understanding of protein-protein interactions during development-associated chromosome segregation.

Table 1.1: Elements of different partitioning systems in prokaryotic model species.

Partitioning systems in bacteria	**Major Elements found in the cells**
Type I segregation system (most common in plasmid and chromosome)	Proteins: ParA and ParB (along with accessory proteins and homologs) Centromere: *parS*
Type II segregation system (*E. coli* plasmid)	Proteins: ParM, ParR, Centromere: *parC*
Type III segregation system (*B. subtilis* plasmid)	Proteins: TubZ, TubR, and Centromere: *tubC*

Table 1.2: Segregation components in different prokaryotic models.

Bacterium	Components of chromosome segregation
E. coli	*oriC,* MinCED, MukBEF, FtsK FtsN, FtsA, FtsZ, NO, XerCED,
B. subtilis	*oriC,* Soj, Spo0J, SpoIIIE, SMC, ScpA, ScpB
C. crescentus	*parS,* ParA, ParB, PopZ, MipZ, TipN, SMC, ScpA, ScpB
C. glutamicum	*parS,* ParA, ParB, PldP, SMC
M. smegmatis	*parS,* ParA, ParB, SMC, FtsK
S. coelicolor	*parS,* ParA, ParB, ParJ, FtsK, SMC, ScpA, ScpB

Table 1.3: List of putative translocases characterized in certain model bacterial species.

Bacterium	***B. subtilis***	***E. coli***	***S. coelicolor***
Different translocases identified	SpoIIIE SftA	FtsK	FtsK SffA SmeA

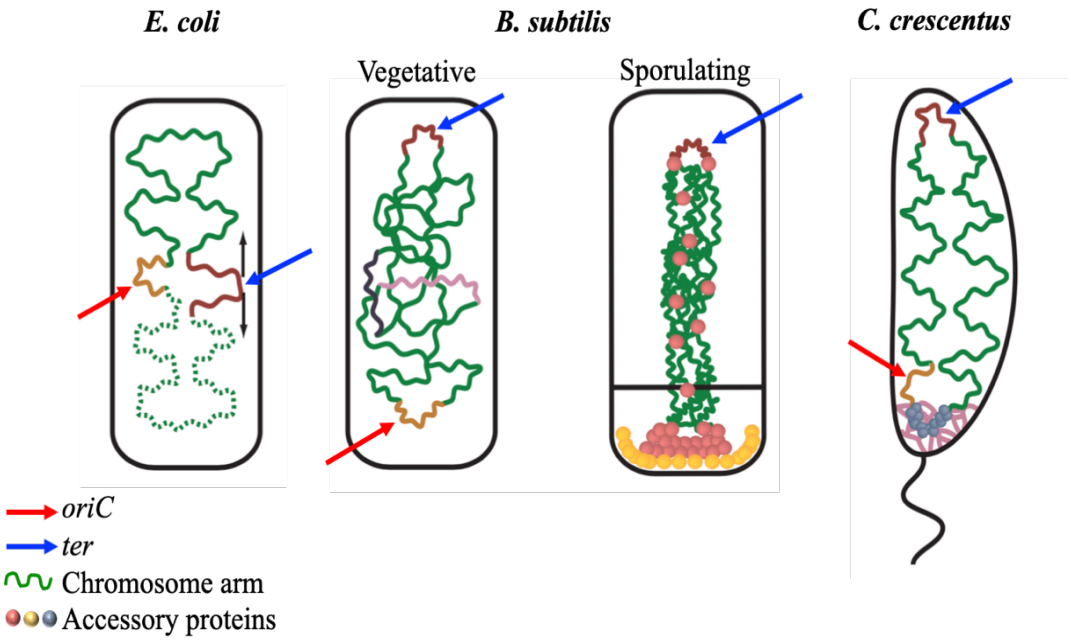

Figure 1.1: Position of specific chromosomal loci in different bacterial cells.

This schematic describes the position of the basic chromosomal elements in different bacterial species. The *oriC* elements are pointed by RED arrows, the *ter* elements are pointed by BLUE arrows, the chromosome arms are highlighted in GREEN, and accessory proteins are represented by small spheres. In *E.coli,* the *oriC* and *ter* elements are arranged around the midcell. In *B. subtilis,* the *oriC* and *ter* elements are arranged at opposite poles in the vegetative cells, and the *ter* elements can be seen at the pole in the sporulating cell. The *oriC* is at the pole in the prespore with accessory proteins like RacA. Similarly, in *C. crescentus*, the *oriC* and *ter* elements are found at the opposite poles and the accessory proteins near the *oriC*. (Adapted from Toro & Shapiro (2010)).

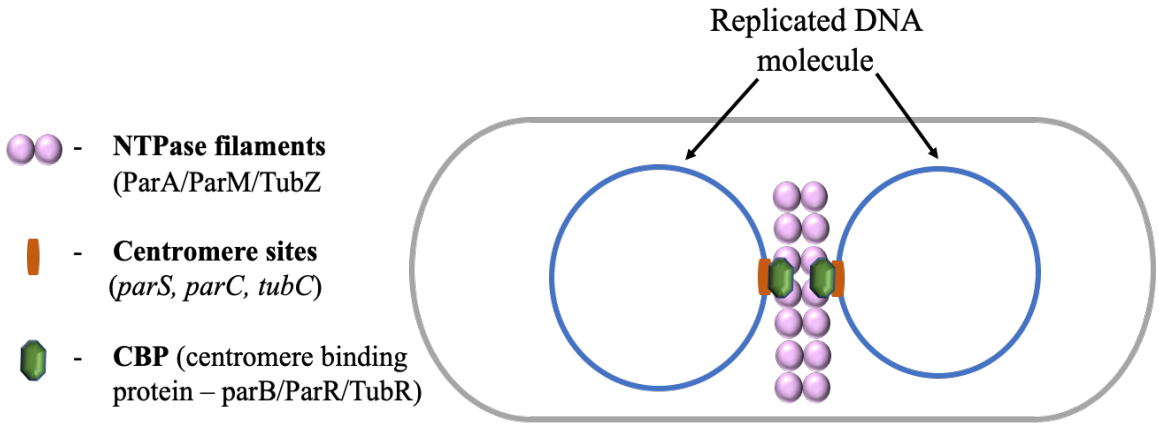

Figure 1.2: A basic partitioning system model.

This schematic displays a simplified version of proteins involved within a cell, which are common to different partitioning systems. Along the centromeric sites (orange) of the replicated plasmid genome (shown as blue circles), the NTPase (ATPase/GTPase protein) shown as pink spheres forms a filament like structure to position the centromere binding protein (in green) and form this nucleoprotein complex by binding to the centromeric sites. This process ensures that the genome is equally segregated and the cell can proceed towards division.

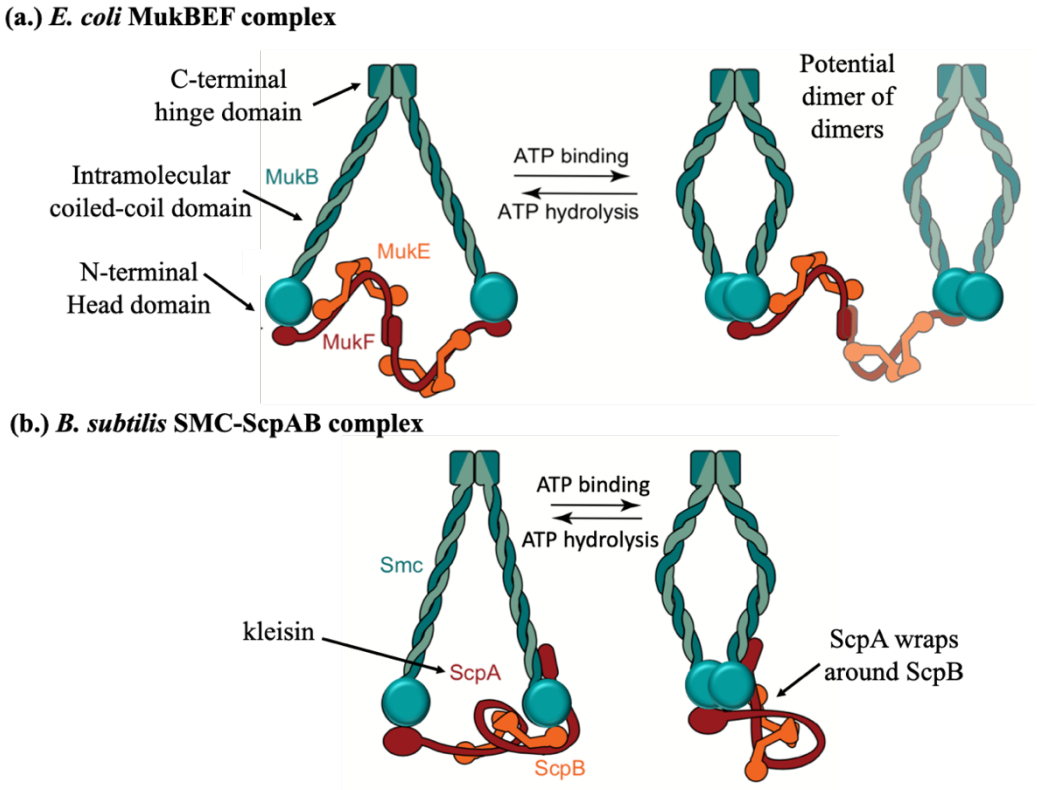

Figure 1.3: A simplified model of SMC dimerization.

Displayed is the cartoon representation and interaction of SMC protein with its accessory ScpA and ScpB proteins in an ATP-dependent fashion. (a.) Shows *E. coli* MukB (SMC) protein dimerizing and binding to MukE and MukF at the head domain. Each monomer contains the head N-terminal domain, the coiled coil domain and the hinge domain. It is hypothesized that MukE and MukF interact with each other and aid MukB in chromosomal remodeling. It is also postulated that this dimer structure further dimerizes via MukE and MukF interactions. (b.) In *B. subtilis,* the SMC dimerizes similarly at the hinge domain, and binds to ScpA and ScpB (Kleisin) proteins at its head via interaction of ScpA and ScpB, where ScpA monomer wraps around ScpB dimer. (Adapted from Nolivos & Sherratt (2014)).

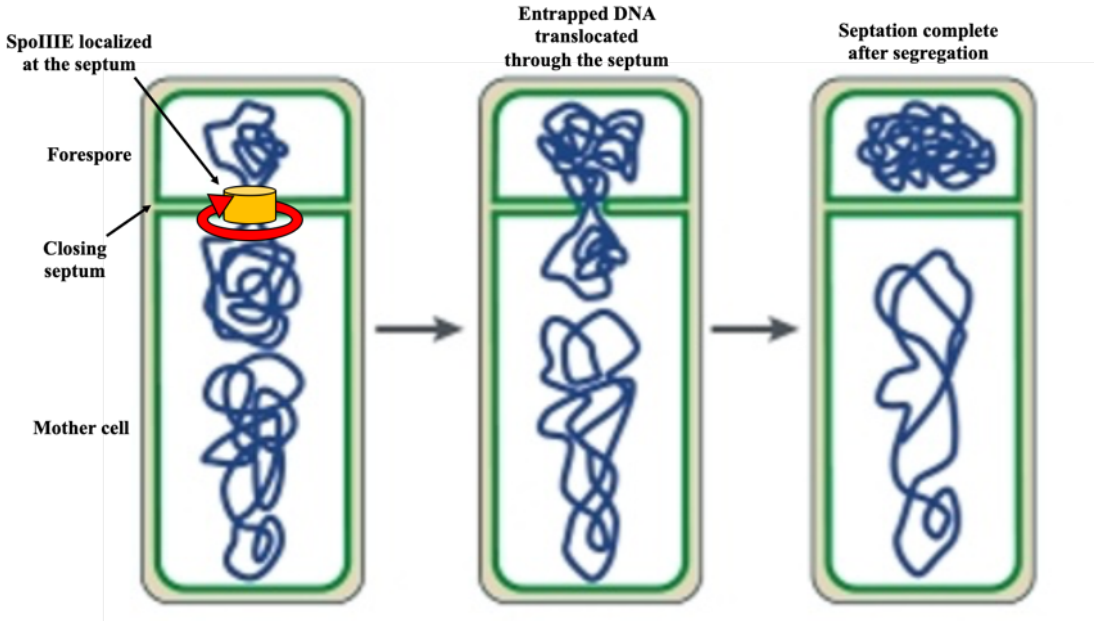

Figure 1.4: Model of DNA movement through the sporulation septum in *B. subtilis*.

Above is a schematic of chromosome movement through the septum in *B. subtilis* during sporulation. SpoIIIE localizes and assembles at the closing septum between the mother cell and pre-spore. The replicated nucleoid is bisected by the newly formed septum, and about 1/3 of the genome is entrapped by the prespore, leaving 2/3 of the chromosome trapped in the mother cell. This trapped portion of the nucleoid is then translocated by SpoIIIE into the prespore compartment through the septum via a plasmid conjugation-like mechanism. (Adapted from Errington et al. (2001)).

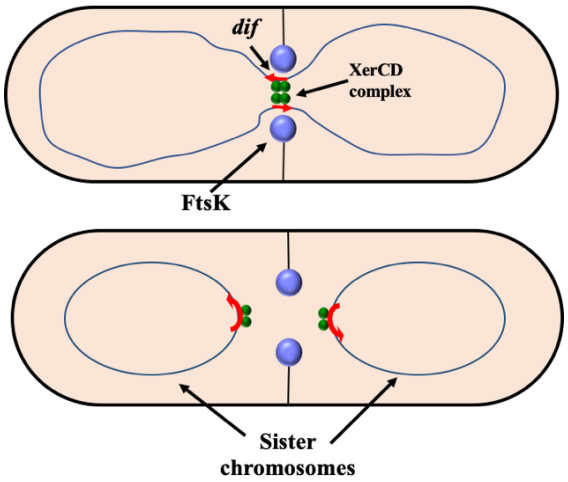

Figure 1.5: Schematic of the role of FtsK in a dividing *E. coli* cell.

Above is a basic diagram showing localization of FtsK in *E. coli* invaginating septum at midcell to interact with the *dif* sites-Xer protein complex near the replicated chromosomes. FtsK is involved in stimulating decatenation and resolution of the sister chromosomes by the Xer/*dif* complex. The cytosolic C-terminal domain of FtsK acts as a DNA translocase that aids in terminating replication by catalyzing decatenation of the sister chromosome dimer resolution in a *dif*-site specific manner by activating the XerCD protein complex by hexamerizing at the midcell. The FtsK motor also moves the trapped DNA to the opposite sides. (Adapted from Errington et al. (2001)).

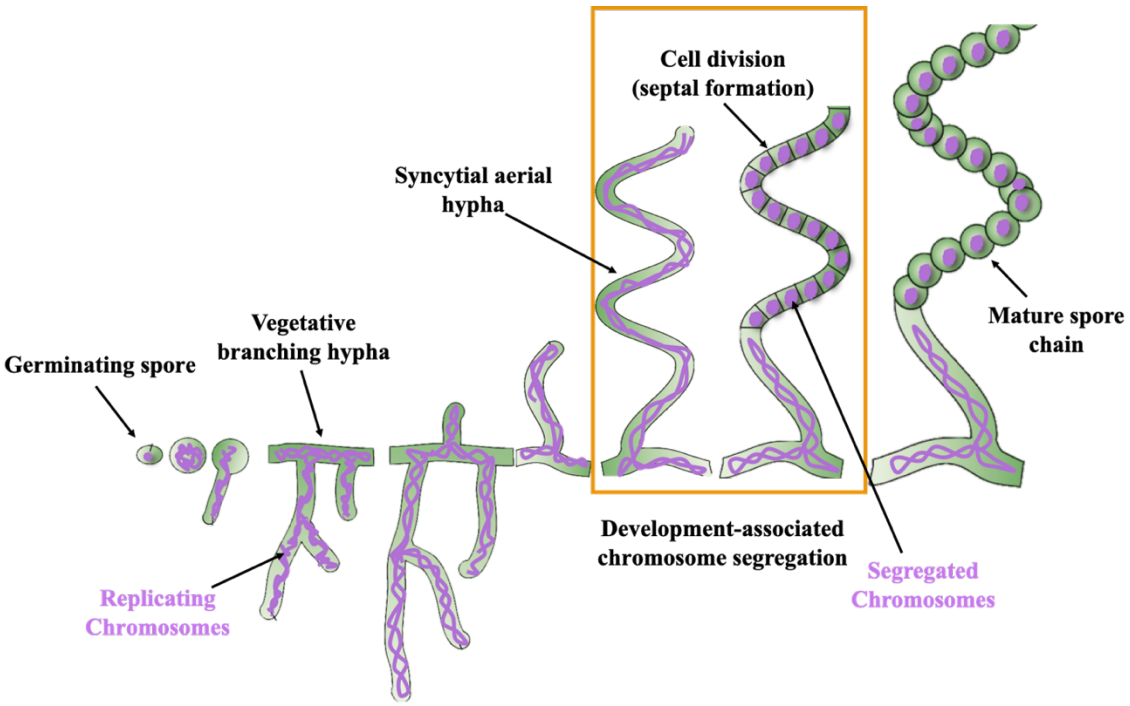

Figure 1.6: **Development-associated chromosome segregation in *S. coelicolor*.**

The diagram depicts the general life cycle of *S. coelicolor*, showing the unique progression from spore germination into substrate (vegetative) mycelium and branching into aerial mycelium. These syncytial aerial hyphae contain multiple replicated copies of the genome (highlighted in purple), which condense and segregate into unicellular compartments prior to septation. This process is known as the development-associated chromosome segregation. This advances the cell towards division, and these prespore compartments eventually metamorphose into mature spore chains. (Adapted from Flärdh & Buttner (2009)).

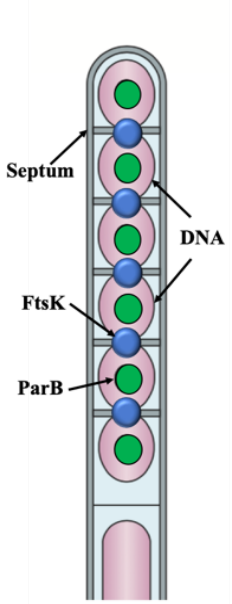

Figure 1.7: DNA translocation by FtsK in *S. coelicolor.*

A basic schematic showing the pre-divisional hypha of *S. coelicolor* FtsK during chromosome segregation. The diagram above shows FtsK lodged in the septa along with protein ParB localized between the sept a in the predivisional aerial sporogenic cell. This multinucleoid hypha needs to accurately partition and segregate the genomes between the closing septum of the daughter cells, during which FtsK is hypothesized to translocate and direct DNA movement by specific sequences present on the chromosome. (Adapted from Flärdh & Buttner (2009)).

References

Anderson, R. P., Roth, J. R. (1977). Tandem genetic duplications in phage and in bacteria. *Annual Rev Microb.*, *31*, 473-505.

Ates, L.S., Houben, E. N. G., Bitter, W. (2016). Type VII secretion: a highly versatile secretion system. *Microbiology Spectrum*, *4*, 1-21.

Ausmees, N., Wahlstedt, H., Bagchi, S., Elliot, M. A., Buttner M. J., Flärdh, K. (2007). SmeA, a small membrane protein with multiple functions in *Streptomyces* sporulation including targeting of a SpoIIIE/FtsK-like protein to cell division septa. *Mol Microbiol.*, *65*, 1458-1473.

Badrinarayanan, A., Reyes-Lamothe, R., Uphoff, S., Leake, M. C., Sherratt, D. J. (2012). In vivo architecture and action of bacterial structural maintenance of chromosome proteins. *Science*, *338*, 528-531.

Badrinarayanan, A., Le, T. B. K., Laub, M. T. (2015). Bacterial chromosome organization and segregation. *Annu Rev Cell Dev Bio.*, *31*, 171-199.

Bao, K., Cohen, S. N. (2001). Terminal proteins essential for the replication of linear plasmids and chromosomes in *Streptomyces*. *Genes Dev.*, *15*, 1518-1527.

Barre, F. X. (2007). FtsK and SpoIIIE: the tale of the conserved tails. *Mol Microbiol.*, *66*, 1051-1055.

Begg, K. J., Dewar, S. J., Donachie, W. D. (1995). A new *Escherichia coli* cell division gene, *ftsK*. *J Bacteriol.*, *177*, 6211-6222.

Bergé, M., Viollier, P. H. (2018). End-in-sight: cell polarization by the polygamic organizer PopZ. *Trends Microbiol.*, *26*, 363-375.

Bentley, S. D., Chater, K. F., Cerdeño-Tárraga, A. M., Challis, G. L., Thomson, N. R., James, K. D., Harris, D.E., Quail, M. A., Kieser, H., Harper, D., Bateman, A., Brown, S., Chandra, G., Chen, C. W., Collins, M., Cronin, A., Fraser, A., Goble, A., Hidalgo, J., Hornsby, T., Howarth, S., Huang, C. H., Kieser, T., Larke, L., Murphy, L., Oliver, K., O'Neil, S., Rabbinowitsch, E., Rajandream, M. A., Rutherford, K., Rutter, S., Seeger, K., Saunders, D., Sharp, S., Squares, R., Squares, S., Taylor, K., Warren, T., Wietzorrek, A., Woodward, J., Barrell, B. G., Parkhill, J., Hopwood, D. A. (2002). Complete genome sequence of the model actinomycete *Stretomyces coelicolor* A3(2). *Nature*, *417*, 141-147.

Bibb, M. J. (2005). Regulation of secondary metabolism in *Streptomycetes*. *Curr Opin Microbiol.*, *8*, 208-215.

Bignell, C., Thomas, C. M. (2001). The bacterial ParA-ParB partitioning proteins. *J Biotech.*, *9*, 1-34.

Bisicchia, P., Steel, B., Debela, M. H. M., Löwe, J., Sherratt, D. (2013). The N-terminal membrane-spanning domain of the *Escherichia coli* DNA translocase FtsK hexamerizes at midcell. *mBio*, *4*, 1-13.

Böhm, K., Giacomelli, G., Schmidt, A., Imhof, A., Koszul, R., Marbouty, M., Bramkamp, M. (2019). Chromosome organization by a conserved condensin-ParB system in the actinobacterium *Corynebacterium glutamicum*. *bioRxiv*, *(Pre-print)*, 1-44, doi: 10 1101/649749.

Brown, P. J., Kysela, D. T., Brun, Y. V. (2011). Polarity and the diversity of growth mechanisms in bacteria. *Sem Cell Dev Biol.*, *22*, 790-798.

Bürmann, F., Sawant, P., Bramkamp, M. (2012). Identification of interaction partners of the dynamin-like protein DynA from *Bacillus subtilis*. *Commun Integr Biol.*, *5*, 362-369.

Cho, H., McManus, H. R., Dove, S. L., Bernhardt, T. G. (2011). Nucleoid occlusion factor SlmA is a DNA-activated FtsZ polymerization antagonist. *Proc Natl Acad Sci U S A.*, *108*, 3773-3778.

de Boer, P. A. (2010). Advances in understanding *E. coli* cell fission. *Curr Opin Microbiol.*, *13*, 730-737.

Dedrick, R. M., Wildschutte, H., McCormick, J. R. (2009). Genetic Interactions of *smc*, *ftsK*, and *parB* genes in *Stretomyces coelicolor*and their developmental genome segregation phenotypes. *J Bacteriol.*, *191*, 320–332.

Ditkowski, B., Troć, P., Ginda, K., Donczew, M., Chater, K. F., Zakrzewska-Czerwińska, J., Jakimowicz, D. (2010). The actinobacterial signature protein ParJ (SCO1662) regulates ParA polymerization and affects chromosome segregation and cell division during *Streptomyces* sporulation. *Mol Microbiol.*, *78*, 1403-1415.

Donovan, C., Schwaiger, A., Kramer, R., Bramkamp, M. (2010). Subcellular localization and characterization of the ParAB system from *Corynebacterium glutamicum*. *J Bacteriol.*, *192*, 3441-3451.

Donovan, C., Sieger, B., Kramer, R., Bramkamp, M. (2012). A synthetic *Escherichia coli* system identifies a conserved origin tethering factor in Actinobacteria. *Mol Microbiol.*, *84*, 105-116.

Donovan, C., Schauss, A., Krämer, R., Bramkamp, M. (2013). Chromosome segregation impacts on cell growth and division site selection in *Corynebacterium glutamicum*. *PLOS One*., *8*, 1-7.

Donovan, C., Bramkamp, M. (2014). Cell division in Corynebacterineae. *Front Microbiol.*, *5*, 1-16.

Du, S., Lutkenhaus, J. (2012). MipZ: one for the pole, two for the DNA. *Mol Cell.*, *46*, 239-240.

Du, S., Lutkenhaus, J. (2017). Assembly and activation of the *Escherichia coli* divisome. *Mol Microbiol.*, *105*, 177-187.

Duan, Y., Huey, J. D., Herman, J. K. (2016). The DnaA inhibitor SirA acts in the same pathway as Soj (ParA) to facilitate *oriC* segregation during *Bacillus subtilis* sporulation. *Mol Microbiol.*, *102*, 530-544.

Errington, J., Bath, J., Wu, L. J. (2001). DNA transport in bacteria. *Nature Rev Mol Cell Biol.*, *2*, 538-545.

Errington, J., Daniel, R. A., Scheffers, D. J. (2003). Cytokinesis in bacteria. *Mol Biol Rev.*, *67*, 52-65.

Errington, J., Murray, H., Wu, L. J. (2005). Diversity and redundancy in bacterial chromosome segregation mechanisms. *Phil Trans Royal Society B., 360*, 497-505.

Flärdh, K. (2003). Growth polarity and cell division in *Streptomyces*. *Curr Opin Microbiol.*, *6*, 564-571.

Flärdh, K., Buttner, M. J. (2009). *Streptomyces* morphogenetics: dissecting differentiation in a filamentous bacterium. *Nature Rev Microbiol.*, *7*, 36-49.

Ginda, K., Santi, I., Bousbaine, D., Zakrzewska-Czerwińska, J., Jakimowicz, D., McKinney, J. (2017). The studies of ParA and ParB dynamics reveal asymmetry of chromosome segregation in mycobacteria. *Mol Microbiol.*, *105*, 453-468.

Goley, E. D., Yeh, Y. C., Hong, S. H., Fero, M. J., Abeliuk, E., McAdams, H. H., Shapiro, L. (2011). Assembly of the *Caulobacter* cell division machine. *Mol Microbiol.*, *80*, 1680–1698.

Gordon, G. H., Wright, A. (2000). DNA Segregation in bacteria. *Annu Rev Microbiol.*, *54*, 681–708.

Gruber S, Errington J. (2009). Recruitment of condensin to replication origin regions by ParB/SpoOJ promotes chromosome segregation in *B. subtilis*. *Cell*, *137*, 685-696.

Hajduka, I. V., Rodrigues, C. D. A., Harry, E. J. (2016). Connecting the dots of the bacterial cell cycle: Coordinating chromosome replication and segregation with cell division. *Sem Cell Dev Biol.*, *53*, 2-9.

Hett, E. C., Rubin, E. J. (2008). Bacterial growth and cell division: a Mycobacterial perspective. *Microbiol Mol Biol Rev.*, *72*, 126–156.

Higo, A., Hara, H., Horinouchi, S., Ohnishi, Y. (2012). Genome-wide distribution of AdpA, a global regulator for secondary metabolism and morphological differentiation in *Streptomyces*, revealed the extent and complexity of the AdpA regulatory network. *DNA Research*, *19*, 259-273.

Hiraga, S., Niki, H., Ogura, T., Ichinose, C., Mori, H., Ezaki, B. (1989). Chromosome partitioning in *Escherichia coli*: novel mutants producing anucleate cells. *J Bacteriol.*, *171*, 1496-1505.

Holmes, N. A., Walshaw, J., Leggett, R. M., Thibessard, A., Dalton, K. A., Gillespie, M. D., Kelemen, G. H. (2013). Coiled-coil protein Scy is a key component of a multiprotein assembly controlling polarized growth in *Streptomyces*. *Proc Natl Acad Sci U S A.*, *110*, 397-406.

Hsiao, N. H., Kirby, R. (2008). Comparative genomics of *Streptomyces avermitilis*, *Streptomyces cattleya*, *Streptomyces maritimus* and *Kitasatospora aureofaciens* using a *Stretomyces coelicolor* microarray system. *Antonie Van Leeuwenhoek*, *93*, 1-25.

Jacob, F., Brenner, S. (1963). On the regulation of DNA synthesis in bacteria: the hypothesis of the replicon. *C R Hebd Seances Acad Sci D.*, *256*, 298-300.

Jakimowicz, D., Gust, B., Zakrzewska-Czerwinska, J., Chater, K. F. (2005). Developmental-stage-specific assembly of ParB complexes in *Stretomyces coelicolor* hyphae. *J Bacteriol.*, *187*, 3572-3580.

Jakimowicz, D., Brzostek, A., Rumijowska-Galewicz, A., Zydek, P., Dołzbłasz, A., Smulczyk-Krawczyszyn, A., Zimniak, T., Wojtasz, L., Zawilak-Pawlik, A., Kois, A., Dziadek, J., Zakrzewska-Czerwińska, J. (2007). Characterization of the mycobacterial chromosome segregation protein ParB and identification of its target in *Mycobacterium smegmatis*. *Microbiology*, *153*, 4050-4060.

Jakimowicz, D., Zydek, P., Kois, A., Zakrzewska-Czerwinska, J., Chater, K. F. (2007). Alignment of multiple chromosomes along helical ParA scaffolding in sporulating *Streptomyces* hyphae. *Mol Microbiol.*, *65*, 625-64.

Jensen, R. B., Lurz, R., Gerdes, K. (1998). Mechanism of DNA segregation in prokaryotes: replicon pairing by *parC* of plasmid R1. *Proc Natl Acad Sci U S A.*, *95*, 8550-8555.

Jensen, R. B., Shapiro, L. (1999). Chromosome segregation during the prokaryotic cell division cycle. *Curr Opin Cell Biol.*, *11*, 726-31.

Jiang, C., Caccamo, P. D., Brun, Y. V. (2015). Mechanisms of bacterial morphogenesis: evolutionary cell biology approaches provide new insights. *Bioessays*, *37*, 413-425.

Kaimer, C., González-Pastor, J. E, Graumann, P. L. (2009). SpoIIIE and a novel type of DNA translocase, SftA, couple chromosome segregation with cell division in *Bacillus subtilis*. *Mol Microbiol.*, *74*, 810-25.

Kaimer, C., Schenk, K., Graumann, P. L. (2011). Two DNA translocases synergistically affect chromosome dimer resolution in *Bacillus subtilis*. *J Bacteriol.*, *193*,1334-40.

Kaiser, B. K., Stoddard, B. L. (2011). DNA recognition and transcriptional regulation by the WhiA sporulation factor. *Nature Sci Rep., 1*, 1-9.

Kois, A., Swiatek, M., Jakimowicz, D., Zakrzewska-Czerwinska, J. (2009). SMC protein dependent chromosome condensation during aerial hyphal development in *Streptomyces*. *J Bacteriol.*, *191*, 310-319.

Larsen, R. A., Cusumano, C., Fujioka, A., Lim-Fong, G., Patterson, P., Pogliano, J. (2007). Treadmilling of a prokaryotic tubulin-like protein, TubZ, required for plasmid stability in *Bacillus thuringiensis*. *Genes Dev.*, *21*, 1340-1352.

Le, T. B. K., Laub, M. T. (2014). New approaches to understanding the spatial organization of bacterial genomes. *Curr Opin Microbiol.*, *5*, 15-21.

Lee, P. S., Grossman, A. D. (2006). The chromosome partitioning proteins Soj (ParA) and Spo0J (ParB) contribute to accurate chromosome partitioning, separation of replicated sister origins, and regulation of replication initiation in *Bacillus subtilis*. *Mol Microbiol.*, *60*, 853-869.

Lesterlin, C., Pages, C., Dubarry, N., Dasgupta, S., Cornet, F. (2008). Asymmetry of chromosome replichores renders the DNA translocase activity of FtsK essential for cell division and cell shape maintenance in *Escherichia coli*. *PLoS Genetics*, *4*, 1-11.

Lim, J. H., Oh, B. H. (2009). Structural and functional similarities between two bacterial chromosome compacting machineries. *Biochem Biophys Res Commun.*, *386*, 415-419.

Liu, G., Draper, G. C., Donachie, W. D. (1998). FtsK is a bifunctional protein involved in cell division and chromosome localization in *Escherichia coli*. *Mol Microbiol.*, *29*, 893-903.

Liu, N., Chistol, G., Cui, Y., Bustamante, C. (2018). Mechanochemical coupling and bi-phasic force-velocity dependence in the ultra-fast ring ATPase SpoIIIE. *eLIFE*, *7*, 1-15.

Livny, J., Yamaichi, Y., Waldor, M. K. (2007). Distribution of centromere-like *parS* sites in bacteria: insights from comparative genomics. *J Bacteriol.*, *189*, 8693-8703.

Lutkenhaus, J., Pichoff, S., Du, S. (2012). Bacterial cytokinesis: From Z ring to divisome. *Cytoskeleton*, *69*, 778-790.

Männik, J., Bailey, M. W. (2015). Spatial coordination between chromosomes and cell division proteins in *Escherichia coli*. *Front Microbiol.*, *6*, 1-8.

Matsuhashi, M., Tamaki, S., Curtis, S. J, Strominger, J. L. (1979). Mutational evidence for identity of penicillin-binding protein 5 in *Escherichia coli* with the major D-Alanine carboxypeptidase IA activity. *J Bacteriol.*, *137*, 644-647.

McCormick, J. R., Su, E. P., Driks, A., Losick, R. (1994). Growth and viability of *Stretomyces coelicolor* mutant for the cell division gene *ftsZ*. *Mol Microbiol.*, *14*, 243-254.

McCormick, J. R., Flärdh, K. (2012). Signals and regulators that govern *Streptomyces* development. *FEMS Microbiol Rev.*, *36*, 206-231.

Mori, H., Kondo, A., Ohshima, A., Ogura, T., Hiraga, S. (1986). Structure and function of the F plasmid genes essential for partitioning. *J Mol Biol.*, *192*, 1-15.

Monteiro, J. M., Pereira, A. R., Reichmann, N. T., Saraiva, B. M., Fernandes, P. B., Veiga, H., Tavares, A. C., Santos, M., Ferreira, M. T., Macário, V., VanNieuwenhze, M. S., Filipe, S. R., Pinho, M. G. (2018). Peptidoglycan synthesis drives an FtsZ-treadmilling-independent step of cytokinesis. *Nature*, *554*, 528-532.

Najjar, N. E., Andari, J. E., Kaimer, C., Fritz, G., Rösch, T. C., Graumann, P. L. (2018). Single-molecule tracking of DNA translocases in *Bacillus subtilis* reveals strikingly different dynamics of SftA, SpoIIIE, and FtsA. *Appl Environ Microbiol.*, *84*, 1-16.

Niki, H., Jaffe, A., Imamura, R., Ogura, T., Hiraga, S. (1991). The new gene *mukB* codes for a 177 kd protein with coiled-coil domains involved in chromosome partitioning of *E. coli*. *EMBO J.*, *10*, 183-193.

Niki, H., Yamaichi, Y., Hiraga, H. (2000). Dynamic organization of chromosomal DNA in *Escherichia coli*. *Genes Dev.*, *14*, 212-223.

Nolivos, S., Sherratt, D. (2014). The bacterial chromosome: architecture and action of bacterial SMC and SMC-like complexes. *FEMS Microbiol Rev.*, *38*, 380-392.

Pettis, G. S., Cohen, S. N. (1996). Plasmid transfer and expression of the transfer (*tra*) gene product of plasmid pIJ101 are temporally regulated during the *Streptomyces lividans* life cycle. *Mol Microbiol.*, *19*, 1127-1135.

Ptacin, J. L., Lee, S. F., Garner, E. C., Toro, E., Eckart, M., Comolli, L. R., Shapiro, L. (2010). A spindle-like apparatus guides bacterial chromosome segregation. *Nature Cell Biol.*, *12*, 791-798.

Quisel, J. D., Grossman, A. D. (2000). Control of sporulation gene expression in *Bacillus subtilis* by the chromosome partitioning proteins Soj (ParA) and Spo0J (ParB). *J Bacteriol.*, *182*, 3446-3451.

Ramirez-Diaz, D. A., Garcìa-Soriano, D. A., Raso, A., Mücksch, J., Feingold, M., Rivas, G., Schwille, P. (2018). Treadmilling analysis reveals new insights into dynamic FtsZ ring architecture. *PLOS Biology*, *16*, 1-20.

Ramamurthi, K. S., Losick, R. (2009). Negative membrane curvature as a cue for subcellular localization of a bacterial protein. *Proc Natl Acad Sci U S A.*, *106*, 13541-13545.

Reyes-Lamothe, R., Nicolas, E., Sherratt, D. J. (2012). Chromosome replication and segregation in bacteria. *Annu Rev Genet.*, *46*, 121-43.

Ruban-Ośmiałowska, B., Jakimowicz, D., Smulczyk-Krawczyszyn, A., Chater, K. F., Zakrzewska-Czerwińska, J. (2006). Replisome localization in vegetative and aerial hyphae of *Streptomyces coelicolor*. *J Bacteriol.*, *188*, 7311-7316.

Salje, J., Gayathri, P., Lowe, J. (2010). The ParMRC system: molecular mechanisms of plasmid segregation by actin-like filaments. *Nature Rev Microbiol.*, *8*, 683-692.

Santi, I., McKinney, J. D. (2015). Chromosome organization and replisome dynamics in *Mycobacterium smegmatis*. *mBio*, *6*, 1-14.

Sharp, M. D., Pogliano, K. (1999). An in vivo membrane fusion assay implicates SpoIIIE in the final stages of engulfment during *Bacillus subtilis* sporulation. *Proc Natl Acad Sci U S A.*, *96*, 14553-14558.

Sharp, M. D., Pogliano, K. (2003). The membrane domain of SpoIIIE is required for membrane fusion during *Bacillus subtilis* sporulation. *J Bacteriol.*, *185*, 2005-2008.

Shen, B., Lutkenhaus, J. (2010). Examination of the interaction between FtsZ and MinCN in *E. coli* suggests how MinC disrupts Z rings. *Mol Microbiol.*, *75*, 1285-1298.

Shrempf, H. (2008). Streptomycetaceae: Life style, genome, metabolism and habitats. *In eLS, (Ed) Chichester John Wiley and Sons Ltd*., *23*, 1-7 doi.

Shwarts, M. A., Shapiro, L. (2011). An SMC ATPase mutant disrupts chromosome segregation in *Caulobacter*. *Mol Microbiol.*, *82*, 1359-1374.

Strakova, E., Bobek, J., Zikova, A., Rehulka, P., Benada, O., Rehulkova, H., Kofronova, O., Vohradsky, J. (2012). Systems insight into the spore germination of *Streptomyces coelicolor*. *Journal of Proteome Research*, *12*, 525-536.

Strahl, H., Errington, J. (2017). Bacterial membranes: structure, domains, and function. *Annu Rev Microbiol.*, *71*, 519-538.

Strunnikov, A. V. (2006). SMC complexes in bacterial chromosome condensation and segregation. *Plasmid*, *55*, 135-144.

Sullivan, N. L., Marquis, K. A., Rudner, D. Z. (2009). Recruitment of SMC by ParB-*parS* organizes the origin region and promotes efficient chromosome segregation. *Cell*, *137*, 697-707.

Surovtsev, I. V., Jacobs-Wagner, C. (2018). Subcellular organization: a critical feature of bacterial cell replication. *Cell*, *172*, 1271-1293.

Thanbichler, M. (2009). Spatial regulation in *Caulobacter crescentus*. *Curr Opin Microbiol.*, *12*, 715-721.

Toro, E., Hong, S. H., McAdams, H. H., Shapiro, L. (2008). *Caulobacter* requires a dedicated mechanism to initiate chromosome segregation. *Proc Natl Acad Sci U S A.*, *105*, 15435-15440.

Toro, E., Shapiro, L. (2010). Bacterial chromosome organization and segregation. *Cold Spring Harb Perspect Biol., 2*, 1-15.

Trojanowski, D., Ginda, K., Pióro, M., Hołówka, J., Skut, P., Jakimowicz, D., Zakrzewska-Czerwińska, J. (2015). Choreography of the *Mycobacterium* replication machinery during the cell cycle. *mBio*, *6*, 1-12.

Tzeng, L., Singer, M. (2005). DNA replication during sporulation in *Myxococcus xanthus* fruiting bodies. *Proc Natl Acad Sci U S A.*, *102*, 14428-14433.

van den Ent, F., Moller-Jensen, J., Amos, L. A., Gerdes, K., Lowe, J. (2002). F-actin-like filaments formed by plasmid segregation protein ParM. *EMBO J*, *21*, 6935-6943.

Viollier, P. H., Thanbichler, M., McGrath, P. T., West, L., Meewan, M., McAdams, H. H., Shapiro, L. (2004). Rapid and sequential movement of individual chromosomal loci to specific subcellular locations during bacterial DNA replication. *Proc Natl Acad Sci U S A.*, *101*, 9257-9262.

Volkov, A., Mascarenhas, J., Andrei-Selmer, C., Ulrich, H. D., Graumann, P. L. (2003). A prokaryotic condensin/cohesin-like complex can actively compact chromosomes from a single position on the nucleoid and binds to DNA as a ring-like structure. *Mol Cell Biol.*, *23*, 5638-5650.

Vollmer, W., Blanot, D., de Pedro, M. A. (2008). Peptidoglycan structure and architecture. *FEMS Microbiol Rev.*, *32*, 149-167.

Walker, J. E., Saraste, M., Runswick, M. J., Gay, N. J. (1982). Distantly related sequences in the alpha- and beta-subunits of ATP synthase, myosin, kinases and other ATP-requiring enzymes and a common nucleotide binding fold. *EMBO J.*, *1*, 945-951.

Wang, S. C., West, L., Shapiro, L. (2006). The bifunctional FtsK protein mediates chromosome partitioning and cell division in *Caulobacter*. *J Bacteriol.*, *188*,1497–1508.

Wang, L., Yu, Y., He, X., Zhou, X., Deng, Z., Chater, K. F., Tao, M. (2007). Role of an FtsK-like protein in genetic stability in *Stretomyces coelicolor* A3(2). *J Bacteriol.*, *189*, 2310-2318.

Wang, X., Liu, X., Possoz, C., Sherratt, D. J. (2006). The two *Escherichia coli* chromosome arms locate to separate cell halves. *Genes Dev.*, *20*, 1727-1731.

Woese, C. R. (1957). Radiation inactivation of *Bacillus megaterium* spores and its interpretation. *Arch Biochem Biophys.*, *74*, 28-45.

Wu, L. J., Errington, J. (1994). *Bacillus subtilis* spoIIIE protein required for DNA segregation during asymmetric cell division. *Science*, *264*, 572-575.

Wu, L. J., Errington, J. (1997). Septal localization of the SpoIIIE chromosome partitioning protein in *Bacillus subtilis*. *EMBO J.*, *16*, 2161-2169.

Yamanaka, K., Ogura, T., Niki, H., Hiraga, S. (1996). Identification of two new genes, *mukE* and *mukF*, involved in chromosome partitioning in *Escherichia coli*. *Mol Gen Genet.*, *250*, 241-251.

Yang, C. C., Huang, C. H., Li, C. Y., Tsay, Y. G., Lee, S. C., Chen, C. W. (2002). The terminal proteins of linear *Streptomyces* chromosomes and plasmids: a novel class of replication priming proteins. *Mol Microbiol.*, *43*, 297-305.

Yang, M. C., Losick, R. (2001). Cytological evidence for association of the ends of the linear chromosome in *Streptomyces coelicolor*. *J Bacteriol.*, *183*, 5180-5186.

Yu, X. C., Weihe, E. K., Margolin, W. (1998). Role of the C terminus of FtsK in *Escherichia coli* chromosome segregation. *J Bacteriol.*, *180*, 6424-6428.

Chapter 2: Genetic Analysis of HfkA, an FtsK-like Protein in Development-Associated Chromosome Segregation

Abstract

The DNA translocase FtsK has been a protein of interest for the last ~30 years is crucial for chromosome segregation and cell division. Highly conserved across different phyla, FtsK belongs to the FtsK/SpoIIIE/Tra family of DNA translocases. These proteins drive segregating DNA towards the correct side of the cell membrane during vegetative septation, sporulation, and conjugation. This family of proteins is also known to share homology with protein translocation motors of type VII secretion systems in bacteria.

In *S. coelicolor*, FtsK is known to play a role in its unique life cycle during development-associated segregation and division. However, an *ftsK* deletion in *S. coelicolor* does not cause an overt phenotype. In this study, a gene encoding a novel FtsK homolog protein Sco4508 was genetically analyzed for functionality during development-associated chromosome segregation. Sco4508 was named HfkA (Homolog of FtsK protein A). An *hfkA* deletion in *S. coelicolor* did not have a segregation defect, however, a *hfkA ftsK* double deletion had a phenotype of 8% anucleate spores. Genetic complementation studies suggest that HfkA and FtsK are redundant in function. Preliminary evidence suggests that the HfkA-EGFP fusion protein weakly localizes only in the absence of a functional FtsK protein in the cell.

A series of other double, triple and quadruple segregation gene mutants were also isolated and phenotypes were analyzed. The Δ*hfkA* Δ*parB* and Δ*hfkA* Δ*smc* double mutants had a similar segregation phenotype to Δ*parB* (11.8%) and Δ*smc* (6.4%) single mutants based on anucleate spores. Of the various triple mutants isolated, Δ*hfkA* Δ*ftsK*

Δ*smc* (16.2%) and Δ*hfkA* Δ*ftsK* Δ*parB* (18.1%) showed heightened segregation defects. The quadruple mutant Δ*hfkA* Δ*ftsK* Δ*smc* Δ*parB* (20%) was viable, and did not show an additive or severe phenotype over a triple mutant strain. Finally, a quadruple mutant (14%) containing a truncated Δ*ftsK'* deletion had a less deleterious effect on segregation relative to the congenic strain with a complete *ftsK* deletion.

Further bioinformatic analysis revealed that HfkA shares considerable homology with another FtsK-like protein (Sco5734, a type VII system secretory protein), which contains conserved structural motifs for protein translocation. This suggests HfkA may also be involved as a type VII secretion system protein in the cell, and this secretion system plays a role in successful chromosome segregation.

INTRODUCTION

Development-associated chromosome segregation in *Streptomyces*

A unique process of development occurs in certain bacteria during which the parent cell differentiates into a different type of daughter cell. When sporulating bacteria like *Bacillus* and *Streptomyces* undergo development, several critical processes like chromosome condensation, partitioning, and segregation occur in a coordinated manner. *Streptomyces* are Gram-positive filamentous soil bacteria, which grow with a unique and complex developmental cycle that synchronizes several cellular processes in a harmonized fashion (Flärdh & Buttner, 2009). During this multifaceted process, other highly regulated activities like antibiotic synthesis and secondary metabolite production also occur (Niu et al., 2016).

Streptomyces species are known to naturally produce a widespread variety of biologically-active compounds, synthesis of which is strictly regulated by complex molecular signals. These compounds are commercially used for pharmaceutical applications such as antibiotics, anti-infection, and anti-cancer drugs, which makes it an organism of interest for laboratories across the world (Bibb, 2005; Hopwood, 2007; McCormick & Flärdh, 2012). The physiological processes leading to production of these compounds are coordinated with the morphological differentiation of the aerial *Streptomyces* filaments. The molecular stimuli triggering these differentiation events are regulated by environmental factors like nutrition and signaling cascades. These cascades are operated by pathway-specific cellular regulatory networks present like *bld* and *whi* genes, which play pivotal roles driving several downstream developmental processes (Chandra & Chater, 2008; McCormick & Flärdh, 2012). Therefore, a key to

understanding secondary metabolic processes and their industrial and medical applications is to closely examine the players involved in these individual cellular events.

S. coelicolor has been studied as a well-established non-pathogenic model for teasing apart genetic configurations during morphological development and differentiation. It has also been used to understand the functional organization and apparatus of disease-causing *Actinobacteria* like *Mycobacterium tuberculosis*, which has similarities to *S. coelicolor* in its cellular constitutions and life cycle. During development, distinct pathways of chromosome replication, condensation, partitioning, and DNA translocation occur in a coherent fashion to advance the cell towards development-associated chromosome segregation. Several proteins are involved during these processes like the chromosome condensation protein SMC, partitioning proteins (ParA and ParB), and DNA translocases (FtsK/SpoIIIE like proteins), which work together in a synchronized fashion to facilitate chromosome segregation (McCormick & Flärdh, 2012). The role of DNA translocases in *S. coelicolor* still remains elusive, and therefore it is necessary to explore further.

DNA translocases are conserved

DNA translocases are commonly found in bacterial cells as FtsK/SpoIIIE-like proteins, which are conserved across prokaryotic phyla, and are known to conduct several cellular functions in different bacterial species. These DNA translocation motor proteins have multifaceted functions within the cell. From replication, to growth, sporulation, chromosome segregation, and cell division, FtsK/SpoIIIE proteins play important specific roles in different model bacteria like *E. coli*, *B. subtilis*, and *S. coelicolor* (Figure 2.1). It was noted that even though SpoIIIE was not required for viability in *B. subtilis*, it was

essential in *E. coli,* and in some other unicellular bacteria like *C. crescentus* (Wang et al., 2007; Lesterlin et al., 2008; Surovtsev & Wagner, 2008).

Structure of DNA translocases

FtsK/SpoIIIE-like proteins have multiple domains in their structure. The N-terminus consists of four transmembrane segments attached to a variable linker region. This cytoplasmic linker domain connects the N-terminal membrane anchor to the C-terminal portion of the protein, which contains an α motor domain, a β ATPase domain, and a γ DNA recognition domain (Figure 2.2) (Massey et al., 2006). Truncation mutations of *ftsK* or *spoIIIE* isolated in different species also elucidated the potential effects of the N-terminus or C-terminus deletions (Wang et al., 2006). The FtsK Orienting Polar Sequences (KOPS) on the DNA provide directionality for DNA transport. The KOPS have a consensus sequence of 5′-GGGNAGGG-3′ in *E. coli* (Sivanathan et al*.,* 2006). In *B. subtilis*, SpoIIIE Recognition Sequence (SRS) has a similar consensus sequence of GAG(C/A)AGGG. These consensus sequences are recognized by the specific amino acid residues in the C-terminal γ domain of FtsK/SpoIIIE to direct DNA translocation (Ptacin et al*.,* 2008).

Mechanism of DNA translocation

After being genetically characterized to play a role in cell division and segregation, FtsK has also been analyzed by crystal structure to propose possible mechanisms for DNA translocation (Massey et al*.,* 2006). Occurring as a multidomain protein, FtsK/SpoIIIE plays a role in cell division, chromosome dimer resolution, chromosome segregation, and membrane fusion. The crystallized FtsK protein from *Psuedomonas aeruginosa* led to an important breakthrough in understanding the

mechanism of FtsK/SpoIIIE-like proteins. It was observed that FtsK monomers oligomerized into a hexameric ring. This assembly is similar to RecA, with the central pore of the hexamer large enough to fit dsDNA through it. Further assays also suggested that it was the C-terminal domains of six membrane-anchored monomeric subunits that came together to form this ring (Figure 2.3) (Massey et al., 2006).

Several models of DNA translocation by FtsK have been proposed. It has been previously determined that DNA translocases can move dsDNA up to the rate of approximately 6.7 kb DNA/second *in vitro*. These values were obtained using measurement of single molecules during translocation, where FtsK followed Michaelis–Menten kinetics (Saleh et al., 2004).

Initially, the movement of DNA was observed to cause a specific conformational change in the cleft between the α and the β domains of the C-terminal portions of the folded protein. When the α domain contacts the DNA backbone, the conformational change leads to ATP hydrolysis, and directs the α domain "jaw" away from the β domain, which causes a propulsion or translocation of the DNA. Different models of movement indicate that this conformational change is initiated due to sequence specificity rendered by the γ domain, which recognizes the KOPS present on the DNA. However, this interdomain movement model could not explain the hexamerization, and the lack of ATP hydrolysis with individual monomers. After further analysis, another rotary-inchworm model was hypothesized, in which the contact of the central channel with dsDNA initiated a conformational change. This change led to ATP hydrolysis during the catalytic cycle of each monomer, and drove DNA translocation to about 1.6 bp/subunit with little net rotation (Massey et al., 2006).

Recent work with single molecule imaging demonstrated that the direction of DNA movement is still an elusive process, and is often dependent on other processes and proteins within the cell. Spontaneous reversal of the direction of dsDNA does not appear to be sequence specific, but can be stoichiometric in nature. It can also be caused due to spontaneous short interactions with large molecules in the cell during translocation, where it is unable to bypass its "roadblock", like other larger proteins or the closing septum (Lee et al., 2014). These mechanisms are likely to differ in different bacterial species due to their differential progression through their respective life cycles. It is important to note that these hypothesized mechanisms can shed light on other unknown functions of FtsK, as well as help identify its functional and structural homologs.

Homologs and orthologs of *ftsK*

Even though a few model prokaryotic species have a single unique FtsK/SpoIIIE-like protein, it is not uncommon for more than one protein to be involved in DNA translocation within the divisome or segregation machinery. In *B. subtilis*, the SpoIIIE DNA translocase works together with another SpoIIIE-like protein SftA for chromosome partitioning during vegetative growth (Biller & Burkholder, 2009). Yet, SpoIIIE works differently than FtsK in *E. coli*, as it is also involved in membrane fusion/fission during sporulation (Kaimer & Graumann, 2011). In *Staphylococcus aureus*, membrane bound ATPases of the FtsK/SpoIIIE family traffic DNA or protein cargo for the type VII secretion systems (Jäger et al., 2016). Therefore, different FtsK/SpoIIIE homologs can be involved in different functions in different bacteria.

Role of FtsK/SpoIIIE in *S. coelicolor*

The product of *ftsK* also plays an important role in chromosome segregation in the *Streptomyces* species. The C-terminal domain of FtsK is known to be involved in DNA translocation, whereas the function of the transmembrane domain of FtsK in *S. coelicolor* is not well understood (McCormick & Flärdh, 2012). Therefore, it is important to note that there are still several uncharacterized and putative FtsK-like proteins, which could be the explain the complexity of chromosome segregation and division in this organism. Most of these structural homologs can be found using genome databases and computational analyses, and can then be further scrutinized genetically for their role in segregation. The goal of this project was to elucidate the role of a novel, previously uncharacterized FtsK homolog (Sco4508), named HfkA (Homolog of FtsK protein A), in *S. coelicolor* with other known proteins like FtsK, SMC and ParB during development-associated chromosome segregation.

MATERIALS AND METHODS

Bacterial strains, media, and growth conditions

The *E. coli* and *S. coelicolor* strains used for in this study are listed in Table 2.1 and Table 2.2, respectively.

E. coli strains were grown under standard conditions in either LB, or SOC media (Sambrook et al., 1989). For selection and plasmid propagation, the media was supplemented with ampicillin (100 μg ml^{-1}), apramycin (50 μg ml^{-1}), carbenicillin (100 μg ml^{-1}), chloramphenicol (25 μg ml^{-1}), kanamycin (50 μg ml^{-1}), hygromycin (50 μg ml^{-1}), spectinomycin (50 μg ml^{-1}), viomycin (30 μg ml^{-1}), or neomycin

(30 μg ml^{-1}) as needed. Competent cells from TG1, BW25113 containing the temperature-sensitive plasmid pIJ790 with arabinose-inducible λ RED genes (Gust et al., 2004), and ET12567 containing the non-transmissible plasmid pUZ8002, (MacNeil et al., 1992 and Kieser et al., 2000) were used for basic plasmid propagation, recombineering and conjugation, respectively. All the cosmids and plasmids used in this study are listed in Table 2.3. Standard techniques were used for plasmid and cosmid purification, preparing chemical and electrocompetent cells, and transformation (Sambrook et al., 1989).

All mutant *S. coelicolor* strains were derived from the wild type strain M145 (Keiser *et al,* 2000). *S. coelicolor* strains were grown under standard conditions on solid media on soy flour mannitol agar (MS), R2YE, or minimal medium (MM), with either 0.5% glucose or 1% mannitol as the carbon source (Kieser et al., 2000). *S. coelicolor* was grown in liquid media in ISP2 or YEME at 30°C (Kieser et al., 2000). For selection, the media were supplemented with antibiotics apramycin (25 μg ml^{-1}), kanamycin (50 μg ml^{-1}), hygromycin (200 μg ml^{-1}), nalidixic acid (20 μg ml^{-1}), spectinomycin (100 μg ml^{-1}), neomycin (10 μg ml^{-1}), or thiostrepton (50 μg ml^{-1}) as necessary.

General DNA techniques

Plasmid purification, agarose gel-fractionated DNA recovery, DNA clean up and concentration kits were used as per manufacturer instructions (Zymo Research Corporation). For purification of total genomic DNA, the Wizard Genomic DNA Purification Kit (Promega) was used. All chromosomal mutations were isolated using PCR-directed mutagenesis (Redirect technology) using the λ RED-mediated recombination using mutagenic linear DNA cassettes in *E. coli* (Gust et al., 2004). For

isolation of complementation strains, protoplasts were prepared and transformed using optimized standard protocols (Kieser et al., 2000).

The enzymes used for restriction digestion were from New England Biolabs. For amplification, *Taq* DNA polymerase (New England Biolabs) and a high fidelity Phusion polymerase (Thermofisher) were used. For sequence verification, standard Sanger sequencing method was used as per the manufacturer's protocol (Applied Biosystems genetic analyzer 3130).

Construction of an *aphI* antibiotic cassette

Due to the large number of strains to be constructed and the limited number of antibiotic deletion cassettes available, an additional selection cassette was designed and constructed for this study. The apramycin-resistance gene of the cassette contained in pIJ773 was targeted by a PCR product of pRA4 (containing a neomycin resistance gene *aphI*), amplified with homology to the sequences flanking the apramycin *orf* using specifically designed oligonucleotides. The recombineering resulted in plasmid pSS34 that precisely replaced the *orf* of *acc(3)IV* with that of *aphI*, which was verified by PCR amplification and Sanger sequencing.

Isolation of null strains for a series of genes

Insertion-deletion mutants were isolated for a series of *hfkA*, *ftsK*, *smc*, *parB* single, double, triple and quadruple mutants, using the *in vivo E. coli* λ Red-mediated recombineering technique. Specific oligonucleotides were designed to amplify various disruption antibiotic cassettes (Table 2.4). These mutagenic PCR products were transformed into the *E. coli* strain BW25113/pIJ790 containing the appropriate cosmid to

create mutant cosmids. These cosmids (Table 2.3) were introduced into the chromosome of *S. coelicolor* strain M145, or its derived mutants, via interspecies conjugation.

Construction of a *hfkA* genetic complementation plasmid

The cosmid containing the wild type copy of *hfkA* was digested with *Eco*RI. The ~8 kb fragment, containing the complete *sco4508* gene, along with genes encoding three upstream small hypothetical proteins (including a type VII cargo protein), and a downstream serine/threonine kinase-encoding gene, was purified. This fragment was ligated in the multiple cloning site of the site-specific integration plasmid vector, pSpc152 (derivative of pSET152 conferring spectinomycin resistance from Dedrick et al., 2009). The resultant plasmid, pSS26 was verified by PCR amplification and partial DNA sequencing. pSS26 was introduced into *S. coelicolor* strains where it integrates by site-specific recombination at the ϕC31 *attB* site (Combes et al., 2002).

Genetic complementation strains:

Genetic complementation with *hfkA*

pSS26, containing the wild type *hfkA,* was transformed into the *E. coli* strain ET12567/pUZ8002, and then introduced into Δ*hfkA* mutant strains via inter-species conjugation. Candidates conferring spectinomycin resistance were selected and propagated. To verify these candidates, specific oligonucleotides annealing within the wild type gene were used for PCR amplification using purified genomic DNA as template. For negative controls, the empty vector pSpc152 was also conjugated, and spectinomycin-resistant candidates were selected and screened using PCR.

Genetic complementation with *parB*

The complementation plasmid for *parB*, pIJ6539 (Kim et al. 2000), was transformed into the donor *E. coli* strain ET12567/pUZ8002, and conjugated into *S. coelicolor* strains, where it integrates at the native location by homologous recombination. Single crossovers were identified by selecting for thiostrepton resistance. The isolated candidates were verified by the PCR amplification of the genomic DNA using oligonucleotides designed to anneal within the wild type gene.

Genetic complementation with *ftsK* and *smc*

The complementation plasmids for *ftsK* (pRMD6) and *smc* (pHW35) were available in the laboratory (Dedrick, 2009). They were obtained from the parent low-copy-number bifunctional plasmid pJRM10 (McCormick & Losick, 1996). These plasmids were introduced into the different *S. coelicolor* M145-derived mutant strains by transformation. This was achieved by preparing and transforming the protoplasts (using standard protocol) of different mutant strains with the pRMD6 or pHW35 plasmid DNA, and selecting with thiostrepton. These thiostrepton-resistant candidates were verified by PCR amplification of the genomic DNA using specific oligonucleotides designed to anneal within the wild type gene. For a negative control, the empty plasmid vector pJRM10 was introduced into *S. coelicolor* mutant strains and selected for thiostrepton resistance and verified using PCR.

Construction of the HfkA-EGFP expressing strain

Oligonucleotides Sco4508egfp FWD57 and Sco4508egfp REV63 were used to amplify and add *hfkA* homology to the *egfp-aac(3)IV-oriT* cassette from the cosmid H24-ParB-EGFP (Jakimowicz et al., 2005). This mutagenic PCR product was transformed into

the *E. coli* strain BW25113/pIJ790/StD35 to construct the *hfkA-egfp* cosmid pSS22. The *acc(3)IV* gene of verified *hfkA-egfp* cosmid pSS22 expressing the C-terminal fusion of HfkA-EGFP was targeted by the *Eco*RI-*Hin*dIII fragment of the pIJ778 (containing spectinomycin resistance) to have a compatible selectable marker. The resultant cosmid pSS28 was verified by PCR and partial sequencing analysis. pSS28 was transformed into the donor *E. coli* strain ET12567/pUZ8002, and introduced into the *S. coelicolor* wild type M145 and Δ*hfkA* Δ*ftsK* (SS5) strains by inter-species conjugation. After homologous recombination, double crossover candidates were selected for spectinomycin resistance and screened for the loss of the cosmid backbone (kanamycin sensitivity). These candidates were verified by PCR amplification of the genomic DNA using oligonucleotides specific to the *egfp* fragment and *hfkA* gene fragment. The HfkA-EGFP protein was expressed in both the strains from its native location as the only source of HfkA.

Fluorescence Microscopy

S. coelicolor strains were prepared for confocal microscopy by pressing a coverslip on the growing solid culture to make impression slides, or by using cover slips that were embedded at a 45° angle in the agar medium, and incubated for different lengths of time so that the strains grown on the cover slip. Methanol (100%) was used to fix the cells before staining and mounting. For nucleic acid staining, the cells were stained and mounted in 0.1% propidium iodide. For unfixed cells, the samples were mounted directly in the standard PBS buffer solution. A TCS SP2 Spectral Confocal Microscope System (Leica) and Nikon A1Rsi microscopes were used for confocal imaging. A Zeiss Axio Observer microscope was used for fluorescent imaging of the

EGFP strains. A Nikon Eclipse E400 phase-contrast microscope was used for phase-contrast microscopy to observe the general morphology of the growing cultures. Volocity Demo program (Perkin Elmer Inc, Version 6.1.1) and Image J (https://imagej.nih.gov/ij/) were used to crop images, optimize contrast, and add scale bars.

Growth curve

A growth curve analysis was conducted to determine the growth trend of *Streptomyces* strains in liquid media. For each strain, 100 µl of pregerminated spores were added to 30 ml of ISP2 media containing a fixed concentration of 3.0 x 10^6 spores ml^{-1}. These submerged cultures were grown in a 30°C shaker at 200 rpm. Absorbance was recorded at 600 nm (OD_{600}) every 6 hours after inoculation for 2 days (48 hours) to observe the general growth rate of the vegetative mycelium. The negative control was uninoculated ISP2 media, and the positive control was the wild type M145 strain. The absorbance values were used to generate a growth curve graph.

Viable and direct cell count

Viability counts of wild type and selected mutant strains were determined using the frozen spore preparations. This was analyzed from prepared serial dilutions by direct counts using phase-contrast microscopy using a hemocytometer. The viable counts were calculated after three days of incubation on SFM agar plates.

Developmental phenotypes

The developmental phenotypes for the wild type and mutant strains of *S. coelicolor* were macroscopically observed by plating the strains on different growth media. SFM, R2YE and minimal media (supplemented with glucose or mannitol) were

used to grow these strains and observe general colony morphology, colony coloration, visible secondary metabolite production, sporulation, and growth rates.

Segregation phenotypes

Segregation analysis was conducted using standard microscopy methods, confocal microscopy and post imaging analyses. For each strain, at least two independent candidates were analyzed. For all the strains, a standard method was used for counting the number of anucleate spores. While conducting imaging of any strain, the number of total spores and anucleate spores were counted manually from one end of the slide to the other. This was done by taking a series of images for each strain, which were then processed using ImageJ and Volocity. Merged images of the fluorescent channel (red propidium iodide) and the DIC channel were obtained. These were then used to count the total spores and anucleate number of spores, for each field of view. The total spores could be counted as all the compartments in the DIC spore chains and the anucleate spores were the empty compartments without any red fluorescent signal.

These strains were also analyzed for general growth characteristics and microscopic morphology. Any unusual observations in the shape and size of the spores, particular pattern of spore chains, clustering of mycelium and rate of sporulation were recorded. All the raw observational values were recorded and analyzed in Microsoft Excel. The percentages, averages, and standard deviations of anucleate spores were calculated and used to generate data graphs.

RESULTS

S. coelicolor possesses a novel uncharacterized FtsK homolog

To understand the lack of severe phenotypes and redundancy in previously characterized segregation mutants of *S. coelicolor*, it was essential to find a new target that could be explored for its role in chromosome segregation. Based on the previously characterized chromosome segregation mutants, ParB and SMC proteins are encoded by unique single copy genes which do not have any homologs in the *Streptomyces* chromosome (Dedrick et al., 2009). This left FtsK to be further analyzed for potential homologs. The *Streptomyces* database contains the sequenced genome of *S. coelicolor*. BLAST analysis conducted using the amino acid sequence of FtsK (SCO5750) as a query, revealed several *ftsK/spoIIIE*-like genes harbored in the chromosome (Table 2.5). The search resulted in four genes based on the percentage of similarity of the C-terminal domain of the FtsK protein to the predicted amino acid sequences of the proteins encoded by *ftsK/spoIIIE*-like genes (Figure 2.4). It was predicted that *sco1805* and *sco5633* encode small Tra-like plasmid transfer proteins (Vogelmann et al. 2011), thereby leaving *sco5734* and *sco4508* as the two likely candidates encoding a putative FtsK-like protein. A *sco5734*-null mutant was analyzed, and it was found that it did not have a genome segregation phenotype (Roman et al., 2010). However, it was shown to be involved in a type VII secretion system in *S. coelicolor*, where the deletion of genes *esxA* and *esxB* (encoding small WXG100 cargo proteins secreted by Sco5734) resulted in a mild segregation defect (Roman et al., 2010). This left *sco4508* as the next potential candidate to be analyzed for its role in chromosome segregation in *S. coelicolor*. This protein had not been previously studied and I analyzed its similarity to FtsK.

I found that *sco4508* encodes a 1526 amino acid putative FtsK/SpoIIIE-like protein. It shares 42% identity and 59% similarity over 502 amino acids of the C-terminal domain of the 467 amino acids of FtsK (amino acids 462 to 929 containing its α, β and γ domains) (Figure 2.5). I also observed that protein Sco4508 had a significantly larger linker and C-terminal domain than FtsK. In particular, the Sco4508 polypeptide also extends 400 amino acids after the homologous region to FtsK.

Using ExPASy tools (TMHMM) for secondary structure and topology prediction, the amino acid sequence of Sco4508 showed two putative membrane-spanning segments. BLAST analysis predicted that a large cytoplasmic portion of Sco4508 contains three repeated ATPase domains at its C-terminus, which is similar to the type VII secretion (T7S) system protein Sco5734. On the chromosome, the monocistronic *ftsK* (*sco5750*) is flanked by *sco5749*, which encodes a transcriptional regulator, and *sco5751*, which encodes a putative membrane protein. In comparison, the location of *sco4508* on the chromosome suggests that it is also a monocistronic gene. It is flanked by a gene encoding a serine/threonine protein kinase (*sco4507*), and a gene encoding a small coiled-coil protein (*sco4509*) on the opposite strand (Figure 2.4). BLAST analysis also predicted that Sco4509 belongs to the WXG 100 family cargo protein for the type VII secretion system. Based on these preliminary primary and secondary sequence analyses, Sco4508 was an appealing target to further scrutinize for its role in the chromosome segregation of *S. coelicolor*. Due to its homology to FtsK, Sco4508 was named HfkA (Homolog of FtsK protein A), and is referred to as such for the rest of this study.

hfkA* is dispensable for the growth and viability of *S. coelicolor

A marked *hfkA* insertion-deletion mutant does not have a developmental phenotype

The cosmid StD35 containing *hfkA* (*sco4508)* was verified, and the gene was successfully replaced with an apramycin-resistance cassette using standard recombineering (Gust et al., 2003). The length of the isolated deletion included the entire *hfkA* gene. The deletion was not expected to be polar because *hfkA* is a monocistronic gene. The mutant cosmid pSS12, containing the apramycin-resistance cassette, was introduced into the *S. coelicolor* wild type strain (M145) by interspecies conjugation using an *E. coli* donor strain. Transconjugants were screened for apramycin resistance and kanamycin sensitivity to identify candidates for double homologous recombination. Genomic DNA was isolated from potential candidates, and six candidates were verified by PCR amplification of a region within the wildtype gene. All six predicted mutant candidates were subsequently analyzed for a macroscopic phenotype on different nutrient media (minimal medium glucose, minimal medium mannitol, R2YE and SFM). All six candidates were also analyzed microscopically for segregation defects by staining nucleoids with 0.1% propidium iodide. The mutant candidates showed an average of 1.2% anucleate spores compared to 1% in the wild type, and the difference is not significant, since a significant difference is usually between 2% - 4% anucleate spores. One verified strain candidate SS1 was used for future genetic constructions. Over 1500 spores of the verified *hfkA* null mutant candidate were measured for at least two independent and reproducible studies.

The unmarked and marked *hfkA* deletion strains display no overt phenotype

Due to a limited number of available antibiotic markers, I also isolated an unmarked for mutant strain *hfkA*. The apramycin-disruption cassette was replaced by an unmarked 81 bp scar sequence using FLP-recombinase, by first removing the antibiotic marker from the cosmid, and then altering the cosmid backbone to make it mobilizable. The PCR-verified cosmid pSS19 was introduced into the wild type M145, and screened for gene conversion events by identifying single crossovers, which were selected for apramycin resistance and kanamycin resistance. These identified single crossover candidates were tested by PCR amplification of the genomic DNA for a gene conversion event at *hfkA*. The candidates that tested positive were further propagated without selection to obtain spore lawns. These spores were then harvested, and a dilution series was prepared for each spore stock to be plated to screen for both apramycin and kanamycin sensitivity, to indicate the loss of the integrated cosmid. Six potential candidates were propagated to be purified and verified using PCR amplification of genomic DNA to isolate the strain SS2. Figure 2.8 shows the differences in the length of the PCR products and the way the oligonucleotides were used to verify deletions. The macroscopic and microscopic phenotype of the unmarked Δ*hfkA*::*frt* was similar to the Δ*hfkA*::*acc(3)IV* and wild type M145 with 1.4% and 1% anucleate spores, respectively (Table 2.6). Over 1500 spores were measured for at least two independent and reproducible studies.

ftsK is dispensable for the growth and viability for _S. coelicolor_

Isolation of a marked *ftsK* insertion-deletion mutant lacks a segregation phenotype

Even though several research groups had previously isolated an *ftsK* deletion exhibiting no segregation phenotype (Wang et al., 2007; Ausmees et al., 2007; Dedrick et al., 2009), I independently re-isolated *ftsK* deletion mutants for this study to be congenic with the other isolated strains. The gene *ftsK* (*sco5750*) is harbored on the cosmid St7C7. The cosmid was used to successfully make an insertion-deletion mutation using standard recombineering, where *ftsK* was replaced by an apramycin-resistance cassette. Like *hfkA*, *ftsK* is also a monocistronic gene, which prevents any polar effects of the mutation. The verified mutant cosmid pSS14 was transformed into the *E. coli* donor strain and conjugated into a *S. coelicolor* wild type strain (M145) via interspecies conjugation. The transconjugant candidates were selected for apramycin resistance and kanamycin sensitivity for double homologous recombination. Six candidates were screened by PCR of the genomic DNA by amplifying the flanking region of the wild type gene. Figure 2.8 shows the differences in the length of the PCR products, and the way the oligonucleotides were used to verify different deletions. The verified candidates were plated on standard sporulation and minimal media to observe the developmental phenotype of the Δ*ftsK*::*acc(3)IV* strain. One verified strain SS3 was also used for microscopic analysis to determine the segregation phenotype. Using nucleic acid staining, an average of 1.5% anucleate spores were observed using confocal microscopy, compared to for the wild type strain (1%) (~1500 spores were counted). This strain was used for the rest of the mutant construction.

Isolation of an unmarked and marked *ftsK* deletion mutant strain does not have an effect on development

Similar to the Δ*hfkA* mutant, an unmarked mutant strain of *ftsK* was isolated due to limited availability of antibiotic markers, by replacing the apramycin-disruption cassette with the unmarked 81 bp scar FLP-recombinase sequence. This was conducted in a two-step process as described above to construct the cosmid pSS17. This cosmid was introduced into the wild type M145 strain via an *E. coli* donor strain, and screened for gene conversion events, by selecting single crossovers that were apramycin and kanamycin resistant. PCR amplification was conducted to verify gene conversion events at *ftsK* using genomic DNA as a template, as previously done for the Δ*hfkA* unmarked mutant (Figure 2.8). The verified candidates were further propagated without selection, by harvesting their spores and plated to select for apramycin and kanamycin sensitivity. Two potential independent candidates were isolated and verified, and one was used for further analysis as SS4. The developmental and segregation phenotype of the strain with an unmarked Δ*ftsK*::*frt* was similar to the strain with the marked allele Δ*ftsK::acc(3)IV*, which has 1.5% anucleate spores. Approximately 1500 spores were measured for at least two independent and reproducible studies.

The *hfkA ftsK* double deletion mutant has a segregation phenotype

To understand the role of HfkA as a putative DNA translocase, I isolated an Δ*hfkA* Δ*ftsK* double mutant. The Δ*ftsK*:*acc(3)IV* mutant cosmid pSS14 was introduced into mutant SS2 (Δ*hfkA*:: *frt*) through interspecies conjugation to isolate a double mutant strain. Transconjugants were then selected for apramycin resistance and kanamycin sensitivity to isolate double homologous recombinants. Four candidates were screened via PCR of the genomic DNA to amplify the mutant gene fragments on the chromosome

to verify deletion for both the genes. A verified candidate SS5 was characterized by analyzing macroscopic (developmental) and microscopic (segregation) phenotypes.

For analyzing the developmental phenotype, the strain SS5 was grown on different nutrient media (minimal medium glucose, minimal medium mannitol, R2YE and SFM). SS5 grew normally on the SFM media, and appeared similar to the wild type and single mutant strains. On R2YE media, it displayed some heterogeneity in colony morphology and secondary metabolite production (Figure 2.9). The segregation phenotype was analyzed by staining the strains with 0.1% propidium iodide, and imaging with a confocal microscope. It was observed that 8% of the ~1500 spores were anucleate (Figure 2.10). This was a more severe phenotype than the individual gene deletion mutants, and is as strong as the segregation defect in Δ*smc* (see below). The phenotype suggests that HfkA might have a role in chromosome segregation by acting as an additional DNA translocase in the cell.

Genetic complementation of the Δ*hfkA* Δ*ftsK* double deletion strain with *hfkA*$^+$ or *ftsK*$^+$ restores proper developmental genome segregation

Genetic complementation studies were conducted on the double mutant strain SS5 using the complementation plasmids pSS26 (*hfkA*$^+$) and pRMD6 (*ftsK*$^+$). The *hfkA* complementation plasmid was introduced in SS5 via inter-species conjugation and selected for spectinomycin resistance. pSS26 integrates at the ϕC31 *attB* site of the *S. coelicolor* chromosome. Candidates were colony purified, and verified using PCR amplification of the genomic DNA to isolate the strain SS10. The *ftsK* complementation plasmid was introduced into the double mutant by preparing and transforming protoplasts of SS5 with pRMD6, and selecting for thiostrepton resistance. pRMD6 is in an

autonomously replicating low-copy-number plasmid derived from SCP2* (McCormick and Losick, 1996). The positive candidates were colony purified and screened by PCR of the genomic DNA to isolate the strain SS12. Negative control strains with the empty vectors pSpc152 and pJRM10, respectively, were also isolated using conjugation and protoplast transformation.

These genetically complemented strains were analyzed for developmental and segregation phenotypes (Figure 2.11). Strains complemented individually with *hfkA*$^+$ and *ftsK*$^+$, showed a correction in the segregation defect close to the single mutant. Compared to the double mutant Δ*hfkA* Δ*ftsK* (8%), the complemented strain Δ*hfkA* Δ*ftsK* /*hfkA*$^+$ showed a 2.4% segregation phenotype (compared to 1.5% in Δ*ftsK*) and Δ*hfkA* Δ*ftsK* /*ftsK*$^+$ had a segregation defect of 1.4% (compared to 1.2% in Δ*hfkA*) (Table 2.6). This indicated that the phenotype was a result of the loss of these two genes, and not an unlinked mutation (Figure 2.11). Together the loss of these gene products had a more significant effect on segregation compared to being deleted individually, and appear to be redundant in function (Figure 2.12). My interpretation is that HfkA could be functioning as an auxiliary DNA translocase in the absence of FtsK, as both HfkA and FtsK were able to genetically complement the segregation phenotype of the double deletion successfully.

Faint HfkA-EGFP foci localize in the predivisional hypha of Δ*ftsK*

If HfkA is a putative DNA translocase, it would be expected to have a similar localization pattern as FtsK. I constructed the *hfkA-egfp* strain SS8 by replacing *hfkA* at its native location on the chromosome with *hfkA-egfp-acc(3)IV-oriT*, such that the fusion gene is the only source of HfkA. However, when investigated using fluorescent

microscopy, unlike a *ftsK-egfp* strain, the *hfkA-egfp* strain did not have any observable EGFP localization patterns at different time points (vegetative, predivisional and sporulating hypha) (data not shown). This could suggest that HfkA-EGFP may not localize into an observable pattern or even be expressed when a functional copy of the native FtsK protein also exists in the cell. I speculated that FtsK could potentially be the primary translocase, and HfkA could be working as a compensating auxiliary translocase only in its absence. As this original fusion strain had a functional copy of *ftsK*, an alternative approach to construct another *hfkA-egfp* strain was tried. A modified *egfp-aadA-oriT* cassette was used to construct a spectinomycin resistant *hfkA-egfp* strain in a Δ*ftsK* mutant background. This SS21 strain (Δ*ftsK hfkA-egfp*) was isolated by introducing the modified *hfkA-egfp* plasmid pSS28 into the *S. coelicolor* Δ*hfkA* Δ*ftsK* double mutant strain SS5. This enabled me to observe the localization of HfkA-EGFP from its native location in the absence of a functional FtsK protein (Figure 2.13). Preliminary analysis of this strain showed weak yet observable EGFP foci in the pre-divisional hypha stage (Figure 2.14). These foci were not visible once sporulation was complete. This suggested that HfkA could be expressed and localizing only in the absence of a functional FtsK protein. However, a Δ*ftsK hfkA-egfp/ftsK*$^{+}$ complementation strain was not constructed to confirm whether these faint HfkA-EGFP foci were a result of the Δ*ftsK* deletion. An Δ*hfkA ftsK-egfp* strain was also not constructed to directly compare the localization of FtsK protein in the absence of HfkA.

When I checked for a segregation phenotype of the Δ*ftsK hfkA-egfp* strain, I observed that the percentage of anucleate spores for this strain (1.9%) was similar to the Δ*ftsK* mutant strain (1.5%). It was also close to the segregation phenotype of the

complementation strain Δ*hfkA* Δ*ftsK*/*hfkA*$^{+}$ (2.4%). This indicated that in addition to giving localization information, the Δ*ftsK hfkA-egfp* strain (SS21) also acted as a genetic complement for the double mutant strain Δ*hfkA* Δ*ftsK* (8%). In SS21, *hfkA* was expressed as *hfkA-egfp* from its native locus on the chromosome, and was able to restore the double mutant segregation phenotype back to the single mutant phenotype, which implies that the fusion protein is functional.

A null deletion of *smc* exhibits an overt segregation phenotype

Previously, *smc* deletions were isolated in *S. coelicolor* by traditional cloning methods where most of the *smc* gene was replaced by a hygromycin or apramycin resistance-cassette (Dedrick et al., 2009; Kois et al., 2009). An independent *smc* insertion-deletion mutant was isolated for this study for marker compatibility, and to be congenic with the other strains. The *smc* gene (*sco5577*) is harbored on cosmid SC7A1. The cosmid was used to successfully make an insertion-deletion mutant by recombineering to delete the entire *smc* gene, and it was replaced by a hygromycin-resistance cassette from plasmid pIJ10700. The verified mutant cosmid pSS33 was transformed into the *E. coli* donor strain and introduced into the *S. coelicolor* wild type strain (M145) via interspecies conjugation. The transconjugant candidates were selected for hygromycin resistance and kanamycin sensitivity for double homologous recombination. Three candidates were screened by PCR of the genomic DNA by amplifying the flanking region of the wild type *smc* gene. The verified strain SS66 was also used for microscopic analysis to determine the segregation phenotype of 6.4%, that was similar to the previously isolated mutants, which had 7% anucleate spores (~1200 spores were measured) (Figure 2.16). The strain was complemented using the *smc*$^{+}$

plasmid pHW35 and the segregation defect was reduced to 1.7%, which is consistent with previously isolated data by Dedrick et al. (2009). This indicated that the segregation phenotype was a result of the *smc* deletion, and it when it was genetically complemented, the segregation phenotype reverted back to wild type.

A null deletion of *parB* confirms a prominent segregation phenotype

Previously, a *parB* deletion was isolated in *S. coelicolor* where the *parB* gene was replaced by an unmarked 81 bp scar (Kim et al., 2000). To isolate a compatibly marked insertion-deletion of *parB* for the current mutant series, a new *aphI* deletion cassette was constructed (pSS34). This cassette was targeted to the *parB*-harboring cosmid H24 by standard recombineering. An additional step was conducted first by changing the backbone resistance marker (*aphII*) on cosmid H24. This gene confers kanamycin resistance and neomycin resistance for the wildtype *ParB* cosmid H24, and *aphII* was changed using the spectinomycin-resistance gene *aadA* by recombineering. This resulted in pSS35, which was targeted subsequently by the neomycin-deletion cassette (pSS34) to obtain the *parB* mutant cosmid pSS36, which was Δ*parB*::*aphI* (neomycin resistant) (Figure 2.15). Cosmid pSS36 was conjugated into the *S. coelicolor* wild type strain (M145) via interspecies conjugation. The transconjugant candidates were selected for neomycin resistance and spectinomycin sensitivity for double homologous recombination. Three candidates were screened by PCR of the genomic DNA by amplifying the flanking region of the wild type *parB* gene. The verified mutant strain SS68 was analyzed for a segregation phenotype, and it showed 11.8% anucleate spores. When this mutant was complemented with $parB^{+}$, it had 2.90% anucleate spores, which is consistent with the previously isolated mutant and complemented strains (Dedrick et al.,

2009). This indicates that the segregation phenotype was a result of the *parB* deletion, and when it was genetically complemented, the phenotype reverted close to the wild type strain. Therefore, *parB* was the most important gene tested in this study, as loss of this gene caused the highest segregation defect amongst all the other genes studied.

Isolation of a series of double deletion mutants shows a higher segregation defect phenotype but does not affect growth and viability

Using the mutant cosmids and single deletion strains, I isolated a series of double mutant strains and genetically complemented them to analyze segregation phenotypes (Table 2.8).

Isolation of Δ*hfkA* Δ*parB,* Δ*hfkA* Δ*smc,* Δ*ftsK* Δ*parB,* Δ*ftsK* Δ*smc* and Δ*parB* Δ*smc* double mutant strains

Double deletions were isolated using the Δ*hfkA*::*acc(3)IV* mutant cosmid, pSS13, and Δ*ftsK*::*acc(3)IV* mutant cosmid, pSS15, by introducing them into the *S. coelicolor* Δ*parB* strain J3305 and Δ*smc* strain HJ2 via interspecies conjugation. The transconjugants were selected for apramycin resistance and kanamycin sensitivity and verified using PCR amplification of the specific gene, *hfkA* or *ftsK*.

Δ*hfkA* Δ*parB* was named SS22, and it showed a segregation defect of 13.4% anucleate spores, which was successfully complemented by $parB^{+}$(2.30%). Complementation with $hfkA^{+}$ did not have a major effect on the mutant phenotype, and the complemented strain had 12.1% anucleate spores, which is similar to the Δ*parB* single mutant phenotype (11.8%). This indicated that the loss of HfkA in the cell did not cause a severe segregation phenotype to a strain already lacking ParB (Figure 2.16).

Similarly, the Δ*hfkA* Δ*smc* double deletion was observed to have a segregation defect of 7.60% and a normal developmental phenotype (Table 2.7). Genetic complementation of this double mutant with *smc*$^+$ led to the restoration of the segregation phenotype back to nearly wild type (1.70%). Complementation with *hfkA*$^+$ did not have any effect on the mutant phenotype, and there were 6.8% anucleate spores observed, similar to the Δ*smc* mutant phenotype. This indicated that the loss of HfkA did not cause an overt phenotype in the cell already lacking SMC.

The Δ*ftsK* Δ*parB* double deletion strain contained a complete deletion of both genes. The strain appeared similar to the wild type strain during its development on solid media. A segregation phenotype of 14.10% anucleate cells was observed for this mutant, which was complemented by *parB*$^+$ (2.8%). Complementation with *ftsK*$^+$ did not have any effect on the mutant phenotype, and there were 13.6% anucleate spores observed, which was similar to the Δ*parB* mutant phenotype (11.8%). This indicated that a complete loss of FtsK does not cause an overt phenotype in the cell already lacking ParB.

Similarly, the Δ*ftsK* Δ*smc* mutant strain was isolated containing complete deletions of both genes (Figure 2.16). The developmental phenotype of the strain appeared like the wild type strain and it showed an 8.3% segregation defect, which was similar to the segregation defect caused by a single Δ*smc* deletion strain (6.7%). This phenotype was rescued by genetic complementation of the double mutant by *smc*$^+$ to 2.10% (similar to 3% as observed in the Δ*smc/smc*$^+$ complementation strain), and complementation by *ftsK*$^+$ did not have any effect on the mutant phenotype (Table 2.8).

This also indicates that *S. coelicolor* can segregate DNA in a reliable fashion, whether one or two key genes are deleted. However, it was observed that in a double

mutant like Δ*parB* Δ*smc,* a higher segregation defect of 18.8% was observed, which was partially complemented by *parB*$^+$ (5.6%) and *smc*$^+$ (14.6%). This was consistent with the previously isolated strain by Dedrick et al. (2009), where the Δ*parB* Δ*smc* mutant had a high segregation defect of 24%. Based on previous observations and my own research, it can be implied that certain proteins in the segregation machinery have a more central role, like ParB and SMC, and deletion of the genes encoding those proteins together, causes a much higher segregation defect than the deletion of other genes like *ftsK* and *hfkA*.

Isolation of a series of triple and quadruple deletion mutants shows an additive effect on developmental phenotypes but it does not affect growth and viability

As discussed in the previous sections, the single mutants Δ*parB* and Δ*smc* display a segregation defect of 11.8% and 6.4% anucleate spores, respectively. When these deletions are combined, a Δ*parB* Δ*smc* double mutant displays a higher segregation phenotype of 18.8%, which appears to be additive of the two individual mutations. This could indicate that the two genes are working in series within the cell. In comparison, the Δ*hfkA* and Δ*ftsK* single mutants each have a segregation phenotype of 1% anucleate spores. However, the double mutant Δ*hfkA* Δ*ftsK* showed a higher segregation phenotype of 8%. Hence, it could be implied that these two genes were working together in parallel, and not in series. This caused an increased segregation phenotype, which is not directly additive of the individual deletions of *hfkA* and *ftsK*.

I determined that the next step was to test if the segregation defect values were consistent when these double deletions (Δ*parB* Δ*smc* and Δ*hfkA* Δ*ftsK)* were combined

with other genes, or if there were any more unique deviations from these results. Consequently, I isolated a series of triple and quadruple deletion strains.

The triple deletion strains Δ*hfkA* Δ*ftsK* Δ*smc* (SS25) and Δ*hfkA* Δ*ftsK* Δ*parB* (SS39) were isolated by using the Δ*smc*::*hyg* mutant cosmid pSS31, and the Δ*parB*::*aphI* mutant cosmid pSS36, respectively. These cosmids were conjugated into the double mutant strain Δ*hfkA* Δ*ftsK* strain SS5, and selected for hygromycin and neomycin resistance, respectively. These mutant strains showed normal growth on solid media and were then analyzed for their segregation phenotypes.

The segregation defect of the Δ*hfkA* Δ*ftsK* Δ*smc* triple mutant appears to be additive (16.2%) of the Δ*hfkA* Δ*ftsK* double mutant (8%) and Δ*smc* mutant (6.4%) segregation phenotypes. Each wild type gene alone can partially complement the phenotype almost back to the double or single mutant phenotypes (Figure 2.19(c)). Therefore, the effect observed in the triple mutant strain is the result of the deletion of these genes, and not an unlinked mutation.

Similarly, the Δ*hfkA* Δ*ftsK* Δ*parB* triple mutant was determined to have a segregation defect of 18.1%, and shows additive properties of the Δ*hfkA* Δ*ftsK* double mutant (8%) and Δ*parB* mutant (11.8%) segregation phenotypes. Genetic complementation with $parB^{+}$ partially rescued the segregation defect to 5.4% anucleate spores, which was close to the Δ*hfkA* Δ*ftsK* double mutant phenotype (8%). Like the Δ*smc*-containing triple mutant, this also indicates that the effect of the deletion of *parB* was additive to the segregation defect of the Δ*hfkA* Δ*ftsK* mutant (Figure 2.19(d)).

The two other triple mutants Δ*ftsK* Δ*smc* Δ*parB* (SS51) and Δ*hfkA* Δ*smc* Δ*parB* (SS40) were also isolated in a similar fashion and analyzed for segregation (Table 2.8).

There were no significant deviations in the percentage of anucleate spores of SS51 and SS40 triple mutant strains when compared to the Δ*parB* Δ*smc* double mutant. This demonstrates that the loss of *parB* and *smc* together causes the highest segregation defect seen so far, hence playing a pivotal role during chromosome segregation.

Subsequently, I wanted to observe the effect of all the four deletions combined together in a quadruple mutant. A Δ*hfkA* Δ*ftsK* Δ*smc* Δ*parB* quadruple deletion strain was isolated for this study (Figure 2.18). This strain was isolated by conjugating the Δ*parB*::*aphI* mutant cosmid pSS36 into the *S. coelicolor* triple mutant Δ*hfkA* Δ*ftsK* Δ*smc* strain SS25, resulting in strain SS56. This mutant strain appeared to grow normally on solid media and was then analyzed for segregation.

The segregation defect of the Δ*hfkA* Δ*ftsK* Δ*smc* Δ*parB* quadruple mutant (20% anucleate spores) does not show additive properties of the previously shown Δ*hfkA* Δ*ftsK* (8%) and Δ*parB* Δ*smc* (18.8%) double mutant strains. The additive effect should have been higher (~27%) than what was observed (20%). This could indicate that ParB and SMC play a significant role during segregation, unlike other proteins such as FtsK and HfkA. I found that this defect could not be genetically complemented with either $hfkA^+$ or $ftsK^+$ (they might be complementing up to a 1% defect on their own). Also, this strain was complemented by $parB^+$ (13.8%) and smc^+ (14.2%) similar to a triple mutant phenotype, hence suggesting that this defect is mainly caused due to the deletion of *parB* and *smc* (Figure 2.19(e)).

Isolation of a quadruple deletion mutant containing a truncated *ftsK'* allele displays a unique and less severe segregation phenotype

Given the results observed so far, which show the marginal effects of a complete *ftsK* deletion, I wanted to collect additional data using a previously published truncated deletion of *ftsK'* (Dedrick et al., 2009). This truncated *ftsK'* allele contained a C-terminal truncation (where one membrane spanning domain, the linker domain and the DNA motor domain of FtsK were deleted), and it showed a higher segregation defect of 15% anucleate spores. Based on results from this study, it was indicated that a complete deletion of *ftsK* has a different segregation phenotype than its truncated version, which is much more severe than a complete *ftsK* deletion.

A previously isolated double mutant Δ*ftsK'* Δ*parB* exhibited a phenotype of 13%, which could not be genetically complemented with either a copy of *parB* or *ftsK*. This could be explained by the segregation defects of the individual Δ*parB* (12%) and Δ*ftsK'* (15%) mutants, and how a strain containing a truncated deletion of *ftsK'* had a similar phenotype to a Δ*parB* mutant. Similarly, the Δ*ftsK'* Δ*smc* deletion displayed a segregation phenotype of 13%, which was also not additive of the individual defects of the truncated Δ*ftsK*' mutant (15%) and the Δ*smc* mutant (7%). However, a Δ*ftsK'* Δ*smc* Δ*parB* triple mutant RMD6 was found to have a segregation defect of only 10%, which was unusual as it was less than the segregation defects observed for the individual *ftsK'* and *parB* deletions (Dedrick et al., 2009).

Due to the unique characteristics of this *ftsK'* mutant, I wanted to combine it with this study to see if there were any significant differences observed in the segregation phenotypes when the *hfkA* deletion was added to the previously isolated

Δ*ftsK'* Δ*smc* Δ*parB* mutant. The Δ*hfkA* Δ*ftsK'* Δ*smc* Δ*parB* quadruple strain (SS63) was constructed by conjugating a newly constructed Δ*hfkA*::*vph* mutant cosmid pSS38 into the existing *S. coelicolor* triple mutant Δ*ftsK'* Δ*ftsK* Δ*smc* strain RMD6 (Dedrick *et al*. 2009), which contained a truncated deletion of *ftsK'*. The Δ*hfkA* Δ*ftsK'* Δ*smc* Δ*parB* mutant strain grew robustly unlike the previously isolated triple and quadruple mutants, and had a segregation defect of 14% (Figure 2.18). Although this was lower than the quadruple mutant SS56 with a complete deletion of *ftsK* (20.0%), the phenotype of this strain was similar to the Δ*ftsK'* Δ*smc* Δ*parB* phenotype (11.02%). This defect was not genetically complemented by *hfkA*$^{+}$, and was slightly exacerbated when complemented by a copy of *ftsK*$^{+}$ (15.6%), indicating that *ftsK*$^{+}$ is dominant to *ftsK'*. It can be inferred that the truncated version of Δ*ftsK'* somehow positively affects chromosome segregation by an unknown mechanism and could potentially interact with or involve other cellular proteins as players during this process. This could lead to future investigation of known and novel target proteins and their potential role in segregation.

Deletion of segregation genes does not affect vegetative growth and viability

Most of the strains in Table 2.7 were also analyzed for vegetative growth in liquid media. A growth curve was generated by measuring OD_{600} (Figure 2.20) and suggests that these deletions do not affect vegetative growth or sporulation. Even though a slight delay in the exponential phase was observed for certain mutant strains, all strains were able to accumulate to the same amount by 48 hours (during the log phase).

I also wanted to look at the spore viability of these selected strains (Table 2.7) as some of their segregation defects were as high as 20% anucleate spores. The spores were directly counted using serial dilutions by phase-contrast microscopy, and plated for viable

count on SFM media. Spores of the wild type strain were 60.5% viable. As expected, all the single and double mutants had similar viability. However, interestingly all triple and quadruple mutant spores were ~42% viable. This could be explained as the difference in viability between these mutants and wild type (~18% out of 60.5%) is roughly equal to the observed segregation defect (20% anucleate spores) as reported in the earlier sections, and those spores didn't have the genetic material to further propagate. This indicated that with the segregation defect of ~20% ($1/5^{th}$ of all spores), the spores only lose their viability by less than 2-fold compared to the wild type strain. These values suggest that these deletions do not impact growth and viability of *S. coelicolor,* which is unlike other organisms, where the viability drops by several logs or even becomes a synthetic lethal when any of these key genes is deleted.

Altogether, the results from this study indicate that *hfkA* is not a central DNA motor for chromosome segregation in *S. coelicolor*. The most severe segregation phenotypes were mainly caused by deleting the *parB* and *smc* genes. These genes encode a partitioning system protein, and a chromosome condensation protein, respectively. Both *ftsK* and *hfkA* are individually dispensable during segregation and there is an unknown function of the truncation deletion of *ftsK* that has a less severe effect on segregation (only in the presence of other deletions). This suggests that there are still unknown targets of segregation proteins which need to be explored for playing a significant role in chromosome segregation.

DISCUSSION

S. coelicolor has distinct proteins in the cell that conduct several overlapping events during prokaryotic developmental genome segregation. Based on previous research, it has been proven that the SMC protein is involved in the restructuring and condensation of the replicated genome along with its accessory proteins ScpA and ScpB (Dedrick et al., 2009; Kois et al., 2009). It is now also known that a ParABS chromosome partitioning system exists in *S. coelicolor,* where ParB binds to the condensed DNA at the *parS* sites near its *oriC*, which is spatially oriented with the help of a Walker-type ATPase protein ParA (Kim et al., 2000; Jakimowicz et al*.,* 2007). In order to complete chromosome segregation, the DNA translocase motor FtsK is employed by the cell to efficiently move the genome to the daughter cells (Wu and Errington; 1994; Wang et al., 2007; Kois et al., 2009).

Different research groups have observed that the deletion of these genes has a varying effect on the segregation phenotype. A *parB* mutant has a segregation defect of 13% anucleate spores, the *smc* mutant has a defect of 7% anucleate spores, which is higher and more significant than an *ftsK* mutant that has a segregation phenotype of 1% anucleate spores. When any two of these genes were deleted at a time, the mutations had an additive effect on the phenotype, where the segregation defect (% anucleate spores) was roughly equal to the sum of individual mutations. The triple deletion strains exhibited segregation phenotypes which were similarly additive in nature, and did not cause a severe increase in the anucleate spores. Yet in each case, the strains were viable and able to segregate their genomes to a sufficient degree unlike being synthetically lethal or synthetic sick. This redundancy and lack of a very strong phenotype (for the

triple mutants) in the genome segregation machinery raised the question of finding new targets to explore for a role in chromosome segregation. It has been known that the *S. coelicolor* genome contains several *ftsK*-like genes, and these homologs are therefore the next likely targets for investigation. Certain proteins like SmeA (Sco1415), a small membrane protein and SffA (Sco1416), an FtsK/SpoIIIE-like protein, were analyzed for their hypothesized role in segregation as putative DNA translocases (Ausmees et al., 2007). These proteins were identified as targets of regulatory proteins like WhiH in *S. coelicolor*, and WhiAB in *S. venezuelae* to form a novel sporulation locus on the chromosome. A Δ*smeA-sffA* deletion mutant was isolated, and observed to have a mild segregation defect of 0.6% anucleate spores (compared to 0.1% anucleate spores in the wild type strain). Upon further experimentation, it was determined that even though the double deletion did not seem to affect segregation even mildly, localization of SffA was SmeA-dependent, and their deletion had a pleiotropic effect on the entire sporulation process. It was also concluded that SffA does not have a DNA translocase function, but a different unknown role in sporulation (Ausmees et al., 2007).

This study examined the role of a previously uncharacterized homolog of FtsK in *S. coelicolor*. The sequence alignment and homology of the protein Sco4508 suggested it could be a putative FtsK-like DNA translocase. It was predicted to contain two N-terminal membrane spanning segments and a C-terminal ATPase domain similar to FtsK. Sco4508 was designated as HfkA (Homolog of FtsK protein A), and hypothesized to operate as a FtsK-like protein during chromosome segregation. During genetic analysis it was shown that an Δ*hfkA* mutant did not have an overt effect on segregation, and it showed 1% anucleate spores (similar to the wild type strain). However, when analyzed

together, an Δ*hfkA* Δ*ftsK* double mutant exhibited a very mild yet observable segregation phenotype of 8% anucleate spores, which is similar to the segregation phenotype of a Δ*smc* mutant (~7% anucleate spores).

Upon genetic complementation of the Δ*hfkA* Δ*ftsK* double mutant, when either of the two genes were individually complemented, the segregation phenotype was recovered back to wild type. Preliminary localization studies suggested that HfkA-EGFP might only localize in the absence of the wild type FtsK protein. This revealed that even though these two genes were potentially redundant in function, HfkA could possibly be working as a secondary translocase in the cell in the absence of FtsK, and hence rescuing the segregation pathway. One of the models that could be postulated on how this may occur is if the levels of HfkA are upregulated in an Δ*ftsK* background, this could increase the expression of HfkA in the cell. The HfkA monomers could oligomerize during segregation and translocate the DNA directly in an FtsK-like fashion, or indirectly by acting as an auxiliary protein and supporting DNA translocation assisted by other unknown cellular proteins.

In other species like *Staphylococcus aureus* and *B. subtilis*, it has been observed that secondary translocases do exist and often work using independent pathways. The two homologs FtsK and SpoIIIE in *S. aureus* work independently, where SpoIIIE drives translocation in the cells advancing towards septation, and does not require FtsK. However, when both these genes are deleted, it has a three times higher segregation phenotype (0.9% anucleate cells) compared to wild type (0.3%) of the replicated nucleoids (Veiga et al., 2017). This was reminiscent of the segregation defect observed in this study, where the double deletion of the two translocases causes a marginal, yet higher

segregation defect (8% anucleate cells), which is 8-fold compared to wild type (1%). This could provide an explanation for why more than one translocase often exists within the cell. In *S. coelicolor*, HfkA could be acting as an auxiliary translocase indirectly interacting with the segregation machinery of the cell, which does not need FtsK to function. Yet when both *hfkA* and *ftsK* are deleted, it causes a mild segregation phenotype.

It is remarkable to observe that several segregation mutants isolated for other bacterial species have little to mild phenotypes in *S. coelicolor*. Loss of these vital chromosome segregation genes in other bacteria (*ftsK* in *E. coli* and *smc spoIIIE* in *B. subtilis*) leads to synthetic lethal phenotypes with log drops in anucleate and viable cells. However, in *S. coelicolor*, only a 10-fold decrease is observed in anucleate cells. One of the hypotheses that could explain this is the redundancy of the *S. coelicolor* genome which could exist since it grows as a syncytium. This multicellular organism has developed complex redundant pathways to ensure proper chromosome management and cell survival. These pathways could be working in coordination, or independently as parallel circuits with overlapping functions.

ESX/type VII secretion modulates development

Another FtsK-like protein in *S. coelicolor*, Sco5734, has been characterized as a type VII secretion system protein (Roman et al., 2010). Therefore, it was worth exploring to see if HfkA also had characteristics to function as a putative secretory protein, which if lost could cause developmental effects, including segregation.

Secretion systems exist in bacteria to effectively interact with their environment by protein export through their complex cell envelope, and their role has been

investigated in physiology, virulence and pathogenicity. Previously discovered and studied secretion systems in gram-negative bacteria like *E. coli*, are type I-VI. The discovery of these secretion systems transformed the field of host-pathogen interaction research. The type VII secretion (T7S) systems were initially discovered in gram positive bacteria in both high GC *Actinobacteria* (*Mycobacterium*), and low GC *firmicutes* (*Bacillus*) species. The components of this system are characterized into two main categories, the Esx proteins, common in both *Actinobacteria* and *Firmicutes*; and PE and PPE proteins, which are *Mycobacterium* specific (Ates et al., 2016). The multiple T7S systems discovered in *M. tuberculosis* were designated Esx-1 to Esx-5, which all have their respective secretory components. The proteins forming this system are well studied, and are known to consist of a membrane complex and T7S substrates. The membrane complex protein EccC has been identified as the hallmark player in secretion, and is conserved across *Mycobacterium* and *Firmicutes* (Ess proteins in *S. aureus*). These proteins are predicted to have transmembrane domains with two membrane spanning segments, and three nucleotide binding domains (NBD), containing Walker A and Walker B boxes. These proteins show homology to several FtsK/SpoIIIE ATPases found in the cell. It has been predicted that these Ecc proteins also form hexameric ring structures like FtsK/SpoIIIE proteins (Ates et al., 2016; Bottai et al., 2016; Unnikrishnan et al., 2017). The most well studied are the EsxA and EsxB substrates of the Esx-1 T7S system.

In *B. subtilis*, *yuk/yue* locus codes for a non-essential Esx system. This locus contains several *yuk* genes involved in the T7S system. YukBA is homologous to EccC in *M. tuberculosis,* and is an FtsK/SpoIIIE family ATPase. This YukBA protein is necessary

for the secretion of the substrate YukE. However, the loss of this locus did not seem to have any effect on the growth and development of the cell (Huppert et al., 2014).

In *Streptomyces* species, a T7S system at the *esx* locus has been identified and investigated for secretory function. In *S. scabies*, the EccC protein secretes EsxA and EsxB. However, in this case, instead of affecting virulence, this secretion system plays a role in development causing a delay in sporulation and the formation of abnormally shaped spore chains (Fyans et al., 2013). Similarly, in *S. coelicolor*, the Esx system was characterized to have two secreted proteins EsxA and EsxB. An *esxAB* deletion in *S. coelicolor* caused developmental aberrations like delayed sporulation, abnormal spore size and nucleoid density. The *ftsK/spoIIIE*-like gene *sco5734* was characterized as a component of the Esx system. Disruption of this gene caused no effect on sporulation in *S. coelicolor* (Roman et al., 2010). As mentioned previously, a phylogenetic alignment between Sco5734 and HfkA reveals homology shared between the amino acid sequences of these two proteins (Figure 2.22). Even though HfkA has not been previously characterized as a secretion system component, it has a remarkable similarity to Sco5734 amino acid sequence, indicating that there may be another T7S system in *S. coelicolor* which has not been discovered, and HfkA could be an EccC-like protein with all the characteristics of an Esx-system membrane complex.

However, it can also be observed that HfkA, though similar to Sco5734, has certain distinctions within its structure. Like Sco5734, HfkA contains three Walker A boxes within its C-terminal domain. These Walker A boxes are conserved sequences within the protein that can form three-dimensional structures, and interact with ATP. In two out of the three Walker A boxes, HfkA contains an arginine (R) in place of a lysine

(K) in Sco5734, which signifies the uniqueness of this locus as this lysine residue is known to be important for nucleotide binding (Figure 2.22). The presence of arginine in place of lysine could potentially alter the structure, folding, and thus function of HfkA, which can lead to loss or gain of functional properties of HfkA within the cell as compared to Sco5734. This could imply despite the similarities, HfkA and Sco5734 may not have identical functions in the T7S system.

It is also known that in non-pathogenic bacteria, secretion system proteins conduct developmental functions, which could account for the segregation phenotype observed in Δ*hfkA* Δ*ftsK*. It can therefore be postulated that even though HfkA shares homology with FtsK, it is a part of an unknown T7S system (Figure 2.21). It can further be seen that the gene *sco4509*, which encodes a putative T7S system WXG100 cargo protein, flanks the *hfkA* locus. This locus is found in a unique region of the *S. coelicolor* genome, which is not conserved in other species like *Streptomyces venezuelae*. This region of the chromosome is also known as a plasticity island, where genes performing a broad array of functions can evolve and rearrange to adapt to the environment. It could explain why genomes of only some species contain these regions, and they are not widely present in many *Streptomyces* species.

These observations could thereby also indicate that the segregation defect shown in this study could only be a secondary and indirect function of HfkA. It can be hypothesized that HfkA is primarily a putative and uncharacterized EccC-like T7S system component, secreting a protein in the extracellular space that plays a role in chromosome segregation.

Models for DNA segregation

Based on the different aspects of DNA segregation explored in this study, and the roles of DNA translocases, I propose different mechanisms for efficient chromosome segregation during development in *S. coelicolor*.

Considering the Δ*hfkA* Δ*ftsK* mutant phenotype, and the preliminary weak localization of HfkA-EGFP in a Δ*ftsK* background, one of the models I suggest is that HfkA works as an auxiliary DNA translocase in the cell. I presume that it is expressed and is functional only in the absence of FtsK, although this was not measured. This could indicate that there is competition between FtsK and HfkA, where FtsK is primarily expressed, and functions as the main DNA motor.

It is also conceivable that since FtsK is dispensable for growth and segregation in *S. coelicolor* (according to this study as well as three previous studies), an essential DNA motor protein is yet to be identified, which could be the linchpin holding the entire segregation machinery together. This motor would have to look unlike the typical DNA motors.

According to the sequence alignment of HfkA, it shares homology with the T7S protein Sco5734 and therefore could be a potential motor translocating either DNA or protein. This can be supported by the presence of Sco4509 (a predicted cargo protein) and represent synteny between these two chromosomal loci. If HfkA is a protein motor, it could be postulated that instead of directly translocating the DNA, HfkA interacts with the terminal proteins at the end of the linear *S. coelicolor* chromosome. It is known that the Telomere-associated proteins (Tap) are covalently bound to the 5' overhangs of the linear replicons (Bao and Cohen, 2003). These terminal proteins could be potentially

interacting via protein-protein interactions with an existing protein motor (HfkA) in the cell, to drive translocation of the chromosome indirectly. It can be hypothesized that HfkA is a bifunctional motor in the cell working to ensure proper translocation of protein or DNA as needed, perhaps by possessing different Walker A boxes for each function.

HfkA could also be mitigating segregation by providing a structural anchor and a scaffold by oligomerizing, and tethering its C-terminal domain to supply ATPase activity to aid other proteins in the cell, and to compensate for lack of key segregation proteins. This could ensure viability and adequate chromosome segregation. Since FtsK weakly interacts with ParA in a bacterial two hybrid system (Appendix II), it can be suggested that this interaction may be a result of a protein-protein collision activity within the cell. This could happen while the ParA helical filaments depolymerize and briefly interact with the assembling and oligomerizing FtsK. In the absence of FtsK, HfkA could be interacting with ParA instead and aiding the same process (not experimentally tested). Since a *parA* deletion has the highest segregation phenotype of 26% of any segregation mutant tested, perhaps another function of ParA is aiding chromosome segregation in addition to localizing ParB at the *oriC* sites the before genomes are segregated (Jakimowicz et al., 2007). This could compel further investigation into ParA, HfkA, and FtsK interactions *in vivo,* and shed light on functions and interactions of these proteins.

Ultimately, since *S. coelicolor* shows remarkable redundancy during chromosome segregation, it can be debated if it is the mistakes in the chromosome segregation machinery that causes these anucleate phenotypes. These anucleate cells could also be the result of a faulty replication process, where there are not enough replicated chromosomes for the dividing apical cell. This could also unveil unknown functions of these

segregation proteins during DNA replication. Other proteins like Nucleoid-Associated Proteins (NAPs) could also contribute to chromosome segregation as they are known to have a function in in a variety of cellular processes like DNA repair and chromosome restructuring (Bradshaw et al., 2013). It can be speculated that if NAPs are the pleiotropic regulators of gene expression and protection of the chromosome by performing DNA repair, they may have a function in chromosome segregation as well. Other proteins like SsgA-like (SALPs) proteins, which are cell division sporulation-associated proteins, can also be involved in segregation as it is known that segregation and septum formation are coordinated in the cell (Jakimowicz & van Wezel, 2012).

To ascertain which of these models explains the role of HfkA, and which other cellular proteins are involved, further examination is required that could also explain the redundancy in the segregation pathway.

SUMMARY AND FUTURE DIRECTIONS

The life cycle of bacteria is intricate, exhibiting unique morphological and developmental features in different model bacterial species. From simple unicellular organisms, to multicellular differentiating species, there is a vast array of complex processes conducted by bacteria. The bacterial nucleoid possesses conserved structural features that enable the cell to grow and divide efficiently. These specific chromosomal architectural facets dictate the spatial orientation of requisite chromosomal elements, advancing replicated genomes towards progression of the cell cycle, and successful cell division.

This study investigated the role of an *ftsK*-like gene *sco4508* in development-

associated chromosome segregation. Sco4508 was named HfkA (Homolog of FtsK protein A) and it was analyzed for function during segregation by isolating a series of mutants along with *ftsK*, *parB* and *smc*. All the mutant strains were derived from the wild type M145 strain (Appendix I).

Single mutants of Δ*hfkA* and Δ*ftsK* did not have an overt segregation phenotype, whereas the double Δ*hfkA* Δ*ftsK* deletion had a segregation phenotype. This defect was individually complemented indicating that *hfkA* and *ftsK* are redundant, and that HfkA could be a potential DNA translocase.

A series of double, triple and quadruple mutants were isolated and analyzed for segregation phenotypes. In almost all the cases, the segregation defect was primarily due to the loss of *parB* and/or *smc,* indicating that they are the known key players in segregation. Out of the known segregation proteins, ParA was not tested in this study. It was noted that a quadruple mutant Δ*hfkA* Δ*ftsK* Δ*smc* Δ*parB* containing a complete *ftsK* deletion had a more severe segregation defect than the quadruple mutant Δ*hfkA* Δ*ftsK'* Δ*smc* Δ*parB* with a truncated deletion of *ftsK'*. This implied that the truncated version of FtsK' less severely affects segregation by an unknown mechanism and players, and the individual complete deletion of FtsK and HfkA does not impact the segregation process.

It was also observed that HfkA (Sco4508) had similarity in amino acid sequence features and predicted N-terminal membrane spanning and C-terminal Walker A domains to another FtsK-like protein Sco5734, which is a characterized T7S system protein. This implies that HfkA could also be part of a protein secretion system, and possibly play a secondary role in chromosome segregation indirectly. Conversely, in addition to primarily being a DNA translocase, HfkA could be acting as a protein secretion system

component when the cell requires that activity as its secondary function.

To identify new targets for chromosome segregation, several known proteins were tested to interact with the C-terminal of FtsK (Appendix II). Novel interactions for FtsK with ParA and ParJ proteins were identified, which would have to be corroborated by doing pull down assays or FRET analysis. These data indicate that segregation is a complex phenomenon with several proteins involved in parallel processes, which can have overlapping functions.

Several experimental approaches can be utilized to determine which of the discussed models could reveal the role of HfkA in the segregation pathway. To confirm if localization of HfkA-EGFP is dependent on the absence of FtsK, the *hfkA-egfp* Δ*ftsK* strain could be genetically complemented with $ftsK^{+}$. If expressing FtsK abolishes the HfkA-EGFP foci in the pre-divisional hyphae, it would confirm the hypothesis that HfkA works as an auxiliary DNA translocase in the absence of FtsK and vice-versa. To see if *hfkA* is transcriptionally expressed in the presence or absence of FtsK, qRT-PCR and Northern blot studies could be conducted.

If HfkA is a type VII secretory motor, it would need to be explored to identify its secreted cargo, as well as effect of the cargo proteins on chromosome segregation. One of the potential targets is the gene encoding the protein Sco4509, which is divergently expressed from the same locus as *sco4508*. It is predicted to belong to the WXG 100 family cargo protein of the T7S system. If Sco4509 is the secreted cargo for HfkA, it could have a potential role in segregation or sporulation (similar to EsxAB proteins). Also, to investigate whether HfkA directly translocates DNA in a non-sequence specific fashion, it would be crucial to check HfkA for DNA binding by performing ChIP-seq

analysis or EMSA, as previously done for SpoIIIE (Besprozvannaya & Burton, 2014). This would be decisive in determining whether HfkA is a DNA motor, which binds to specific or non-specific sequences to translocate DNA.

To identify interactions of HfkA with other cellular proteins, it can be cloned into a bacterial two-hybrid system, and screened for interactions with known cell division and segregation proteins. Novel interactions with unknown proteins could be identified by testing HfkA against a chromosomal library. This could also shed light on whether HfkA interacts with itself in the cell, indicating oligomerization. These interactions could be verified using other protein-protein interaction assays like a pull down technique, FRET or surface plasmon resonance (SPR) (Ditkowski et al., 2010). Finding novel interacting proteins with key proteins like FtsK (and HfkA) can also shed light on the extent of its functionality (Berezuk et al., 2018).

Table 2.1: *E. coli* strains used in this study.

Strain	Genotype	Source
BW25113	F$^-$ Δ(*araD-araB*)*567* Δ*lac Z4787* (*::rrnB-3*) *rph-1* Δ(*rhaD-rhaB*)*568 hsdR514*	Datsenko & Wanner, 2000
ET12567	F$^-$ *dam-13*::Tn*9 dcm-6 hsdM hsdR recF143 zjj-201*::Tn*10 galK2 galT22 ara-14 lacY1 xyl-5 leuB6 thi-1 tonA31 rpsL136 hisG4 tsx-78 mtl-1 glnV44*	MacNeil et al., 1992
BT340	F-, Δ*(argF-lac)169*, φ80d*lacZ58*(M15), *glnX44*(AS), *λ*, *rfbC1*, *gyrA96*(NalR), *recA1*, *endA1*, *spoT1*, *thiE1*, *hsdR17*/ pCP20	Cherepanov & Wackernagel, 1995
TG1	*supE thi-1* Δ(*lac-proAB*) Δ(*mcrB-hsdSM*)*5* (*rK-mK*) / F′ *traD36 proAB lacI^{q}ZΔM15*	Sambrook et al., 1989
TOP10	F$^-$ *mcrA* Δ(*mrr-hsdRMS-mcrBC*) Φ*80lacZΔM15/ΔlacX74 deoR recA1 araD139* Δ(*araA-leu*)*697 galU galK*	Invitrogen
BTH101	*F- cya-99 araD139 galE15 galK16 rpsL1 hsdR2 mcrA1 mcrB1*	Euromedex

Table 2.2. *S. coelicolor* strains used in this study.

Name	Genotype	Isolation	Source
M145	Wild type, prototroph SCP1$^-$ SCP2$^-$	-	Kieser et al., 2000
J2537	Δ*parB*::*acc(3)IV*	-	Kim et al., 2000
J3305	Δ*parB*::*frt*	-	Kois et al., 2009
HJ2	Δ*smc*::*hyg*	-	Dedrick et al., 2009
RMD1	*ftsK-egfp acc(3)IV*	-	Dedrick et al., 2009
RMD6	Δ*smc*::*hyg* Δ*parB*::*acc(3)IV* Δ*ftsK*::*aphI*	-	Dedrick et al., 2009
SS1	Δ*hfkA*::*acc(3)IV*	M145 x pSS12	This Study
SS2	Δ*hfkA*::*frt*	M145 x pSS21	This Study
SS3	Δ*ftsK*::*acc(3)IV*	M145 x pSS14	This Study
SS4	Δ*ftsK*::*frt*	M145 x pSS17	This Study
SS5	Δ*hfkA*::*frt* Δ*ftsK*::*acc(3)IV*	SS2 x pSS14	This Study
SS8	*hfkA-egfp acc(3)IV*	M145 x pSS22	This Study
SS10	Δ*hfkA*::*frt* Δ*ftsK*::*acc(3)IV/ hfkA*$^+$	SS5 x pSS26	This Study
SS11	Δ*hfkA*::*frt* Δ*ftsK*::*acc(3)IV/* pSpc152	SS5 x pSpc152	This Study
SS12	Δ*hfkA*::*frt* Δ*ftsK*::*acc(3)IV*/*ftsK*$^+$	SS5 x pRMD6	This Study
SS13	Δ*hfkA*::*frt* Δ*ftsK*::*acc(3)IV*/pJRM10	SS5 x pJRM10	This Study
SS21	Δ*ftsK*::*acc(3)IV hfkA-egfp aadA*	SS5 x pSS29	This Study
SS22	Δ*hfkA*::*acc(3)IV* Δ*parB*::*frt*	J3305 x pSS12	This Study

SS23	Δ*hfkA*::*acc(3)IV* Δ*smc*::*hyg*	HJ2 x pSS12	This Study
SS25	Δ*hfkA*::*frt* Δ*ftsK*::*acc(3)IV* Δ*smc*::*hyg*	SS5 x pSS33	This Study
SS26	Δ*ftsK*::*acc(3)IV* Δ*smc*::*hyg*	HJ2 x pSS14	This Study
SS27	Δ*ftsK*::*acc(3)IV* Δ*smc*::*hyg*/*ftsK*$^+$	SS26 x pRMD6	This Study
SS28	Δ*ftsK*::*acc(3)IV* Δ*smc*::*hyg*/*smc*$^+$	SS26 x pHW35	This Study
SS29	Δ*hfkA*::*frt* Δ*ftsK*::*acc(3)IV* Δ*smc*::*hyg*/*hfkA*$^+$	SS25 x pSS26	This Study
SS30	Δ*hfkA*::*frt* Δ*ftsK*::*acc(3)IV* Δ*smc*::*hyg*/*ftsK*$^+$	SS25 x pJRM10	This Study
SS31	Δ*hfkA*::*frt* Δ*ftsK*::*acc(3)IV* Δ*smc*::*hyg*/*smc*$^+$	SS25 x pHW35	This Study
SS32	Δ*ftsK*::*acc(3)IV* Δ*smc*::*hyg*/pJRM10	SS26 x pJMR10	This Study
SS33	Δ*hfkA*::*frt* Δ*ftsK*::*acc(3)IV* Δ*smc*::*hyg*/pJRM10	SS25 x pJRM10	This Study
SS34	Δ*hfkA*::*frt* Δ*ftsK*::*acc(3)IV* Δ*smc*::*hyg*/pSpc152	SS25 x pScp152	This Study
SS35	Δ*ftsK*::*acc(3)IV* Δ*parB*::*frt*	J3305 x pSS14	This Study
SS36	Δ*ftsK*::*acc(3)IV* Δ*parB*::*frt*/*ftsK*$^+$	SS35 x pRMD6	This Study
SS37	Δ*ftsK*::*acc(3)IV* Δ*parB*::*frt*/*parB*$^+$	SS35 x pIJ6539	This Study
SS38	Δ*ftsK*::*acc(3)IV* Δ*parB*::*frt*/pJRM10	SS35 x pJRM10	This Study
SS39	Δ*hfkA*::*frt* Δ*ftsK*::*acc(3)IV* Δ*parB*::*aphI*	SS5 x pSS37	This Study
SS40	Δ*hfkA*::*acc(3)IV* Δ*smc*::*hyg* Δ*parB*::*aphI*	SS23 x pSS37	This Study
SS41	Δ*hfkA*::*frt* Δ*ftsK*::*acc(3)IV* Δ*parB*::*aphI*/*hfkA*$^+$	SS39 x pSS26	This Study
SS42	Δ*hfkA*::*frt* Δ*ftsK*::*acc(3)IV* Δ*parB*::*aphI*/*ftsK*$^+$	SS39 x pRMD6	This Study
SS43	Δ*hfkA*::*frt* Δ*ftsK*::*acc(3)IV* Δ*parB*::*aphI*/*parB*$^+$	SS39 x pIJ6539	This Study
SS44	Δ*hfkA*::*acc(3)IV* Δ*smc*::*hyg* Δ*parB*::*aphI*/*hfkA*$^+$	SS40 x pSS26	This Study
SS45	Δ*hfkA*::*acc(3)IV* Δ*smc*::*hyg* Δ*parB*::*aphI*/*smc*$^+$	SS40 x pHW35	This Study

SS46	Δ*hfkA*::*acc(3)IV* Δ*smc*::*hyg* Δ*parB*::*aphI*/*parB*$^+$	SS40 x pSS26	This Study
SS47	Δ*hfkA*::*frt* Δ*ftsK*::*acc(3)IV* Δ*parB*::*aphI*/pSpc152	SS39 x pSpc152	This Study
SS48	Δ*hfkA*::*frt* Δ*ftsK*::*acc(3)IV* Δ*parB*::*aphI*/pJRM10	SS39 x pJRM10	This Study
SS49	Δ*hfkA*::*acc(3)IV* Δ*smc*::*hyg* Δ*parB*::*aphI*/pSpc152	SS40 x pSpc152	This Study
SS50	Δ*hfkA*::*acc(3)IV* Δ*smc*::*hyg* Δ*parB*::*aphI*/pJRM10	SS40 x pJRM10	This Study
SS51	Δ*ftsK*::*acc(3)IV* Δsmc::*hyg* Δ*parB*::*frt*	SS35 x pSS33	This Study
SS52	Δ*ftsK*::*acc(3)IV* Δsmc::*hyg* Δ*parB*::*frt*/*ftsK*$^+$	SS51 x pRMD6	This Study
SS53	Δ*ftsK*::*acc(3)IV* Δsmc::*hyg* Δ*parB*::*frt*/*smc*$^+$	SS51 x pHW35	This Study
SS54	Δ*ftsK*::*acc(3)IV* Δsmc::*hyg* Δ*parB*::*frt*/*parB*$^+$	SS51 x pIJ6539	This Study
SS55	Δ*ftsK*::*acc(3)IV* Δsmc::*hyg* Δ*parB*::*frt*/pJRM10$^+$	SS51 x pJRM10	This Study
SS56	Δ*hfkA*::*frt* Δ*ftsK*::*acc(3)IV* Δ*smc*::*hyg* Δ*parB*::*aphI*	SS25 x pSS37	This Study
SS57	Δ*hfkA*::*frt* Δ*ftsK*::*acc(3)IV* Δ*smc*::*hyg* Δ*parB*::*aphI*/*hfkA*$^+$	SS56 x pSS26	This Study
SS58	Δ*hfkA*::*frt* Δ*ftsK*::*acc(3)IV* Δ*smc*::*hyg* Δ*parB*::*aphI*/*ftsK*$^+$	SS56 x pRMD6	This Study
SS59	Δ*hfkA*::*frt* Δ*ftsK*::*acc(3)IV* Δ*smc*::*hyg* Δ*parB*::*aphI*/*smc*$^+$	SS56 x pHW35	This Study
SS60	Δ*hfkA*::*frt* Δ*ftsK*::*acc(3)IV* Δ*smc*::*hyg* Δ*parB*::*aphI*/*parB*$^+$	SS56 x pIJ6539	This Study
SS61	Δ*hfkA*::*frt* Δ*ftsK*::*acc(3)IV* Δ*smc*::*hyg* Δ*parB*::*aphI*/pSpc152	SS56 x pSpc152	This Study
SS62	Δ*hfkA*::*frt* Δ*ftsK*::*acc(3)IV* Δ*smc*::*hyg* Δ*parB*::*aphI*/pJRM10	SS56 x pJRM10	This Study
SS63	Δ*hfkA*::*vph* Δ*ftsK'*:: *aphI* Δ*smc*::*hyg* Δ*parB*:: *acc(3)IV*	RMD6 x pSS38	This Study

SS64	Δ*hfkA*::*vph* Δ*ftsK'*::*aphI* Δ*smc*::*hyg* Δ*parB*::*acc(3)IV/hfkA*$^{+}$	SS63 x pSS26	This Study
SS65	Δ*hfkA*::*vph* Δ*ftsK'*::*aphI* Δ*smc*::*hyg* Δ*parB*::*acc(3)IV/ftsK*$^{+}$	SS63 x pRMD6	This Study

Table 2.3: Cosmids and plasmids used in this study.

Name	Description	Source
StD35	Cosmid source of *hfkA (sco4508)*; *bla, aphII*	M. Elliot
St7C7	Cosmid source of *ftsK*; *bla, aphII*	Redenbach et al., 1996
StH24	Cosmid source of *parB*; *bla, aphII*	D. Jakimowitz
SC7A1	Cosmid source of *smc*; *bla, aphII*	Redenbach et al., 1996
StH24 *parB-egfp*	*egfp* inserted in-frame at 3' end of *parB* in cosmid StH24; *acc(3)IV, aphII*	D. Jakimowitz
pCR2.1	TA cloning vector	Invitrogen
pKNT25	Bacterial two-hybrid vector used to create a fusion to the N-terminus of the CyaA T25 polypeptide	Euromedex
pKT25	Bacterial two-hybrid vector used to create a fusion to the C-terminus of the CyaA T25 polypeptide	Euromedex
pUT18	Bacterial two-hybrid vector used to create a fusion to the N-terminus of the CyaA T18 polypeptide	Euromedex
pUT18C	Bacterial two-hybrid vector used to create a fusion to the C-terminus of the CyaA T18 polypeptide	Euromedex
pKT25-zip	Bacterial two-hybrid control plasmid, a derivative of pKT25 with the leucine zipper of GCN4 genetically fused in frame to the T25 fragment	Euromedex
pUT18C-zip	Bacterial two-hybrid control plasmid, a derivative of pUT18C with the leucine zipper of GCN4 genetically fused in frame to the T18 fragment	Euromedex
pIJ773	pBluescript II SK(+) derivative containing *aac(3)IV-oriT* disruption cassette flanked by *frt* sites	Gust et al., 2003
pIJ10700	pBluescript II SK(+) derivative containing *hyg-oriT* disruption cassette flanked by *frt* sites	Gust et al., 2003
pIJ780	pBluescript II SK(+) derivative containing *vph-oriT* disruption cassette flanked by *frt* sites	Gust et al., 2003
pIJ778	pBluescript II SK(+) derivative containing *aadA-oriT* disruption cassette flanked by *frt* sites	Gust et al., 2003
pIJ790	λ-RED (*gam*, *bet*, *exo*) *araC rep101*^{ts}	Gust et al., 2003
ParAT18C	*parA* flanked by *Xba*I and *Kpn*I cloned into pUT18C	Jakimowicz et al., 2007
ParAT25	*parA* flanked by *Xba*I and *Kpn*I cloned into pKT25	Jakimowicz et al., 2007

ParJT18C	*parJ* flanked by *Xba*I and *Kpn*I cloned into pUT18C	Jakimowicz et al., 2010
ParJT25	*parB* flanked by *Xba*I and *Kpn*I cloned into pKT25	Jakimowicz et al., 2010
pAEB228	4.2 kb *Pvu*II fragment from SC7C7 containing *ftsK* cloned into *Eco*RV-digested pBluescript *(ftsK* same orientation as *lacZ')*	Dedrick et al., 2009
pRA4	Plasmid pIJ2925 containing the 1.05 kb *aphI* fragment cloned at the *Eco*RI-*Hin*dIII site	Rachel Amino, McCormick laboratory
pSpc152	pSET152 with *acc(3)IV* replaced by *aadA*	Dedrick et al., 2009
pJRM10	bifunctional cloning vector, low-copy-number in *S. coelicolor*, *bla, tsr*	McCormick & Losick 1996
pRMD6	24 kb *Eco*RI-*Hin*dIII fragment from pJRM10 cloned into pAEB228 (*ftsK* complementation plasmid)	Dedrick et al., 2009
pIJ6539	5.3 kb *Eco*RI fragment containing *parB, tsr (parB* complementation plasmid)	Kim et al., 2000
pSS5	2,036 bp fragment of *`ftsK* flanked by *Kpn*I sites cloned into pCR2.1	This Study
pSS6	*Kpn*I fragment of pSS5 cloned into pUT18; *bla*	This Study
pSS7	*Kpn*I fragment of pSS5 cloned into pUT18C; *bla*	This Study
pSS8	*Kpn*I fragment of pSS5 cloned into pKT25; *aphII*	This Study
pSS9	*Kpn*I fragment of pSS5 cloned into pKNT25, *aphII*	This Study
pSS12	cosmid StD35 containing Δ*hfkA*::*acc(3)IV ,* by *in vivo* recombination, *bla, aphII*, *acc(3)IV*	This Study
pSS14	cosmid St7C7 containing Δ*ftsK*::*acc(3)IV ,* by *in vivo* recombination, *bla, aphII*, *acc(3)IV*	This Study
pSS17	St7C7 *ftsK*::*frt* with *aac(3)IV-oriT*, *bla*, *aphII*, *aac(3)IV*	This Study
pSS20	StD35 *hfkA*::*frt* with *aac(3)IV-oriT*, *bla*, *aphII*, *aac(3)IV*	This Study
pSS21	StD35 *ftsK*::*frt* with *aac(3)IV-oriT* in Et25113/pUZ8002, *bla*, *aphII*, *acc(3)IV*, *cat*	This Study
pSS22	*egfp i*nserted in-frame at 3' of *hfkA* in cosmid StD35, *acc(3)IV aphII, bla*	This Study
pSS26	8kb *Eco*RI fragment of StD35 containing *hfkA* cloned in pSpc152, *hfkA* complementation plasmid, *bla*, *aadA*	This Study
pSS28	pSS22 targetted with *aadA-oriT* cassette from pIJ778, resulting in *egfp i*nserted in-frame at 3' of *hfkA i*n cosmid StD35, *aadA, aphII*	This Study

pSS33	cosmid SC7A1 containing Δ*smc*::*hyg,* by *in vivo* recombination, *bla, aphII*, *hyg*	This Study
pSS34	*aphI* Deletion cassette targeting amplified *Pvu*II fragment from pRA4 to the *acc(3)IV-oriT* containing plasmid pIJ773, *bla, aphI*	This Study
pSS35	Cosmid H24 backbone targeted by amplified *Hin*dIII fragment of *aadA* from pJA18 to replace *aphII* to *aadA, bla, aadA*	This Study
pSS36	Modified cosmid pSS35 targeted by amplified *Eco*RI-*Hin*dIII fragment of pSS34 to obtain Δ*parB*::*aphI, bla, aphI*	This Study
pSS38	cosmid StD35 containing Δ*hfkA*::*vph,* by *in vivo* recombination, *bla, aphII*, *vph*	This Study

Table 2.4: **Oligonucleotides used in this study.**

Name	Sequence 5'-3'	Application
Sco5750-F59 long	ATGGAGGGGCGACAC GAACGGGTGAAGCGG TAGGCACACATTCCGG GGATCCGTCGACC	Construction of Δ*ftsK*::*acc(3)IV*
Sco5750-R58 long	TCGGCGAAACGTCGGC GGATCGTCGGCGGAAC CCTTCTCTGTAGGCTG GAGCTGCTTC	Construction of Δ*ftsK*::*acc(3)IV*
Sco5750-F-check-82	AGGACTTGTCAGAGGC TGTAC	PCR amplification of region flanking *ftsK*
Sco5750-R-check+85	CTAACGGGTGAGTCAC GAT	PCR amplification of region flanking *ftsK*
NEWsco4508-F66 SpeI	GGCCGCAGGGGCTCGC CTGGGGAGGACAAGC GTGCGACTGACTAGTA TTCCGGGGATCCGTCG ACC	Construction of Δ*hfkA*::*acc(3)IV*
NEWsco4508-R67 XbaI	CCCGCCCCTTCCACCG GCTCAGCCCGGCACCA CGACCGTGCGTCTAGA TGTAGGCTGGAGCTGC TTC	Construction of Δ*hfkA*::*acc(3)IV*
Sco4508-F-49	ATATCGTCGCCTGGAC TG TG	PCR amplification of region flanking *hfkA*
Sco4508-R+104	GACCTCGACTACGCGT CGAAGA	PCR amplification of region flanking *hfkA*
Sco4508-Fwd3533	ACGAGTTGCAGACGAT GATG	PCR amplification of *hfkA*
Sco4508-Rev851	GTCGTTGAAGTAGTTG GC GA	PCR amplification of *hfkA*
Sco4508fwd841	ATCCTCCTGTTCGCCA AC TAC	PCR amplification of *hfkA*
Sco4508rev1305	AGTTCTCGCTCAGCAC GT AGAAC	PCR amplification of *hfkA*
Sco4508rev2394	TGGTAGTCCTCGATGT CC TTG	PCR amplification of *hfkA*
Sco4508egfp FWD57	CTGGGCGACGGGGAG CTGCGCACGGTCGTGG TGCCGGGCCTGCCGGG CCCGGAGCTG	Construction of *hfkA-egfp*
Sco4508egfp REV63	GGTGCGCAGCGGGGC CGGGGCCCCGCCCCTT	Construction of *hfkA-egfp*

	CCACCGGCACATATGT AGGCTGGAGCTGCTTC	
Sco4508 Check Fwd4302	GAGCCAGATGAAGAA GATCGTC	PCR amplification of Δ*hfkA*
Smc5577 Fwd59long	CGTGGAGTGAGACAG ACCCGAAAGGTAGAG TCCGACGGCATTCCGG GGATCCGTCGACC	Construction of Δ*smc*::*hyg*
Smc5577 Rev58Long	CTGAAGTGGTTATGTG TTCAAGTCTTGAAGAA CGAGGGTTGTAGGCTG GAGCTGCTTC	Construction of Δ*smc*::*hyg*
Smc5577 check F-41	TTCGTGGAGTGAGACA GAC	PCR amplification of region flanking *smc*
Smc5577 check R+63	CGAGAGCTGTGACTTT CAG	PCR amplification of region flanking *smc*
Smc5577 check Fwd368	ACATCCAGGAACTCCT CTC	PCR amplification of *smc*
Smc5577 check Rev2683	GAATCCGTCAACTTGT CCAG	PCR verification of *smc*
parB3887 Fwd59long	ATCCGCGCTATTCGAA GAGGTCTATCCCGCCT TCCGGGGATCCGTCGA CC	Construction of Δ*parB*::*aphI*
parB3887 Rev58Long	GGTCGGCGCGGACCT CTTCACGACGTCGCCT TCTCTGTAGGCTGGAG CTGCTTC	Construction of Δ*parB*::*aphI*
ParBCheckF-237	ATCCAGGATCAAGTGG AGC	PCR amplification of region flanking *parB*
ParBCheckR^{+}576	GTATGCACCGGACACA GTC	PCR amplification of region flanking *parB*
ParBCheckFwd69	TGAAACCGAAGAGCT GACG	PCR amplification of *parB*
ParBCheckRev833	CTTCTTCTGACCCAGG TCGA	PCR amplification of *parB*
oftsK bacth FWD	GGTACCTAACGCCATC CCGCAGCGGCTG	Cloning of `*ftsK* in the BACTH plasmids with *Kpn*I sites
oftsK bacth REV	GGTACCCCTTCAGACT CCCCACGGAT	Cloning of `*ftsK* in the BACTH plasmids with *Kpn*I sites
oftsK Fwd 661	CTGTCGTACACGATGA CCG	PCR amplification of *ftsK*
oftsK Rev 1314	GCAGGGAATAGGTGA TGTCG	PCR amplification of *ftsK*

oftsK Rev+199	ACCTTTACGCCATCGGAATG	PCR amplification of *ftsK*
oftsK993f	CGAGATGAACCGTCCGATGG	PCR amplification of *ftsK*
oftsK1312F	GGCGACATCACCTATTCCCTG	PCR amplification of *ftsK*
oftsK1538F	AGAACATCGCCTACGCCGTCG	PCR amplification of *ftsK*
oftsK1748F	TGGCGAAGATGCCGCACATG	PCR amplification of *ftsK*
oftsK2026F	CACATCGACGACTTCAACCG	PCR amplification of *ftsK*
oftsK2255F	TCGTGACCGGCCTGATCAAGG	PCR amplification of *ftsK*
oftsK2523F	GAAGAAGGAGATCGACGAGG	PCR amplification of *ftsK*

Table 2.5: List of FtsK-like proteins from the *S. coelicolor* genome database.

***ftsK*-like genes from the *S. coelicolor* database**	**Length of the polypeptide (amino acids)**	**Percentage similarity to the FtsK amino acid sequence**	**Percentage similarity to the FtsK C-terminal***	**Length of C-terminal overlap**
SCO5750 (FtsK)	929	100	100	479
SCO5633	768	28	49	199
SCO4508* (HfkA)	1526	31	59	369
SCO5734	1322	27	46	502
SCO1805	244	36	0	79

* The percentage similarity was calculated to the FtsK C-terminal domain containing the α motor domain, the β ATPase domain, and the γ DNA recognition domain.

Table 2.6: Summary of segregation defects observed in *hfkA* and *ftsK* single and double mutant strains.

Strain	% Anucleate spores*
M145 (Wt)	1.0%
Δ*hfkA*	1.2%
Δ*ftsK*	1.5%
Δ*hfkA* Δ*ftsK*	8.0%
Δ*hfkA* Δ*ftsK* /*hfkA*$^{+}$	2.4%
Δ*hfkA* Δ*ftsK*/*ftsK*$^{+}$	1.4%
Δ*hfkA* Δ*ftsK*/pSpc152	8.4%
Δ*hfkA* Δ*ftsK*/pJRM10	8.1%

*~1500 spores were measured for all strains except the negative controls with the empty vectors, for which ~500 spores were measured.

Table 2.7: **Summary table of segregation defect quantified for selected *S. coelicolor* mutant strains during spore formation.**

Strain	% Anucleate spores*
Wt (M145)	1.0%
Δ*hfkA*	1.2%
Δ*ftsK*	1.5%
Δ*smc*	6.4%
Δ*parB*	11.8%
Δ*hfkA* Δ*ftsK*	8.0%
Δ*hfkA* Δ*smc*	7.6%
Δ*ftsK* Δ*smc*	8.3%
Δ*hfkA* Δ*parB*	13.4%
Δ*ftsK* Δ*parB*	14.1%
Δ*parB* Δ*smc*	18.8%
Δ*hfkA* Δ*ftsK* Δ*smc*	16.2%
Δ*hfkA* Δ*ftsK* Δ*parB*	18.1%
Δ*hfkA* Δ*smc* Δ*parB*	18.4%
Δ*ftsK* Δ*smc* Δ*parB*	19.2%
Δ*ftsK′* Δ*smc* Δ*parB*	11.0%
Δ*hfkA* Δ*ftsK* Δ*smc* Δ*parB*	20.0%
Δ*hfkA* Δ*ftsK′* Δ*smc* Δ*parB*	14.0%

* Random spore chains were measured regardless of the spore compartment size.

Table 2.8: **Segregation defect quantified for all *S. coelicolor* strains during spore formation.**

Strain	% Anucleate spores*	Total spores
Wt (M145)	1.0%	1441
SINGLE MUTANTS		
Δ*hfkA*	1.2%	1503
Δ*ftsK*	1.5%	1492
Δ*smc*	6.4%	1228
Δ*smc/smc*$^+$	1.7%	529
Δ*smc*/pJRM10$^+$	7.1%	479
Δ*parB*	11.8%	1399
Δ*parB/parB*+	2.9%	483
DOUBLE MUTANTS		
Δ*hfkA* Δ*ftsK*	8.0%	1534
Δ*hfkA* Δ*ftsK/hfkA*$^+$	2.4%	1386
Δ*hfkA* Δ*ftsK/ftsK*$^+$	1.4%	1322
Δ*hfkA* Δ*ftsK*/pJRM10	8.1%	498
Δ*hfkA* Δ*ftsK*/pSpc152	8.4%	558
Δ*hfkA* Δ*smc*	7.6%	1650
Δ*hfkA* Δ*smc/hfkA*$^+$	6.8%	1339
Δ*hfkA* Δ*smc/smc*$^+$	1.7%	1226
Δ*hfkA* Δ*smc*/pSpc152	8.2%	520
Δ*hfkA* Δ*smc*/pJRM10	7.9%	496
Δ*ftsK* Δ*smc*	8.3%	1464
Δ*ftsK* Δ*smc/ftsK*$^+$	7.8%	1522
Δ*ftsK* Δ*smc/smc*$^+$	2.1%	1582
Δ*ftsK* Δ*smc*/pJRM10	8.1%	478
Δ*hfkA* Δ*parB*	13.4%	1378

Δ*hfkA* Δ*parB/hfkA*$^+$	12.1%	1410
Δ*hfkA* Δ*parB/parB*$^+$	2.3%	1472
Δ*hfkA* Δ*parB*/pSpc152	14.3%	538
Δ*ftsK* Δ*parB*	14.1%	1544
Δ*ftsK* Δ*parB/ftsK*$^+$	13.6%	1491
Δ*ftsK* Δ*parB/parB*$^+$	2.8%	1129
Δ*ftsK* Δ*parB*/pJRM10	13.7%	462
Δ*parB* Δ*smc*	18.8%	1236
Δ*parB* Δ*smc/parB*$^+$	5.6%	1366
Δ*parB* Δ*smc/smc*$^+$	14.6%	1217
Δ*parB* Δ*smc*/pJRM10	19.5%	422
TRIPLE MUTANTS		
Δ*hfkA* Δ*ftsK* Δ*smc*	16.2%	1540
Δ*hfkA* Δ*ftsK* Δ*smc/hfkA*$^+$	10.1%	1621
Δ*hfkA* Δ*ftsK* Δ*smc/ftsK*$^+$	8.9%	1578
Δ*hfkA* Δ*ftsK* Δ*smc/smc*$^+$	7.8%	1432
Δ*hfkA* Δ*ftsK* Δ*smc*/pSpc152	15.3%	412
Δ*hfkA* Δ*ftsK* Δ*smc*/pJRM10	16.8%	522
Δ*hfkA* Δ*ftsK* Δ*parB*	18.1%	1566
Δ*hfkA* Δ*ftsK* Δ*parB/hfkA*$^+$	16.3%	1443
Δ*hfkA* Δ*ftsK* Δ*parB/ftsK*$^+$	14.8%	1287
Δ*hfkA* Δ*ftsK* Δ*parB/parB*$^+$	5.4%	1562
Δ*hfkA* Δ*ftsK* Δ*parB*/pSpc152	16.9%	501
Δ*hfkA* Δ*ftsK* Δ*parB*/pJRM10	18.3%	493
Δ*hfkA* Δ*smc* Δ*parB*	18.4%	1496
Δ*hfkA* Δ*smc* Δ*parB/hfkA*$^+$	17.1%	1538
Δ*hfkA* Δ*smc* Δ*parB/smc*$^+$	13.5%	1564
Δ*hfkA* Δ*smc* Δ*parB/parB*$^+$	4.9%	1428
Δ*hfkA* Δ*smc* Δ*parB*/pSpc152	19.2%	515
Δ*hfkA* Δ*smc* Δ*parB*/pJRM10	18.2%	494

Δ*ftsK* Δ*smc* Δ*parB*	19.2%	1478
Δ*ftsK* Δ*smc* Δ*parB/ftsK*$^+$	16.1%	1511
Δ*ftsK* Δ*smc* Δ*parB/smc*$^+$	5.1%	1487
Δ*ftsK* Δ*smc* Δ*parB*/pJRM10	18.7%	500
Δ*ftsK′* Δ*smc* Δ*parB*	11.0%	1539
Δ*ftsK′* Δ*smc* Δ*parB/ftsK*$^+$	21.4%	571
Δ*ftsK′* Δ*smc* Δ*parB/smc*$^+$	12.7%	512
QUADRUPLE MUTANTS		
Δ*hfkA* Δ*ftsK* Δ*smc* Δ*parB*	20.0%	1596
Δ*hfkA* Δ*ftsK* Δ*smc* Δ*parB/hfkA*$^+$	17.8%	1342
Δ*hfkA* Δ*ftsK* Δ*smc* Δ*parB/ftsK*$^+$	21.0%	1264
Δ*hfkA* Δ*ftsK* Δ*smc* Δ*parB/smc*$^+$	14.2%	1298
Δ*hfkA* Δ*ftsK* Δ*smc* Δ*parB/parB*$^+$	13.8%	1351
Δ*hfkA* Δ*ftsK* Δ*smc* Δ*parB*/pSpc152	22.0%	465
Δ*hfkA* Δ*ftsK* Δ*smc* Δ*parB*/pJRM10	17.2%	489
Δ*hfkA* Δ*ftsK′* Δ*smc* Δ*parB*	14.0%	1529
Δ*hfkA* Δ*ftsK′* Δ*smc* Δ*parB/hfkA*$^+$	16.6%	1320
Δ*hfkA* Δ*ftsK′* Δ*smc* Δ*parB/ftsK*$^+$	15.6%	1426
OTHER STRAINS		
hfkA-egfp in Wt	0.8%	1535
hfkA-egfp in Δ*ftsK*	1.9%	1486

* Random spore chains were measures regardless of the spore compartment size

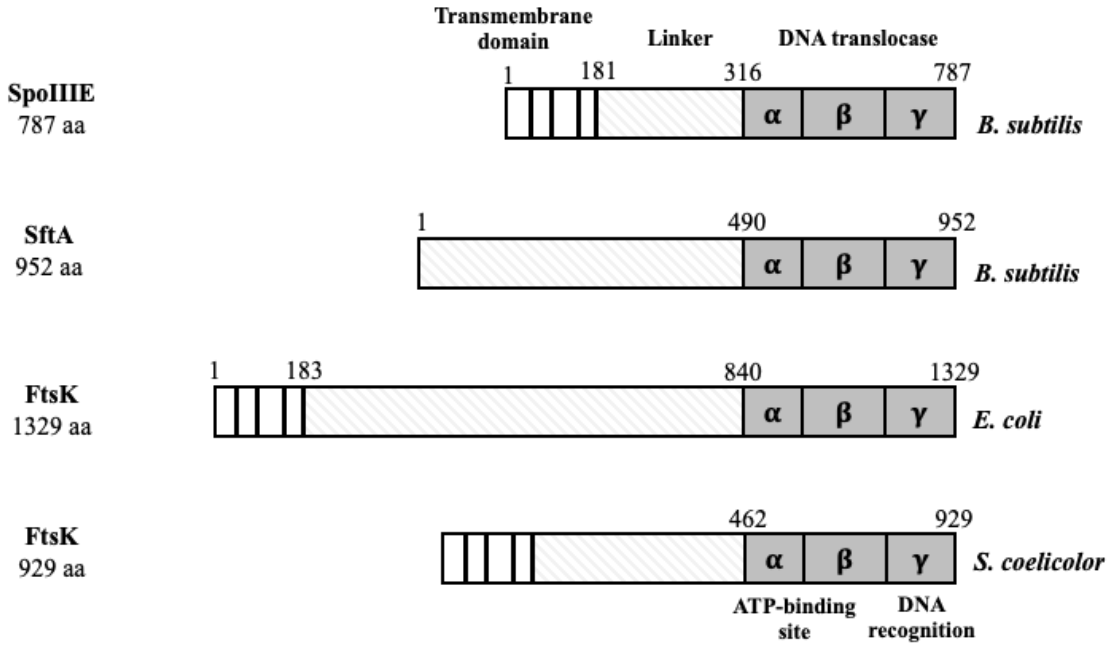

Figure 2.1: Schematic of the FtsK/SpoIIIE polypeptides in bacteria containing different structural domains.

The figure above describes different FtsK/SpoIIIE-like polypeptides in model prokaryotic species. *B. subtilis* contains two DNA translocases. The vertical lines represent the membrane-spanning segments, and the grey α and β boxes represent the ATPase domain, and grey γ box represents the DNA recognition domain. (Adapted from Kaimer et al. (2009)).

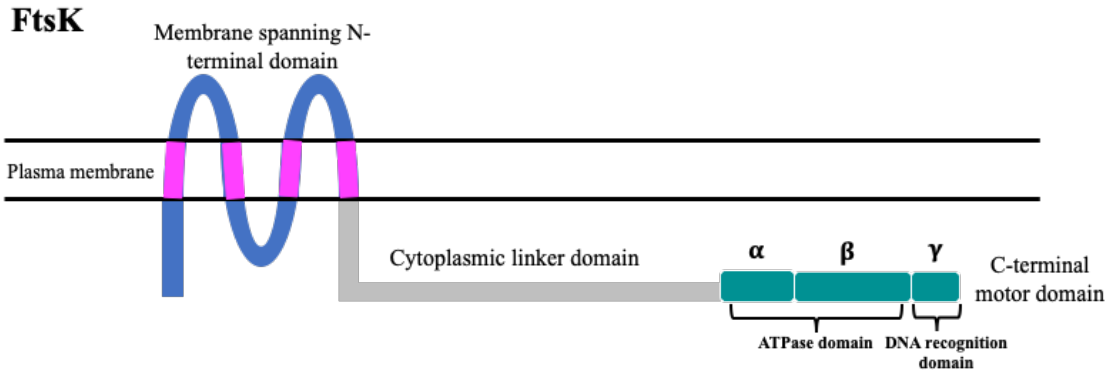

Figure 2.2 The N-terminal domain of FtsK is membrane bound and the C-terminal contains the DNA translocase motor.

Shown is a cartoon version of the FtsK protein within the cell. The different domains of FtsK are labeled and highlighted. The protein contains a N-terminal transmembrane domain (blue) with four membrane-spanning segments (highlighted in pink), followed by a cytoplasmic linker domain (highlighted in grey), and the C-terminal motor domain showing the α and β ATPase, and the γ DNA recognition domains is in teal. (Adapted from Grainge (2010)).

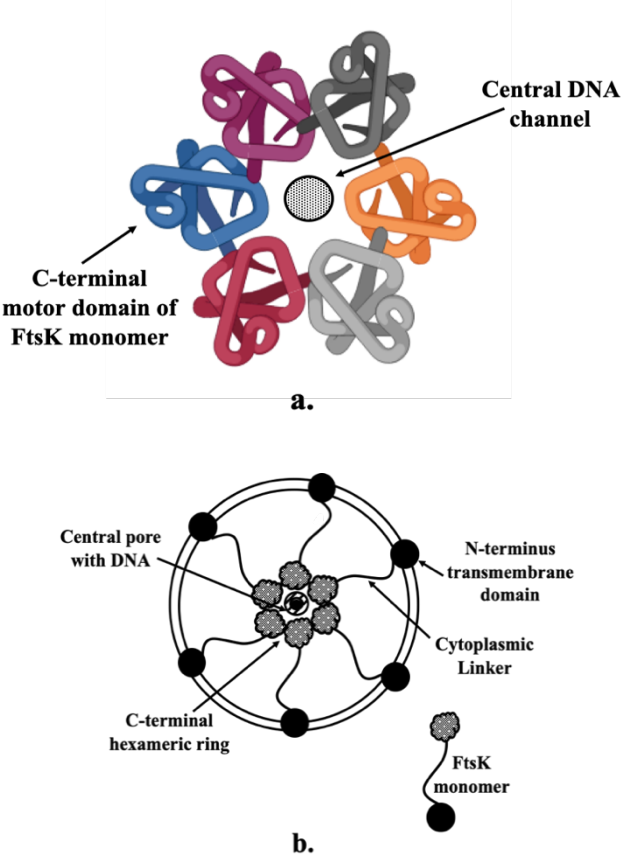

Figure 2.3: **Oligomerization of the C-terminal domains of FtsK forms a hexameric ring around the DNA for translocation.**

This schematic illustrates **(a.)** oligomerization of the C-terminal domain of FtsK into a hexameric ring while being tethered to the membrane at its N-terminal domains in a cross-section of the cell **(b.).** The transmembrane N-terminal domain contains membrane-spanning segments that is responsible for the anchoring to the cell membrane, and the sequence specificity in the C-terminal domain enables its contact with DNA. The central pore of the hexamer is large enough to fit dsDNA through it, which can move dsDNA up to the rate of approximately 6.7 kb DNA/second *in vitro* in *E. coli*. (Adapted from Massey et al., 2006; Dubarry et al., 2010)

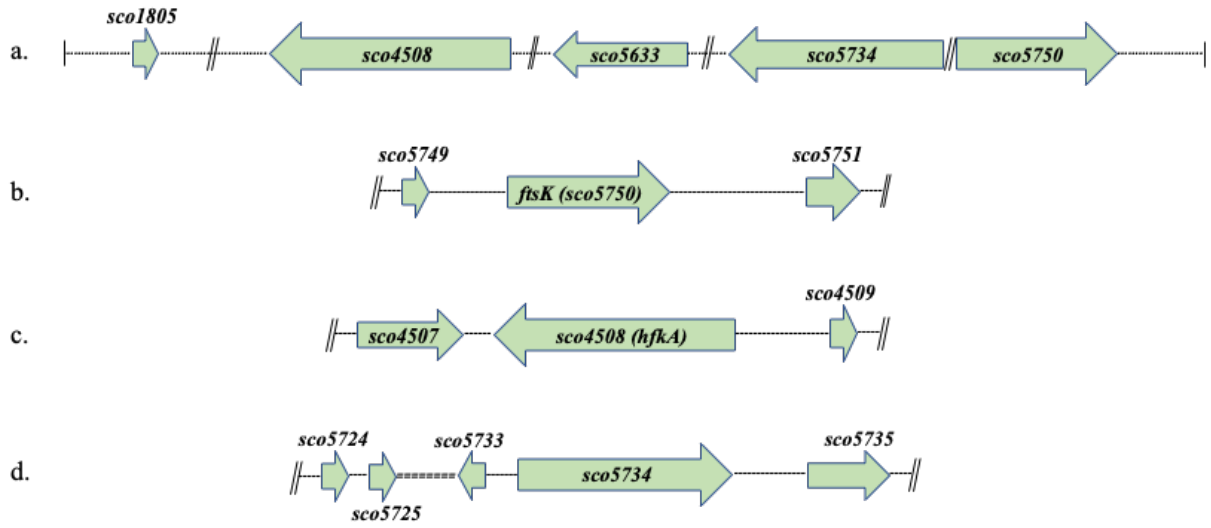

Figure 2.4: Chromosomal loci of *S. coelicolor* depicting *ftsK* and *ftsK*-like genes.

This figure depicts the chromosomal locations of various *S. coelicolor ftsK*-like genes. **(a.)** The physical map of known *ftsK*-like genes encoded throughout the *S. coelicolor* chromosome. *sco5750* is characterized as *ftsK*, and sco4508 is named as *hfkA* (Homolog of FtsK protein A) **(b.)** The physical map of *ftsK* with flanking genes *sco5749* and *sco5751* along with its intergenic regions **(c.)** shows the physical map of *sco4508* with flanking genes *sco4507* and *sco4509* (a putative WXG100 family protein) and the intergenic regions. **(d.)** Depicts the physical map of *sco5734* with its flanking genes *sco5733* and *sco5735* and their intergenic regions. The map also shows the T7S system *esx* locus with *sco5724* (*esxB*) and *sco5725* (*esxA*) cargo proteins, where the disruption of *sco5734* inhibits the secretion of EsxA and EsxB (Roman et al. 2010).

```
FtsK        ------VS------------------------------TAVSPGNLTPMASRPSAAKKQP   24

Sco4508     VRLTLTVVDPYGGGSADVVLDADPESTVGDIAEELAKQVGIAGAQVIPIGHQGQAG----   56
                  *                                 ..:: .:: *:. : .*.

FtsK        AKKAAAPAKGPVKKAAAKKAPAKRAPAKKAA---ARKPAPQPAPNPTNGVY--RLVRALW   79
Sco4508     --TGGAPLVYVDGYAVDPSATVVGSPLREGAVVSLQDPSG-CLPGEPTGLVELRVVGGPG   113
              ...**       *.  .* .  :* ::.*    :.*:    *.  .*:   *:* .

FtsK        LGLAHGVGAVFRGIGQGAKNLDPAHR--KDGVALLLLGVALI--VAAGTWADLKGPV--G   133
Sco4508     AGFVHRLGVGKYDIGSGPAAYVRIEDPEVDARA-LTLSVATDGTCKVAVHSDKEGVTLDG   172
             *:.* :*.   .**.*       .    *. * * *.**      ... :* :* .  *

FtsK        DLVEILVTGAFGRLDLLVPILLGAIAVRLIRHPEKPEANGRIVIGLSALVIGVLGQVHIA   193
Sco4508     ESVQE---RDGDDWPLGAQIAVGNSLVELARYAP-PN--AAL--KWSE------DGVGLD   218
            : *:       .   * . * :*   *.* *:   *:  . :    *       . * :


FtsK        CGSPARSEGM---QAIRDAGGLIGWGAATPLSYTMTDVLAVPLLVLLTVFGLL----VVT   246
Sco4508     YNRPPRLRPAERQTNFRLPSSPRDY-EARPLPWLMALTPLVGAVVAVMVFGRWYYLIMAG   277
             . * * .       :*  ..  .:  * ** : *: .  *  :* : ***      :.

FtsK        ATPVNAIPQRLRQLGVRLGVVHAPETDEFTNDDERYDEQWREALPARPRKR--AQPAAAE   304
Sco4508     LSPILLFANYFNDK-KHGRKSHAKQVKEYEEQKARIEKDAQAALVAERDDRRQAIPDPAV   336
             :*:  : : :.:   :    ** :..*: ::. * ::: : ** *.  .*  * *  *

FtsK        -----------PYDPDAAEQEALSRRRGR---PRRSAVPQPEMNR---------------   335
Sco4508     VLSVATGPRTRLWERRRTDRDHLLLRVGTGQLPSEVVLDDPEQDDHRRQVTWKIEDAPVA   396
                        ::   :::: *  * *    * . .: :** :

FtsK        ----PMDAVDVAAAAAA--AL------DGAVLHGMPPSPLVADLTQGVSTGDRESTTPTP   383
Sco4508     LSLRTLGVVGIAGPGDSARSLGRWAVAQTAALH----SPMDVQFYV-LSENSAQSEWDWV   451
                 :..*.:*. . :  :*      : *.**    **: .::   :* .. :*


FtsK        TPVPAARPQPGK------------------------LKKDATKAAGGEPAGGAVPDLTK   418
Sco4508     RWLPHSRPSGGQDVNVLIGTDAETVGARIGELTQILDARKKAAEQKGGGAQGSSFTDPDI   511
              :* :**. *:                          :*.*::  **   *.:. *

FtsK        TPLPKERDLPPRAEQLQLSGDITYSLPSLDSLTRGGPGKARSA-----------------   461
Sco4508     VV---VWD----------GSRRLRSLPGVVRLLREGPAVSMFAVCIDAEERFLPGECQAF   558
            .      *          ..    ***.:  * * **. :  *

FtsK        ----------------AND---AIVASLTTVFTEFKVDAAVTGFTRG-PTVTRYEVELGP   501
Sco4508     VVAEPRAEESGRQQRDAEARPAQQVAGGFPSFQAWHTNAPAEPEQRARAEKLRLRVE---   615
                           *:      **.    *  ::.:* .    *.     * .**

FtsK        AVKVERITALTKNIA---YAVA-SPDVRIISPIPGKSAVGIEIPNTDREMVNLGDVLRLA   557
Sco4508     EAGVERITGVRPDFVTPAWCLRLARSLSALRDISGETE-DSALPGSS----RLLDVLQLE   670
             . *****.:  ::.   :.:  : .:  :  * *::  .  :*.:.    .* ***:*

FtsK        ESA---------EDDDPMLVAFGKDVEGGYVMHSLAKMPHMLVAGATGSGKSSCINCLIT   608
Sco4508     PPTADAIGARWRMGGQSTMAVIGESYDGPFGIDMRKDGPHGLIAGTTGSGKSELLQTIVA   730
              :          ..:  :..:*:. :* : :.   . ** *:**:******. :: :::

FtsK        SIMMRATPEDVRMILVDPKRVE-LTAYEGIPHLITPIITNP-KRAAEALQWVVREMDLRY   666
Sco4508     ALAVANTPENMTFVLVDYKGGSAFKDCVKLPHTVGMVTDLDAHLVERALESLGAELKRRE   790
            :: :  ***:: ::*** *  . :.    :** :  :     : . .**: :  *:. *

FtsK        DDLAAYGYRHIDDFNRAVREGKVKPPEGSERELQPYPYLLVIVDELADLMMVAPRDVEDA   726
Sco4508     HILAAADAKDIEDYQDLVRRD---------PSHAPVPRLLIVIDEFASMVRDLP-DFVTG   840
            . *** . :.*:*::  **..          .  * * **:::**:*.::   * *.  .

FtsK        IVRITQLARAAGIHLVLATQRPSVDVVTGLIKANVPSRLAFATSSLADSRVILDQPGAEK   786
Sco4508     LVNIAQRGRSLGIHLLLATQRPSGVVS-PEIRANTNLRIALRVTDGGESSDVIDSPEAGH   899
            :*.*:* .*: ****:*******  *    *:**.  *:*: .:. .:*  ::*.* * :

FtsK        LIGKGDG-LFLPMGANKPTRMQGAFVTEEEVATV-VQHCKDQMAPVFREDVTVGT--KQK   842
Sco4508     ISKNTPGRAYVRLGHSSLVPFQSGRVGGRRPGAADPAALAPWVGPLGWEELGRAALTKPK   959
            :  :  *  :: :* .. . :*.. *  .. .:.        :.*:  *::  .:  * *
```

```
FtsK          --KEIDEDIGDDLDLLCQAA-------------------------------------E   861
Sco4508       TESREDDEI-TDLKVLVDAVRDANRSMGIPAQHSPWLPALDEKLLLDEIDVPALAGAAPG   1018
                .. *::*  **.:* :*.

FtsK          LVVSTQFGSTS----MLQRKLRVGFAKAGRLMDLMESRS----IVGPSEGSKARDVLVK-   912
Sco4508       KLPPAPYGIEDLPSDQARRPVVVDFASFGHLMIGGAPRSGRSQVLRTIAGSLARTHSTAD   1078
               :  : :*  .      :* : *.**. *:**     **    ::    ** **   .


FtsK          -----PDELDGVLAV------------------------IRGESEG*-----------   929
Sco4508       VHLYGIDCGNGALNALTRLPHCGAVVGRNQTERVVRLVNRLKGELSRRQDLLADSGFADI   1138
                    *  :*.* .                          ::** .

FtsK          ------------------------------------------------------------   929
Sco4508       GEQRASAEESERLPHIVVLLDRWEGWVPTLGEVDHGSLTDELQTMMREGASVGIHLILTG   1198


FtsK          ------------------------------------------------------------   929
Sco4508       DRTLLVGRIATLTEDKYGLRLADRSDFASLGIPSRKVPEEIPPGRAFRNEAGTETQFALL   1258


FtsK          ------------------------------------------------------------   929
Sco4508       SEDTTGQGQAAAITAIGEAAAARDAGVPRARRPFRVDSLPSRISFPEAWEMHDPEASRSR   1318


FtsK          ------------------------------------------------------------   929
Sco4508       LWALIGIGGDEIVGFGPDLADGVPSFVIAGPAKSGRSTVLMNVAQSLLAQGTRLVVAAPR   1378


FtsK          ------------------------------------------------------------   929
Sco4508       QSPVRQLDGAEGVLKVFTGDDIDEDEFEELIDGASPEEPIAVLVDDGEILEDCDAESQMK   1438


FtsK          ------------------------------------------------------------   929
Sco4508       KIVSRGAERGLALVIAGDEEDVCSGFSGWQVDAKKARRGILLSPQESSSGDLIGLRVSRQ   1498


FtsK          ----------------------------       929
Sco4508       MVGGQVTPGKGMLHLGDGELRTVVVPG*       1525
```

Figure 2.5: Sequence Alignment of FtsK and HfkA (Sco4508) shows the highly conserved amino acids between the C-terminal domain of the polypeptides.

The following alignment shows the region of homology between the known FtsK protein and its uncharacterized homolog, Sco4508 (HfkA). The membrane spanning regions are highlighted in green (predicted using ExPasy proteomics tools), the cytoplasmic regions are highlighted in grey and the motor domain is highlighted in blue. The gamma (γ) domain within the C-terminal containing the DNA recognition sequence (KOPS) is highlighted yellow. Based on the Clustal Omega parameters, the homologous amino acids are represented by asterisk (*) indicates a conserved residue, colon (:) indicates conservation between groups of strongly similar properties, period (.) indicates conservation between

groups of weakly similar properties. There is some homology in the N-terminal domain in the transmembrane spanning segments, which can be narrowed down to 22 amino acids (250-272) in Sco4508 (based on Expasy tools). The shared homology is mostly observed between the cytoplasmic domain where the ATPase domains can be predicted in the 446 amino acids (522-968) of Sco4508. There is also some homology in the 156 amino acids (969-1125) of Sco4508 over the DNA recognition domain of FtsK. It is interesting to see that the C-terminal of Sco4508 extends 399 amino acids longer than FtsK.

```
Sclav4639          SAKPRTGRTSGATAAAKKKAAAGKPGAPAAKGPAGGKTSAKPPAKKATGRKAPAAAARKA       75
Sven5398           TAKPRAGRTTGAAKKAA---P--------------AKSPAKPPAKKAP--AKKAAPAKRA       70
Sgr1771            AAKR-VGRTPGPAKKAA------------------------PAKKTAP--RKSAAPAKRA       48
FtsKSc             --KA-AAPAKG-------------------------------PVKKA----AAKKAPAKRA       49
Sli6011            --KA-AAPAKG-------------------------------PVKKA----AAKKAPAKRA       49
Sav2510            --KA-AVPTKA-------------------------------PAKKA----PAKKAAVRKA       49
FtsKCglu           RSIGELGRRRNEDVLDDF-----------------DDFEEEIATKPATR-----------       34
FtsKMsmeg          SSSRSSGRSRGGAKQGAQ-----------------DGARRKPPTRPAPQ-----------       97
SpoIIIEBs          ------------------------------------------------------------       0
FtsKCcres          ---------------------------------------MSS--------------          3
FtsKMxan           --------------------PTLAAG-----------------IAT--------------       29
FtsKEc             --------------EQTYQQPAAQEPLY--QQP--QPVEQQPVVEP--------------       479
FtsKPaeru          ------------------------------------------------------------       0
Sco4508(HfkA)      ---VE----------LARYAPPNAALK-W-SEDGVGLD--------------------YNRP       222
Sco5734            --------------------------------VSQFV--------------------IKRP       9

Sclav4639          PAKRTAAQKAAPRPA-----PSPTGGLYRLVRALWLGLARTVGALVRGIGRGAKGLDQAH       130
Sven5398           PARKTAAKKAAPRPA-----PSPTGGIYRLARGAWLGVAHAVGAMFRGIGRGAKGLDPAH       125
Sgr1771            PAKKAAARKPAPKPA-----PSPTGGVYRLVRAVWLGAAHGVGAMFRSIGRGAKGLDPAH       103
FtsKSc             PAKKAAARKPAPQPA-----PNPTNGVYRLVRALWLGLAHGVGAVFRGIGQGAKNLDPAH       104
Sli6011            PAKKAAARKPAPQPA-----PNPTNGVYRLVRALWLGLAHGVGAVFRGIGQGAKNLDPAH       104
Sav2510            PARKVAAKKPAPKPA-----PNPTGGVYKLARALWLGVAHAVGAMFRGIGQGAKGLDPAH       104
FtsKCglu           -KSRSKAVEPEPE-------F--DED------------------FDEQSGNR-TSAYVEE       65
FtsKMsmeg          -QRRKPARRPQASPV-----ALAGHKLGQGARAGWLMLAKGAGSTARSVGRA-RDIEPGH       150
SpoIIIEBs          --------------MSVAKK----K------RK--------------SRKKQAKQLN-IK       21
FtsKCcres          -ETFMA----------RAARRSTTELLWDAIRYGWAQPWT-------ARFR---------       36
FtsKMxan           -ARYAAETRRGKTDMTAKKGRAEKAVLSRQEIATRRRALAD------KRMKAGKGGDVTT       82
FtsKEc             -EPVVEETKPARPPLYYFEEVEEKRAREREQLAAWYQPIP-------EPVK---------       522
FtsKPaeru          ---------------MRRKNSDLKDSTTASHAAAWRQQLH-------SRLK---------       29
Sco4508(HfkA)      -PR----LRPAERQT-NFRLPSSPRD-YEARPLPWLMALT--------------------       255
Sco5734            -PR----TLPPDVPS-DELLLEAPPELPRGQQEGVLMQVL--------------------       43

Sclav4639          LTTVFTEFKVDAAVTGFTRGPTVTRYEVELGPAVKVERITALTKNIAYAVASPDV----R       545
Sven5398           LSNVFTEFKVDAAVTGFTRGPTVTRYEVELGPAVKVEKITALTKNIAYAVASPDV----R       550
Sgr1771            LTNVFTEFKVDAAVTGFTRGPTVTRYEIELGPAVKVEKITALAKNIAYAVASPDV----R       536
FtsKSc             LTTVFTEFKVDAAVTGFTRGPTVTRYEVELGPAVKVERITALTKNIAYAVASPDV----R       525
Sli6011            LTTVFTEFKVDAAVTGFTRGPTVTRYEVELGPAVKVERITALTKNIAYAVASPDV----R       525
Sav2510            LSNVFMEFKVDAAVTGFTRGPTVTRYEVELGPAVKVERITALTKNIAYAVASPDV----R       513
FtsKCglu           ITDVFSEFNVDATVTGFSRGPTVTRYEIELGPGVKVSKITNLQSNIAYAVATENV----R       482
FtsKMsmeg          ITSVLEQFKVDAAVTGCTRGPTVTRYEVELGPGVKVEKITALHRNIAYAVATESV----R       510
SpoIIIEBs          LERTFQSFGVKAKVTQVHLGPAVTKYEVYPDVGVKVSKIVNLSDDLALALAAKDI----R       401
FtsKCcres          LESVLAEFGVKGQIDQIRPGPVVTMYELVPAPGVKTARVVALADDIARSMSVISC----R       412
FtsKMxan           LRAKLADFGIVGEVVEIRPGPVVTMYEFLPGPGIKVSKIAALADDLAMAMEAMRV----R       587
FtsKEc             VEARLADFRIKADVVNYSPGPVITRFELNLAPGVKAARISNLSRDLARSLSTVAV----R       923
FtsKPaeru          LEIKLKEFGVEVSVDSVHPGPVITRFEIQPAAGVKVSRISNLAKDLARSLAVISV----R       398
Sco4508(HfkA)      LRLRVEEAGVER-ITGVRPD-------FVTPA---------WCLRLARSLSALRDISGET       652
Sco5734            --------GGVA-YEG-APD-------VMPLP---------GAEALARQLAPLRMGGGD-       403
                                     .       .               :*  :

Sclav4639          IISPIPGKS----AVGIEIPNTDREMVKVGDVLRLADAAEDDHPMLVALGKDVEGGYVMA       601
Sven5398           IISPIPGKS----AVGIEIPNSDREMVNLGDVLRLAAAAEDDHPMLVALGKNVEGGYEMA       606
Sgr1771            IISPIPGKS----AVGIEIPNSDREMVNLGDVLRLADAAEDDHPMLVALGKNVEGGYEMA       592
FtsKSc             IISPIPGKS----AVGIEIPNTDREMVNLGDVLRLAESAEDDDPMLVAFGKDVEGGYVMH       581
Sli6011            IISPIPGKS----AVGIEIPNTDREMVNLGDVLRLAESAEDDDPMLVAFGKDVEGGYVMH       581
Sav2510            IISPIPGKS----AVGIEIPNTDREMVNLGDVLRLADAAEDDHPMLVALGKDVEGGYVMA       569
FtsKCglu           LLTPIPGKS----AVGIEVPNSDREMVRLGDVLNARATVENKDSMLIGLGKDIEGDFVSY       538
FtsKMsmeg          MLAPIPGKS----AVGIEVPNTDREMVRLSDVLTAPSTRRDHHPLVIGLGKDIEGDFVSA       566
SpoIIIEBs          IEAPIPGKS----AIGIEVPNAEVAMVSLKEVLESKLNDRPDAKLLIGLGRNISGEAVLA       457
FtsKCcres          V-AVAQGRN----AIGIEMPNQRRETVYLRDLLSSADYEKASQILPMALGETIGGEPYIA       467
FtsKMxan           IVAPIPGKG----VVGIEVPNRDRETVYLKEIAEQDAFNKGASKLTMCVGKDIEGMPYVL       643
FtsKEc             VVEVIPGKP----YVGLELPNKKRQTVYLREVLDNAKFRDNPSPLTVVLGKDIAGEPVVA       979
FtsKPaeru          VVEVIPGKT----TVGIEIPNEDRQMVRFSEVLSSPEYDEHKSTVPLALGHDIGGRPIIT       454
Sco4508(HfkA)      EDSALPGSSRLLDVLQLEPPTADA-------IGARWRMGGQSTM--AVIGESYDG-PFGI       702
Sco5734            DDEPLLANLDFTELLGLGDAASVD-------VRRTWRPRSTPERLRVPIGVGEDGRPVML       456
                         .      : :             :                .*    *
```

```
Sclav4639          NLAK------MPHILVAGATGSGKSSCINCLITSVMIRATPEDVRMVLVDPKRVE-LTAY       654
Sven5398           NLAK------MPHVLVAGATGSGKSSCINCLITSIMIRATPEDVRMVLVDPKRVE-LTAY       659
Sgr1771            NLAK------MPHVLVAGATGSGKSSCINCLITSIMVRATPDDVRMVLVDPKRVE-LTAY       645
FtsKSc             SLAK------MPHMLVAGATGSGKSSCINCLITSIMMRATPEDVRMILVDPKRVE-LTAY       634
Sli6011            SLAK------MPHMLVAGATGSGKSSCINCLITSIMMRATPEDVRMILVDPKRVE-LTAY       634
Sav2510            NLAK------MPHLLVAGATGSGKSSCINCLITSVMVRATPEDVRMVLVDPKRVE-LTAY       622
FtsKCglu           SVQK------MPHLLVAGSTGSGKSAFVNSLLVSLLTRAKPEEVRLILVDPKMVE-LTPY       591
FtsKMsmeg          NLAK------MPHLLVAGSTGSGKSSFVNSMLVSLLARATPEEVRMILIDPKMVE-LTPY       619
SpoIIIEBs          ELNK------MPHLLVAGATGSGKSVCVNGIITSILMRAKPHEVKMMMIDPKMVE-LNVY       510
FtsKCcres          DLAK------MPHLLIAGTTGSGKSVGVNAMILSILYKLPPEKCRFIMVDPKMLE-LSVY       520
FtsKMxan           DLAK------APHLLIAGTTGSGKSVAVNSMIMSILLKATPEEVRFIMVDPKMLE-LSVY       696
FtsKEc             DLAK------MPHLLVAGTTGSGKSVGVNAMILSMLYKAQPEDVRFIMIDPKMLE-LSVY       1032
FtsKPaeru          DLAK------MPHLLVAGTTGSGKSVGVNAMLLSILFKSTPSEARLIMIDPKMLE-LSIY       507
Sco4508(HfkA)      -----DMRKDGPHGLIAGTTGSGKSELLQTIVAALAVANTPENMTFVLVDYKGGSAFKDC       757
Sco5734            DLKEAAQDGMGPHGLCVGATGSGKSELLRTLVLGLAVTHSSETLNFVLADFKGGATFAGM       516
                                ** * .*:******  :. :: .:          ::: * *    :

Sclav4639          EGIPHLITPIITNPKR----AAEALQWVVREMDLRYDDLA-AFGFRHIDDFNRAVRAGKV       709
Sven5398           EGIPHLITPIITNPKR----AAEALQWVVKEMDLRYDDLA-AFGYRHIDDFNQAIRDGKI       714
Sgr1771            EGIPHLITPIITNPKK----AAEALQWVVREMDLRYDDLA-NFGYRHIDDFNHAVRNGKC       700
FtsKSc             EGIPHLITPIITNPKR----AAEALQWVVREMDLRYDDLA-AYGYRHIDDFNRAVREGKV       689
Sli6011            EGIPHLITPIITNPKR----AAEALQWVVREMDLRYDDLA-AYGYRHIDDFNRAVREGKV       689
Sav2510            EGIPHLITPIITNPKR----AAEALQWVVREMDLRYDDLA-AFGYRHIDDFNEAIRNGKV       677
FtsKCglu           EGIPHLITPIITQPKK----AAAALQWLVEEMEQRYMDMK-QTRVRHIKDFNRKIKSGEI       646
FtsKMsmeg          EGIPHLITPIITEPKK----AAAALGWLVEEMEQRYQDMQ-ASRVRHIDVFNEKVRSGEI       674
SpoIIIEBs          NGIPHLLAPVVTDPKK----ASQALKKVVNEMERRYELFS-HTGTRNIEGYNDYIKRANN       565
FtsKCcres          DGIPHLLAPVVTDPKK----AVVALKWTVREMEDRYRRMS-KIGVRNIGGYNEKANEAAA       575
FtsKMxan           EGIPHLLLPVVTDPKK----AALALRWAVEEMERRYQMLS-EAGVRNIAGFNKLVESTAV       751
FtsKEc             EGIPHLLTEVVTDMKD----AANALRWCVNEMERRYKLMS-ALGVRNLAGYNEKIAEADR       1087
FtsKPaeru          EGIPHLLCPVVTDMKE----AANALRWSVAEMERRYRLMA-AMGVRNLAGFNRKVKDAEE       562
Sco4508(HfkA)      VKLPHTVG-MVTDLDAH--LVERALESLGAELKRREHILA-AADAKDIEDYQDLVRRD--       811
Sco5734            SQMPHVAA-VITNLADDLTLVDRMGDAIRGELQRRQELLRSAGNYANLHDYEKARAAG--       573
                     :**    ::*:       .         *:. *   :       .:  ::

Sclav4639          KP----------------------------------------------------------       711
Sven5398           QL----------------------------------------------------------       716
Sgr1771            KA----------------------------------------------------------       702
FtsKSc             KP----------------------------------------------------------       691
Sli6011            KP----------------------------------------------------------       691
Sav2510            KL----------------------------------------------------------       679
FtsKCglu           ET----------------------------------------------------------       648
FtsKMsmeg          ST----------------------------------------------------------       676
SpoIIIEBs          E-----------------------------------------------------------       566
FtsKCcres          KGEHFERTVQTG------------------------------------------------       587
FtsKMxan           EVKTTTESAPKKKAKPKNVLVLDGESPKSSMPAGGESLGVAAPRDDEDDMLDAQAPEEAE       811
FtsKEc             MMRPIPD-----------------------------------------------------       1094
FtsKPaeru          AGTPLTD-----------------------------------------------------       569
Sco4508(HfkA)      ----------------------------------------------------------       811
Sco5734            ----------------------------------------------------------       573



Sclav4639          -------------------PEGSGRELQPYPYLLVIVDELADLMMVAPRDVEDSVVRITQ       752
Sven5398           -------------------PEGSERELKTYPYLLVIVDELADLMMVAPRDVEDSIVRITQ       757
Sgr1771            -------------------PEGSERELSPYPYLLVIVDELADLMMVAPRDVEDSIVRITQ       743
FtsKSc             -------------------PEGSERELQPYPYLLVIVDELADLMMVAPRDVEDAIVRITQ       732
Sli6011            -------------------PEGSERELQPYPYLLVIVDELADLMMVAPRDVEDAIVRITQ       732
Sav2510            -------------------PEGSERELSPYPYLLVIVDELADLMMVAPRDVEDAIVRITQ       720
FtsKCglu           -------------------PPGSKREYRAYPYIVCVVDELADLMMTAPKEIEESIVRITQ       689
FtsKMsmeg          -------------------PLGSERVYKPYPYIVAIVDELADLMMTAPRDVEDAIVRITQ       717
SpoIIIEBs          ----------------------EGAKQPELPYIVVIVDELADLMMVASSDVEDSITRLSQ       604
FtsKCcres          ---FD--DAGRPI------YETEQIRPEPMPYLVVVIDEVADLMMVAGKDIEGAVQRLAQ       636
FtsKMxan           APELEDESEDTEAMEASESTEPEKKQLKKLPYIVVIIDELADLMMVASREVETYVARLAQ       871
FtsKEc             -----------PYWKPGDSMDAQHPVLKKEPYIVVLVDEFADLMMTVGKKVEELIARLAQ       1143
FtsKPaeru          -----------PLFRRE-SPDDEPPQLSTLPTIVVVVDEFADMMMIVGKKVEELIARIAQ       617
Sco4508(HfkA)      ------------------------PSHAPVPRLLIVIDEFASMVRDLP-DFVTGLVNIAQ       846
Sco5734            ------------------------APLEPLASLVLVIDEFSELLTAKP-DFIDMFIQIGR       608
                                          :: ::**.:.::     ..   . .: :
```

```
Sclav4639          LARAAGIHLVLATQRPSVDVVTGLIKANVPSRLAFATSSLADSRVILDQPGAEKLI-GKG       811
Sven5398           LARAAGIHLVLATQRPSVDVVTGLIKANVPSRLAFATSSLADSRVILDQPGAEKLI-GKG       816
Sgr1771            LARAAGIHLVLATQRPSVDVVTGLIKANVPSRLAFATSSLADSRVILDQPGAEKLI-GKG       802
FtsKSc             LARAAGIHLVLATQRPSVDVVTGLIKANVPSRLAFATSSLADSRVILDQPGAEKLI-GKG       791
Sli6011            LARAAGIHLVLATQRPSVDVVTGLIKANVPSRLAFATSSLADSRVILDQPGAEKLI-GKG       791
Sav2510            LARAAGIHLVLATQRPSVDVVTGLIKANVPSRLAFATSSLADSRVILDQPGAEKLI-GKG       779
FtsKCglu           KARAAGIHLVLATQRPSVDVVTGLIKTNVPSRLAFATSSLTDSRVILDQGGAEKLI-GMG       748
FtsKMsmeg          KARAAGIHLVLATQRPSVDVVTGLIKTNVPSRLAFATSSLTDSRVILDQAGAEKLI-GMG       776
SpoIIIEBs          MARAAGIHLIIATQRPSVDVITGVIKANIPSRIAFSVSSQTDSRTILDMGGAEKLL-GRG       663
FtsKCcres          MARAAGIHLIMATQRPSVDVITGTIKANFPTRISFQVTSKIDARTILGEQGAEQLL-GQG       695
FtsKMxan           MARAAGIHLMVATQRPSTDVVTGVIKANFPTRVSFMLRSKPDSMTILGTVGAEALL-GMG       930
FtsKEc             KARAAGIHLVLATQRPSVDVITGLIKANIPTRIAFTVSSKIDSRTILDQAGAESLL-GMG      1202
FtsKPaeru          KARAAGIHLILATQRPSVDVITGLIKANIPTRIAFQVSSKIDSRTILDQGGAEQLL-GHG       676
Sco4508(HfkA)      RGRSLGIHLLLATQRPSGVVSPE-IRANTNLRIALRVTDGGESSDVIDSPEAGHISKNTP       905
Sco5734            IGRSLGVHLLLASQRLEEGRLRG-LDTYLSYRVGLRTFSAAESRAALGVPDAYHL-PSVP       666
                    .*: *:**::*:** .       : :    *:.:   .  ::   :.   *  :  .

Sclav4639          DGLFLPMGANKPVRMQGAFVTEDEVAAVVQHCKD----QMTPVFREDVVVG-SQQKREV-       865
Sven5398           DGLFLPMGANKPVRMQGAFVTEHEVAAVVQHCKD----QMTPVFRDDVTVG-TKQKKEI-       870
Sgr1771            DGLFLPMGANKPTRMQGAFVTEDEVAAVVQHCKD----QMAPVFRDDVVVG-TKQKKEI-       856
FtsKSc             DGLFLPMGANKPTRMQGAFVTEEEVATVVQHCKD----QMAPVFREDVTVG-TKQKKEI-       845
Sli6011            DGLFLPMGANKPTRMQGAFVTEEEVATVVQHCKD----QMAPVFREDVTVG-TKQKKEI-       845
Sav2510            DGLFLPMGANKPTRMQGAFVTEDEVEAVVQHCKD----QMAPVFRDDVTVG-TKQKKEI-       833
FtsKCglu           DALFIPQGAGKPQRIQGAFVTDEEIQAVVDMAKA----QRQPEYTDGVTEDKASEAKKI-       803
FtsKMsmeg          DGLFLPMGANKPIRMQGAFITDEEIHAVVAATKE----QAEPEFVEGVTAVKAGERKDV-       831
SpoIIIEBs          DMLFLPVGANKPVRVQGAFLSDDEVEKVVDHVIT----QQKAQYQEEMIPEETTETH---       716
FtsKCcres          DMLYMAGG-GRITRLHGPFVSDGEVEAVARFLRD----QGIPQYLDEVTAGGDEEQEEAI       750
FtsKMxan           DMLIMPPTSAHLQRVHGAFVSENEIKKAVDHLKA----QGKPVYDDSILKPRDEDVEGG-       985
FtsKEc             DMLYSGPNSTLPVRVHGAFVRDQEVHAVVQDWKA----RGRPQYVDGITSDSESEGG-A-      1256
FtsKPaeru          DMLYLPPGTGLPIRVHGAFVSDDEVHRVVEAWKL----RGAPDYIEDILAGVDEGGGGG-       731
Sco4508(HfkA)      GRAYVRLGHSSLVPFQSGRVGGRRPGAADPAA------------LAPWVGPLGWEELGR-       952
Sco5734            GSGYLKFGTEEMVRFKAAYVSGPYRGGAPDTSASRVPVERRPSLFTAVHVPVTYAAPDP-       725
                   .             .:.  :       .

Sclav4639          DE---------EIGDDLDLLCQAAEL--VVSTQFGSTSMLQRKLRVGFAKAGRLMDLMES       914
Sven5398           DE---------DIGDDLDLLCQAAEL--VVSTQFGSTSMLQRKLRVGFAKAGRLMDLMES       919
Sgr1771            DE---------DIGDDLDLLCQAAEL--VVSTQFGSTSMLQRKLRVGFAKAGRLMDLMES       905
FtsKSc             DE---------DIGDDLDLLCQAAEL--VVSTQFGSTSMLQRKLRVGFAKAGRLMDLMES       894
Sli6011            DE---------DIGDDLDLLCQAAEL--VVSTQFGSTSMLQRKLRVGFAKAGRLMDLMES       894
Sav2510            DE---------DIGDDLDLLCQAAEL--VVSTQFGSTSMLQRKLRVGFAKAGRLMDLMES       882
FtsKCglu           DA---------DIGNDLEDLLEAVEL--VVTSQMGSTSMLQRKLRIGFAKAGRLMDLMET       852
FtsKMsmeg          DP---------DIGDDLDVFLQAVEL--VVSSQFGSTSMLQRKLRVGFAKAGRLMDLMET       880
SpoIIIEBs          ------------SEVTDELYDEAVEL--IVGMQTASVSMLQRRFRIGYTRAARLIDAMEE       762
FtsKCcres          EGAFSGE------GGANDLYDHAVAV--VTRDRKASTSYIQRRLQIGYNRAASLMERMEK       802
FtsKMxan           -GEE--------DELSDELYDQALAT--VSEMRAVSISMLQRKMRIGYNRAARMIERMER      1034
FtsKEc             -GGFDGA------EELDPLFDQAVQF--VTEKRKASISGVQRQFRIGYNRAARIIEQMEA      1307
FtsKPaeru          -GSFDGGDGSGEGSEDDPLYDEAVRF--VTESRRASISAVQRKLKIGYNRAARMIEAMEM       788
Sco4508(HfkA)      --AA-LTKPKTESREDDEITDLKVLVDAVRDANRSMGIPAQHSPWLPALDEKLLLDEIDV      1009
Sco5734            --ER-DERAAAGRQEDDALADTV--LDVIVQRLEGQG-VAAHQVWLPPLDEAPTMDQVL-       778
                                           :            :   :        :: :


Sclav4639          RSIVGPS-EGSKARDVLVKPEELDGVLALIRGEP--HP----------------------       949
Sven5398           RNIVGPS-EGSKARDVLIKPDELDDVLAVIRGES--GA*---------------------       954
Sgr1771            RNIVGPS-EGSKARDVMVKPDELDGVLAVIRGES--AP----------------------       940
FtsKSc             RSIVGPS-EGSKARDVLVKPDELDGVLAVIRGES--EG----------------------       929
Sli6011            RSIVGPS-EGSKARDVLVKPDELDGVLAVIRGES--EG----------------------       929
Sav2510            RNIVGPS-EGSKARDVLVKADELDGVLAVIRGEA--AP----------------------       917
FtsKCglu           RGVVGPS-EGSKAREVLVKPEELETILWMLKGAD--PADAPKEETWDDEVAAEAEEAANT       909
FtsKMsmeg          RGIVGPS-EGSKAREVLVKPEDLAGTLALIRGGA--DANGAEPEDGEEF-----------       926
SpoIIIEBs          RGVVGPY-EGSKPREVLLSKEKYDELSS---------------------------------       789
FtsKCcres          EGVVGAA-NHAGKREILAPPPPPL-----------------------------------       825
FtsKMxan           DGVVGAA-DGAKPREVLIRGLGDMPGAGAM-----------------------------       1063
FtsKEc             QGIVSEQ-GHNGNREVLAPPPFD-------------------------------------       1329
FtsKPaeru          AGVVTPM-NTNGSREVIAPAPVRD-------------------------------------       811
Sco4508(HfkA)      PALAGAAP-G--------------KLPPAPYGIEDLPSDQARRPVVVDFA------SFGH       1048
Sco5734            PALAVTPERGVQAREYTR-----LGGLTVPLGLIDKPFEQKREVLYQDFSA-----ASGH       828
                     :.
```

Figure 2.6: A multiple sequence alignment of known FtsK/SpoIIIE proteins in different model bacteria shows the conserved amino acid residues in the C-terminal region of the proteins.

A multiple sequence alignment of known FtsK/SpoIIIE proteins in model bacterial species using Clustal Omega. Partial lengths of proteins are aligned to show the different between the N-terminal, linker and C-terminal domains of the respective proteins. An asterisk (*) indicates a conserved residue, colon (:) indicates conservation between groups of strongly similar properties, period (.) indicates conservation between groups of weakly similar properties. The grey highlighted areas show the highest regions of conservation, likely containing the ATPase domains of these proteins. The alignment shows FtsKSc (Sco5750), *S. coelicolor*; Sli601, *S. lividans*, Sav2510, *S. avermitilis*; Sven5398, *S. venezuelae*; Sgr1711, *S. gresius*; Sclav4639, *S. clavicans*; FtsKEc, *E. coli*; FtsKPaeru, *P. aeruginosa*; FtsKCcres, *C. crescentus*; FtsKMxan, *M. xanthus*; SpoIIIEBs, *B. subtilis* protein SpoIIIE; FtsKCglu, *C. glutamicum*; FtsKMsmeg, *M. smegmatis*, Sco4508 (HfkA), *S. coelicolor* FtsK-like protein; Sco5734, *S. coelicolor* FtsK-like protein. It can be observed that FtsK from *E. coli* FtsK has the longest N-terminal region. All proteins have a conserved patch of amino acids, and several conserved residues. The two proteins Sco4508 (HfkA) and Sco5734 are grossly truncated at the C-terminal end, and go on for a considerable length.

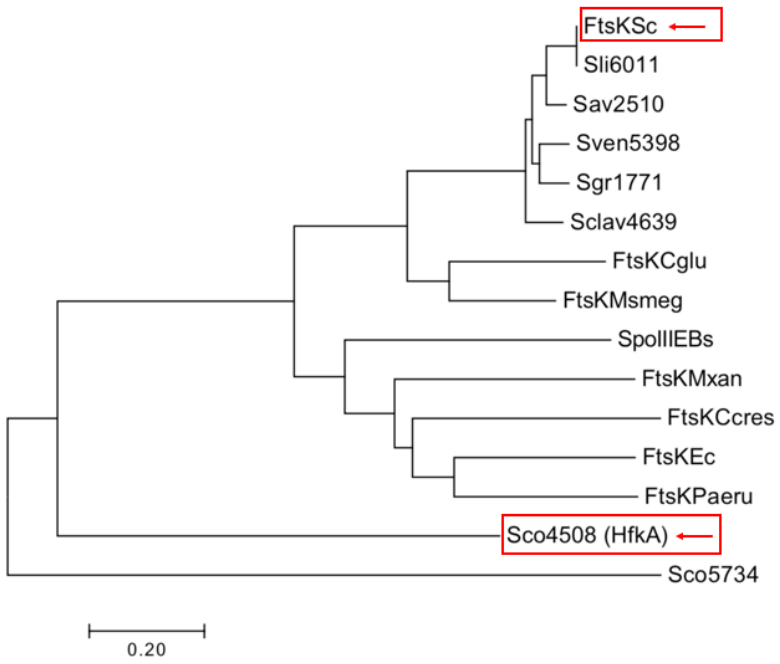

Figure 2.7: Phylogenetic analysis shows that FtsK and HfkA do not group together. This tree was generated using the multiple sequence alignment program Mega 7 of known FtsK proteins in several model bacteria and *Streptomyces* species. It shows FtsKSc (Sco5750), *S. coelicolor*; Sli601, *S. lividans*, Sav2510, *S. avermitilis*; Sven5398, *S. venezuelae*; Sgr1711, *S. gresius*; Sclav4639, *S. clavicans*; FtsKEc, *E. coli*; FtsKPaeru, *P. aeruginosa*; FtsKCcres, *C. crescentus*; FtsKMxan, *M. xanthus*; SpoIIIEBs, *B. subtilis* protein SpoIIIE; FtsKCglu, *C. glutamicum*; FtsKMsmeg, *M. smegmatis*, Sco4508 (HfkA), *S. coelicolor* FtsK-like protein; Sco5734, *S. coelicolor* FtsK-like protein. Two major branches were observed. It can be seen that *S. coelicolor* FtsK groups with FtsK of other multicellular bacteria including other *Streptomyces* species, *C. glutamicum,* and *M. smegmatis.* The other branch showed FtsK proteins in *E. coli*, *C. crescentus, P. aeruginosa* and *M. xanthus*. It can be seen that the two putative FtsK-like proteins, HfkA and Sco5734 grouped separately, indicating that they likely do not contain a DNA motor, and are part of the type VII secretion system.

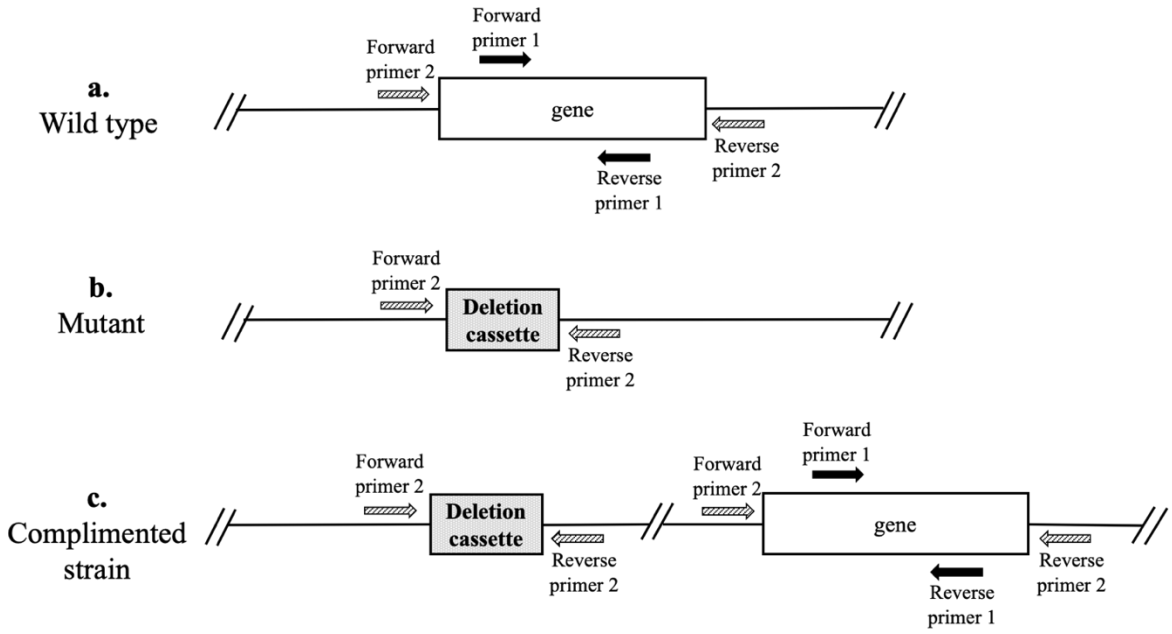

Figure 2.8: **Location of oligonucleotides for PCR amplification for mutation verification.**

This figure describes the locations of the different oligonucleotides designed for each specific gene to verify its presence on the chromosome. Forward primer 1 and reverse primer 1 are internal primers annealing within the gene of interest. These should only result in a PCR product if the wild type gene is present. Forward primer 2 and Reverse primer 2 anneal directly upstream and downstream of the wild type gene, respectively. This should yield a PCR product for both wild type and mutant strains, albeit a different sized product depending on the size of the deletion cassette compared to the original wild type gene.

(a.) shows the wild type gene on the chromosome and the location of the primers. **(b.)** shows the insertion-deletion mutant strain with the deletion cassette in place of the original gene, this strain will not yield any product using the internal primers. (**c.)** shows

a complemented strain with a single copy of the wild type gene as well as the deletion cassette. The genomic DNA obtained from a complemented strain and used as a PCR template should yield both wild type and mutant sized products using the upstream/downstream flanking oligonucleotides, as well as a PCR product using the internal primers. Using the above criteria for PCR verification, all isolated mutant strains were verified this way.

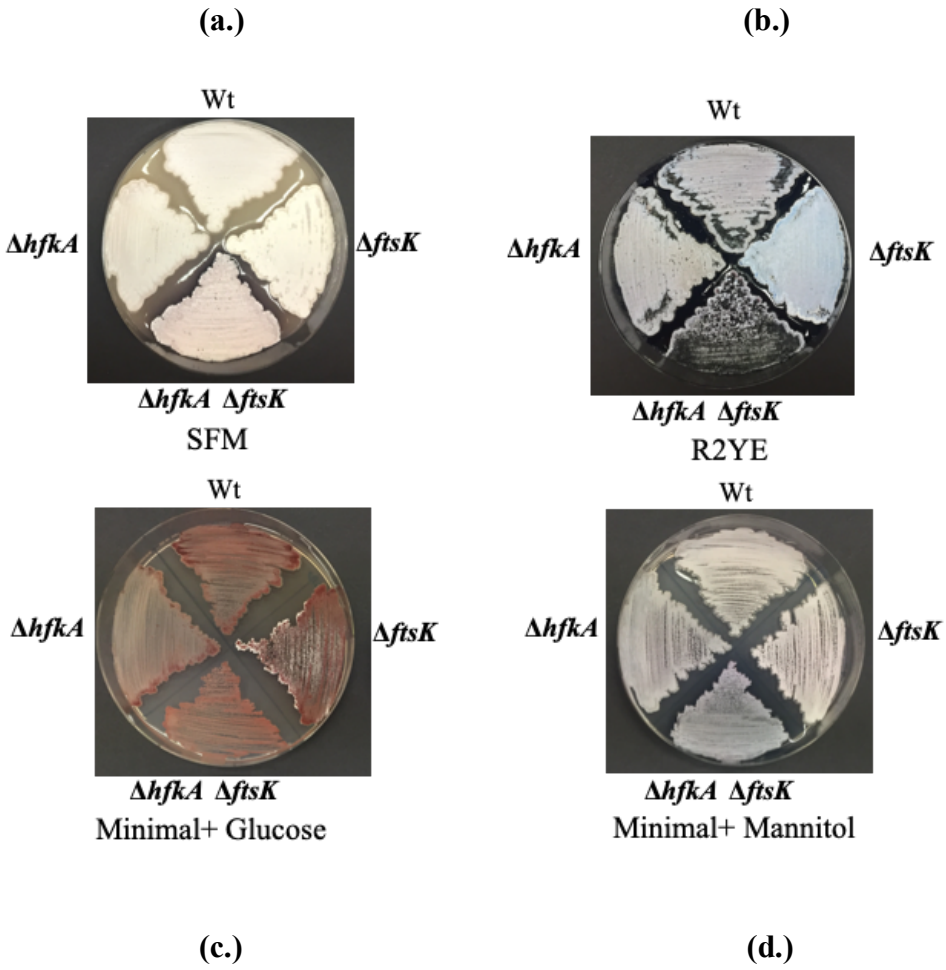

Figure 2.9: *hfkA* and *ftsK* are dispensable for growth and do not have an apparent developmental phenotype in *S. coelicolor.*

Growth and development was observed on different media for the wild type and Δ*hfkA,* Δ*ftsK,* and Δ*hfkA* Δ*ftsK* deletions. Normalized number of spores were inoculated on solid media and plates were grown for 5 days. Panel (a.) shows the mutants grown on sporulating SFM media, (b.) R2YE media,(c.) Minimal media supplemented with glucose, (d.) Minimal media supplemented with mannitol. No overt differences were observed macroscopically. There were slight differences observed in the pigment metabolite production between the strains along with some colony heterogeneity. On R2YE, the aerial mycelium formation of the double mutant strain was slightly delayed.

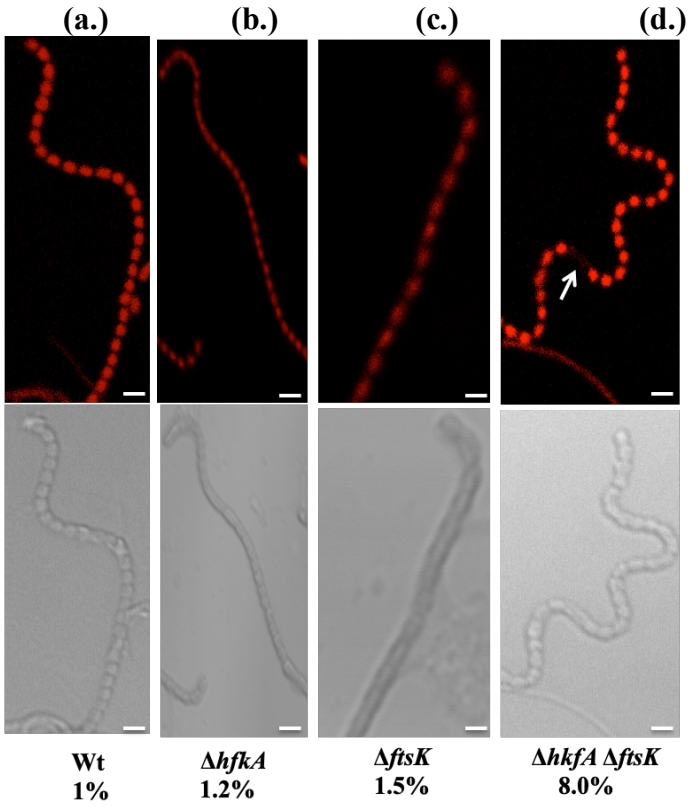

Figure 2.10: **An *hfkA* and *ftsK* double deletion causes an overt segregation phenotype.**

Shown are matching panels of fluorescence and DIC images of the double mutant observed for segregation phenotype. Coverslips were inoculated and hyphae was grown for 4 days on MS agar, fixed and stained with propidum iodide. Top panel shows a propidium iodide image (DNA), and the bottom panel shows a DIC image, of the sporulating aerial hypha. White arrow shows occasional anucleate cells in the spore chain. (a.) Shows the wild type M145 strain, (b.) Shows the single Δ*hfkA* mutant strain SS2, (c.) shows the single Δ*ftsK* mutant SS3, and (d.) shows the Δ*hfkA* Δ*ftsK* double mutant strain SS5. Both single mutants have a wild type-like segregation pattern, whereas the double mutant showed a segregation defect of 8%. Approximatively random 1500 spores were measured. Scale bar is 5 μm.

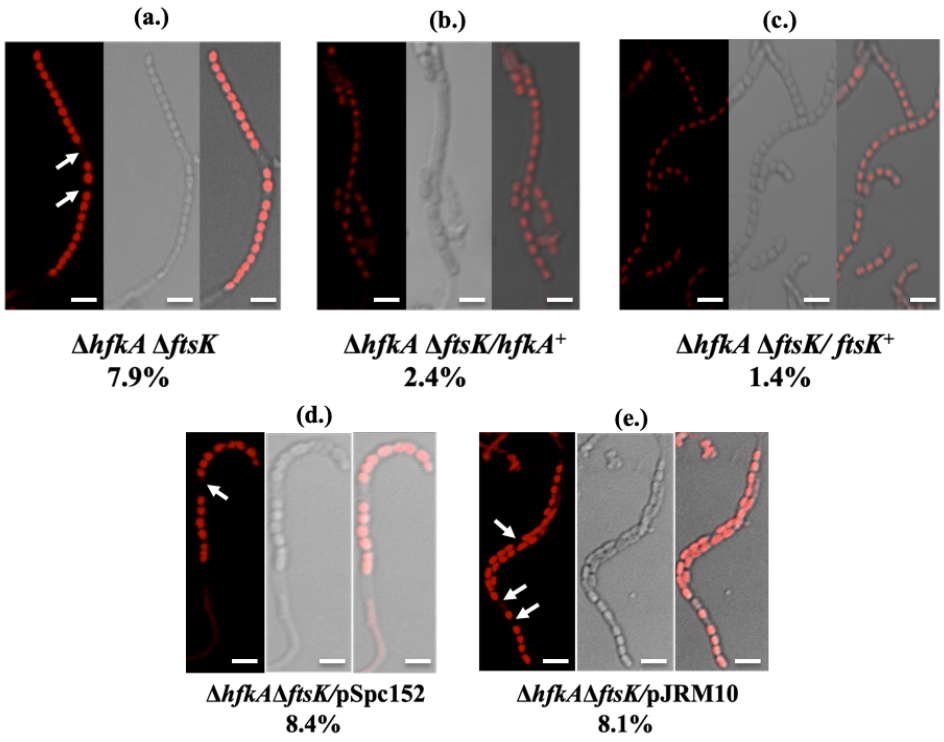

Figure 2.11: **Genetic complementation of Δ*hfkA* Δ*ftsK* double deletion strain with *hfkA*$^+$ or *ftsK*$^+$ restores the segregation phenotype back to wild type.**

Shown are panels of confocal images of the genetic complementation of the Δ*hfkA* Δ*ftsK* double mutant strains (fluorescence, light and merged image). Coverslips were inoculated and hyphae grown for 4 days on SFM (MS) agar, fixed and stained with propidium iodide. (a.) shows the double mutant Δ*hfkA* Δ*ftsK* strain SS5 with an 7.9% segregation phenotype. (b.) shows genetically complemented strain SS10 with 2.4% anucleate spores. (c.) shows genetically complemented strain SS12 with 1.4% anucleate spores. (d.) shows the Δ*hfkA* Δ*ftsK* strain SS1 complemented with the empty vector pSpc152 as a negative control with the segregation defect of 8.4%. (e.) shows the Δ*hfkA* Δ*ftsK* strain SS13 complemented with the empty vector pJRM10 with 8.1% anucleate spores. It can be observed that either *hfkA*$^+$ or *ftsK*$^+$ is able to rescue the double mutant phenotype back to wild type. Scale bar is 5 μm.

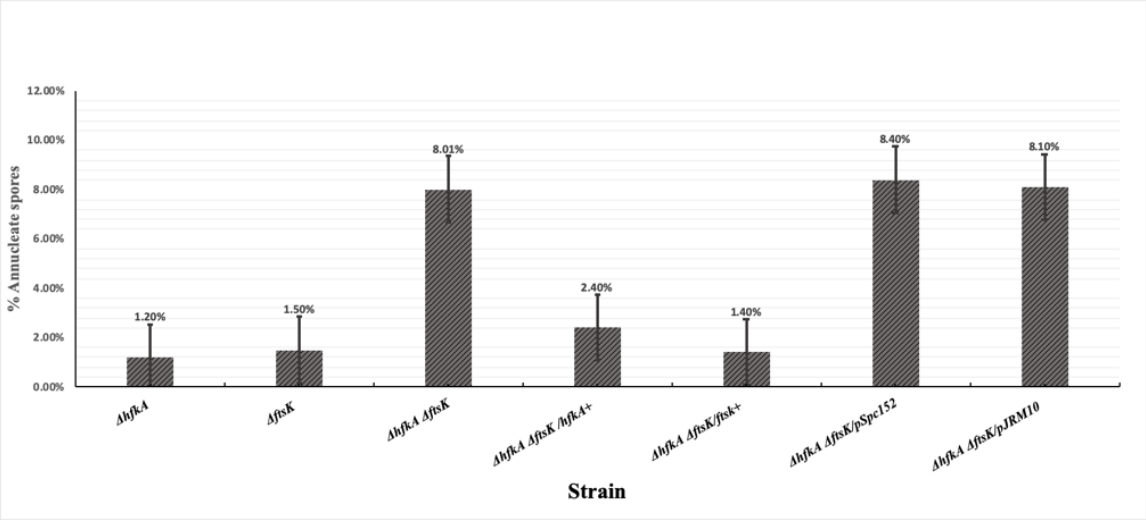

Figure 2.12: Quantification of segregation defect in *hfkA* and *ftsK* single and double mutants showing the restoration of wild type phenotype upon genetic complementation with *hfkA*$^+$ or *ftsK*$^+$.

A summary graph displaying the percent anucleate spores to measured segregation defects for the single and double mutants of *hfkA* and *ftsK*. It can be seen that the Δ*hfkA* Δ*ftsK* double mutant strain SS5 has the most severe phenotype compared to the single mutants Δ*hfkA* strain SS2 and Δ*ftsK* strain SS3. Genetic complementation studies show that phenotype can be rescued by either copy of *hfkA* or *ftsK* back to wild type. Standard error bars are displayed.

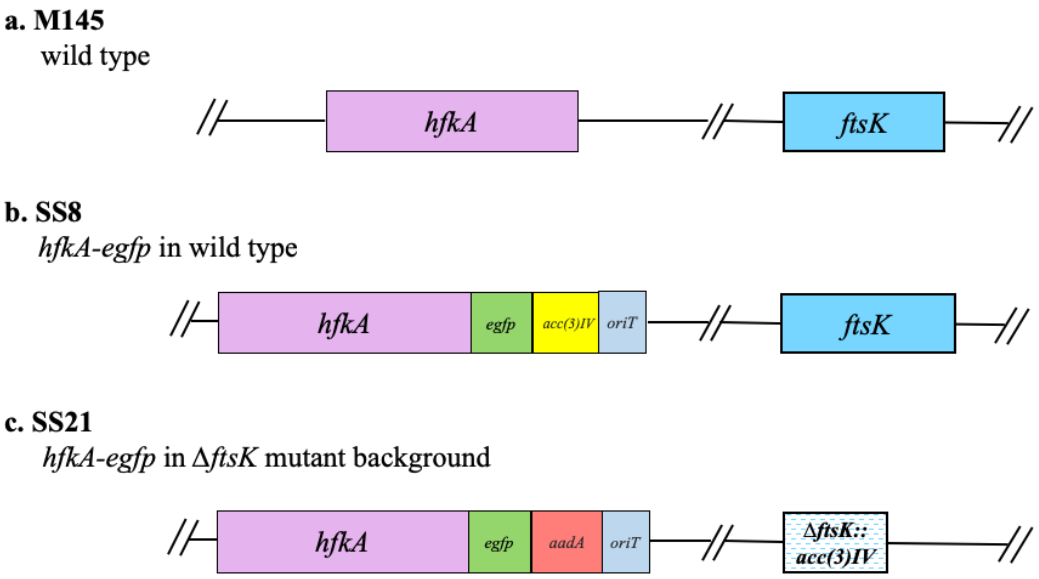

Figure 2.13 Diagram of HfkA-EGFP expressing strains constructed in two different backgrounds to observe localization of HfkA-EGFP in *S. coelicolor.*

The schematic depicts the location of the genes on the chromosome. In (a.) the wild type chromosome shows *hfkA*$^+$ and *ftsK*$^+$ in their representative native locations. (b.) the *hfkA-egfp* strain obtained after homologous recombination of pSS28 in wild type (M145). The *hfkA*$^+$ was replaced with *hfkA-egfp-aadA-oriT* cassette, and therefore the fusion gene is the only copy of *hfkA* in the chromosome. **(c.)** shows the *hfkA-egfp* fusion gene in a mutant background achieved by introducing pSS28 into the Δ*hfkA* Δ*ftsK* (SS5) strain. The Δ*hfkA*::*frt* scar in SS5 was replaced by *hfkA-egfp-aadA-oriT* cassette, at its native location, and thereby the only source on *hfkA* on the chromosome. (Not drawn to scale).

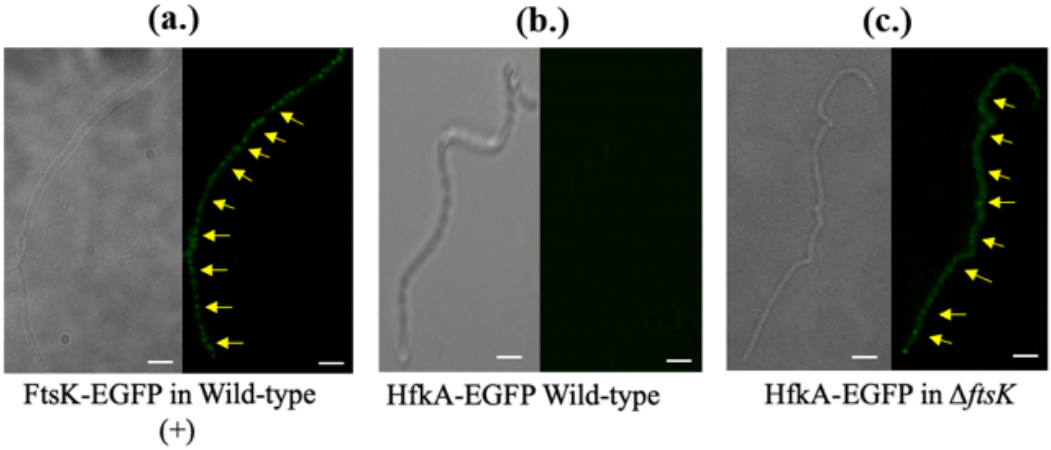

Figure 2.14: Preliminary evidence suggests that HfkA-EGFP weakly localizes in a Δ*ftsK* background.

The panels above show the localization of HfkA-EGFP in the pre-divisional hyphal stage. Cover slips were inoculated and hyphae grown for 2 days on SFM (MS) agar, were mounted unfixed in 1X PBS buffer. The left panel shows fluorescent images and the right panel shows the DIC image (a.) shows the strain RMD1 (Dedrick et al., 2009) expressing FtsK-EGFP as a positive control with distinct EGFP foci visible in a pre-divisional hypha. (b.) shows the HfkA-EGFP strain SS8 in a wild type background with no fluorescent signal detected. (c.) shows the HfkA-EGFP in a Δ*ftsK* mutant strain SS21 background showing diffused, yet distinct EGFP foci present in the pre-divisional hypha. The signal was diffused and not as sharp as the FtsK-EGFP fluorescent signal, suggesting that HfkA could be localizing in the absence of FtsK, but not in the same fashion. Although stoichiometric concentration cannot be determined using this microscopy experiment, it can be interpreted, that HfkA-EGFP assembly is weak and conditional. Scale bar is 5 μm.

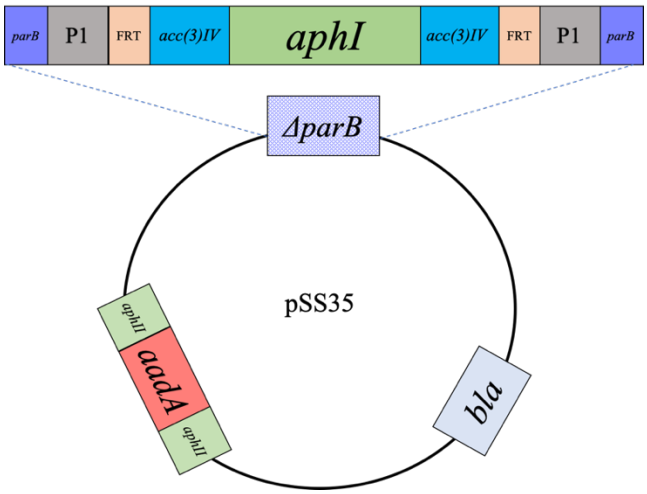

Figure 2.15: **Schematic of the Δ*parB*::*aphI* cosmid constructed by modifying the cosmid backbone and using an *aphI* antibiotic cassette.**

A cartoon representation of an *aphI* deletion cassette used for insertion-deletion of *parB* on the wild type cosmid H24 after a multistep recombineering process. H24 was modified to pSS34 by changing the backbone *aphII* marker to a spectinomycin^{R}, *aadA*. Then, pSS34 was targeted with the *aphI* gene from pSS33 to isolate Δ*parB*::*aphI* mutant cosmid pSS35, which was verified and used for further analysis.

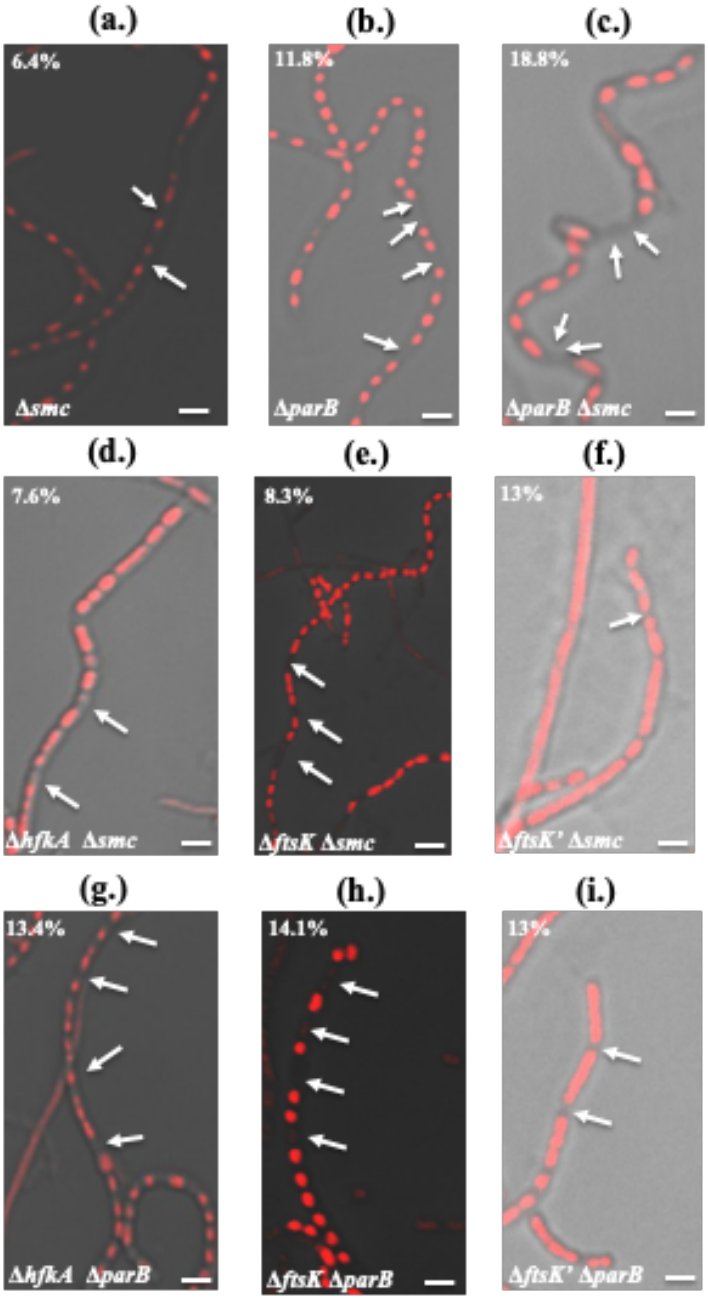

Figure 2.16: **Segregation phenotype of series of single and double mutants shows an overt and higher segregation defect.**

Coverslips were inoculated and hyphae grown for 4 days on SFM agar, fixed and stained with propidium iodide. Previously, it has been shown that single deletions of Δ*hfkA and* Δ*ftsK* have a segregation defect of 1% each. However, the segregation defect of the

truncated Δ*ftsK'* deletion is 15% (as shown by Dedrick et al., (2009)). Here, the single deletions of *smc* and *parB* are shown along with a series of double mutants isolated for this study. (a.) Δ*smc* single deletion strain showing 6.4% anucleate spores. (b.) Δ*parB* single deletion strain with 11.8% anucleate spores. (c.) Δ*parB* Δ*smc* double mutant strain showed the highest segregation defect of 18.8% anucleate spores. (d.) Δ*hfkA* Δ*smc* double deletion showed 7.6% anucleate spores. (e.) Δ*ftsK* Δ*smc* had a similar segregation phenotype of 8.3% anucleate spores. (f.) Δ*ftsK'* Δ*smc* strain RMD3 with 13% anucleate spores (Dedrick et al., 2009). (g.) Δ*hfkA* Δ*parB* strain showed 13.4% anucleate spores. (h.) Δ*ftsK* Δ*parB* exhibited 14.1% anucleate spores. (i.) Δ*ftsK'* Δ*parB* RMD5 with 13% anucleate spores (Dedrick et al., 2009). Some of the double mutants shows a segregation phenotype that is roughly equal to the added sum of the defect (% anucleate spores) of the individual mutations. This could indicate that some of these genes (*parB* and *smc*) may be working in series during the segregation process. Scale bar is 5 μm.

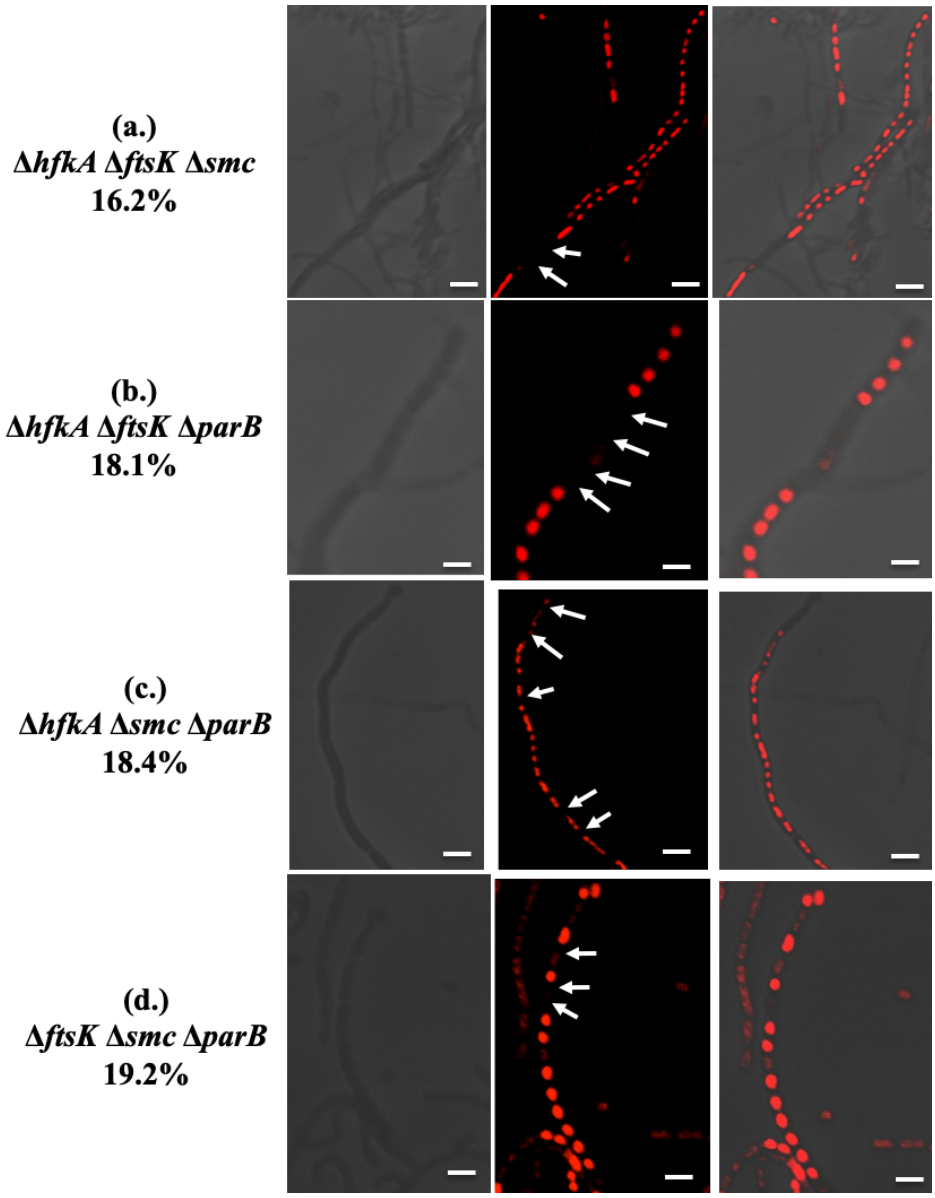

Figure 2.17: **Isolation of a series of triple deletion mutants suggests an additive effect on segregation phenotypes.**

Coverslips were inoculated and hyphae grown for 5 days on SFM agar, fixed and stained with propidium iodide. Panels are DIC, fluorescent, and merged. (a.) Δ*hfkA* Δ*ftskA* Δ*smc* triple mutant strain SS25 showing 16.2% anucleate spores. (b.) Δ*hfkA* Δ*ftskA* Δ*parB* mutant strain SS39 with 18.1% anucleate spores. (c.) Δ*hfkA* Δ*parB* Δ*smc* strain SS40

showed the segregation defect of 18.4% anucleate spores. (d.) Δ*ftsK* Δ*smc* Δ*parB* strain SS51 showed the highest segregation defect of 19.2% anucleate spores. All the strains contained a complete null deletion of *ftsK*. Scale bar is 5 μm.

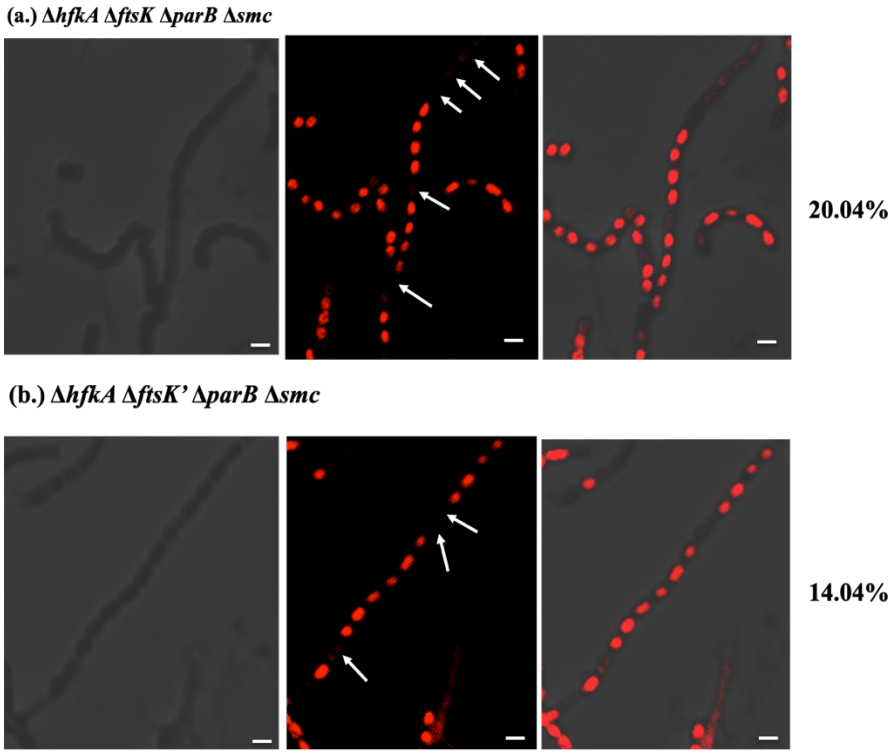

Figure 2.18: **Segregation phenotype of quadruple mutant strains do not show an increased or severe result compared to the triple deletions.**

Coverslips were inoculated and hyphae grown for 5 days on SFM agar, fixed and stained with propidium iodide. Panels are DIC, fluorescent, and merged. (a.) Δ*hfkA* Δ*ftskA* Δ*parB* Δ*smc* quadruple mutant strain SS56 showing 20.04% anucleate spores. This strain contains a complete null deletion of *ftsK* and did not show an increased percentage defect compared to the triple mutant strains (b.) Δ*hfkA* Δ*ftsK'* Δ*parB* Δ*smc* quadruple mutant strain SS63 showing 14.04% anucleate spores contained a truncated deletion of *ftsK*. This strain was derived from the previously isolated triple mutant strain RMD6 (Δ*ftsK'* Δ*parB* Δ*smc*) by Dedrick et al. (2009), containing the same truncated deletion of *ftsK*, and has a less severe phenotype than the complete null deletion. This defect was not much severe than the RMD6 strain (10%) as published by Dedrick et al., (2009). Scale bar is 5 µm.

(a.) Δ*hfkA* Δ*ftsK*

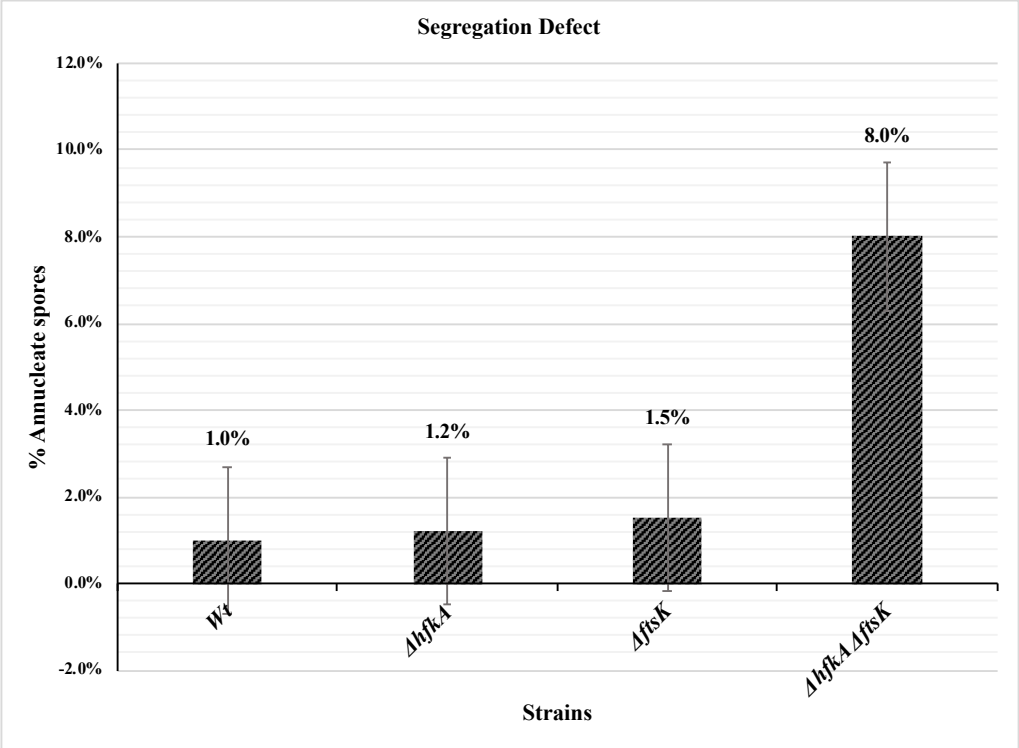

(b.) Δ*parB* Δ*smc*

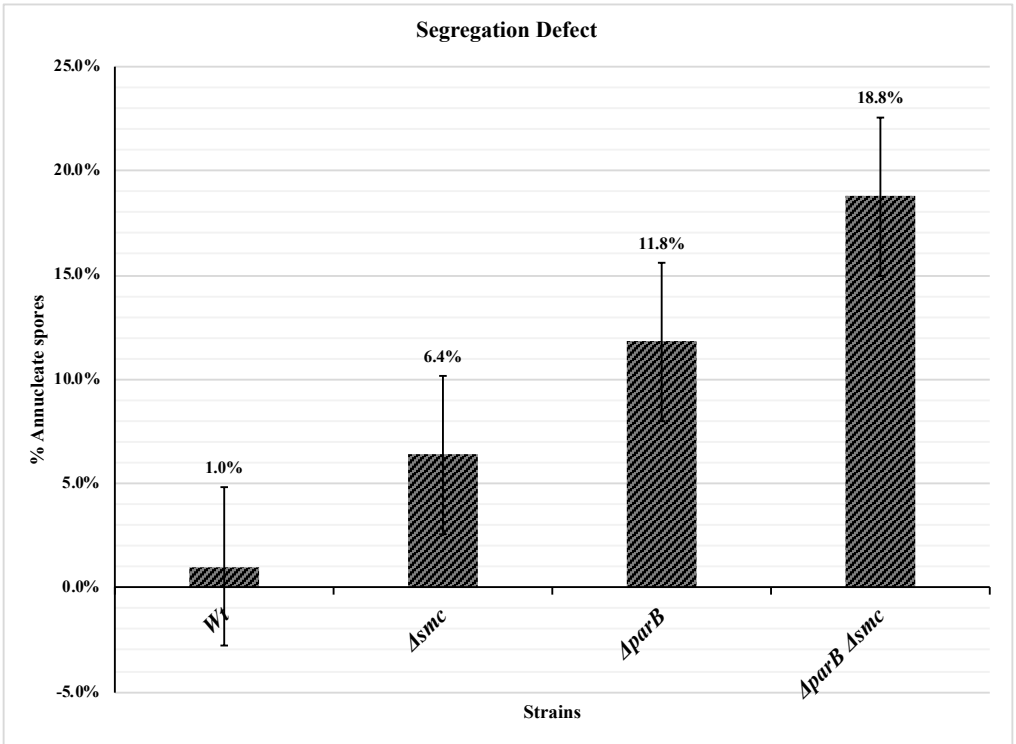

(c.) Δ*hfkA* Δ*ftsK* Δ*smc*

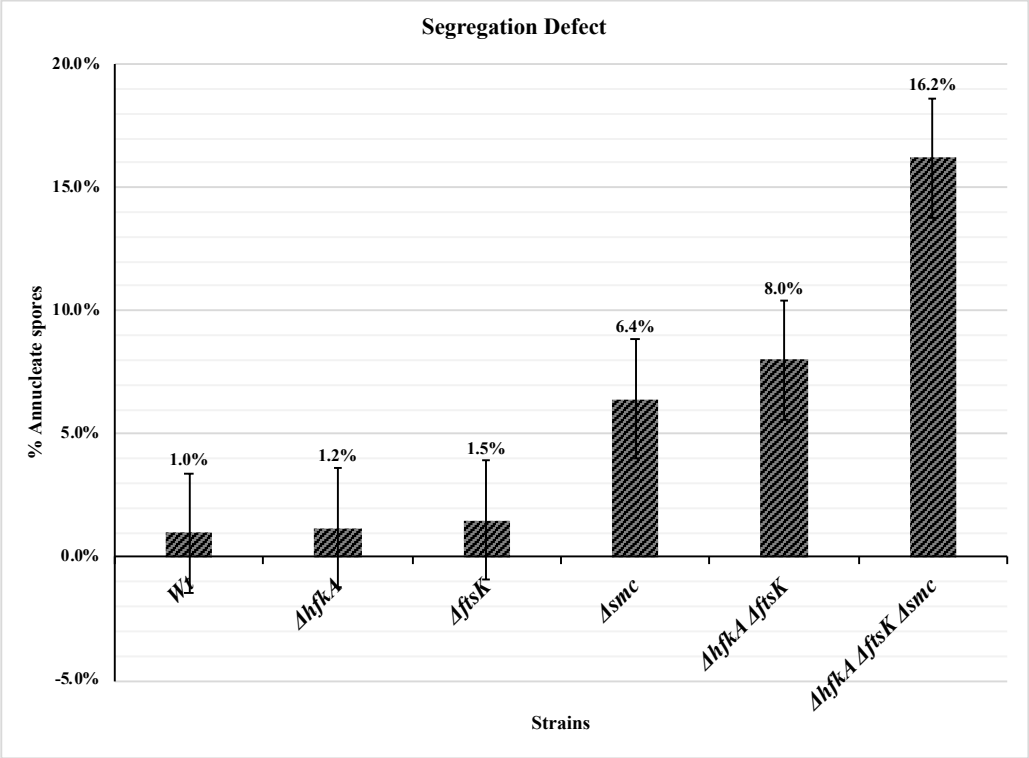

(d.) Δ*hfkA* Δ*ftsK* Δ*parB*

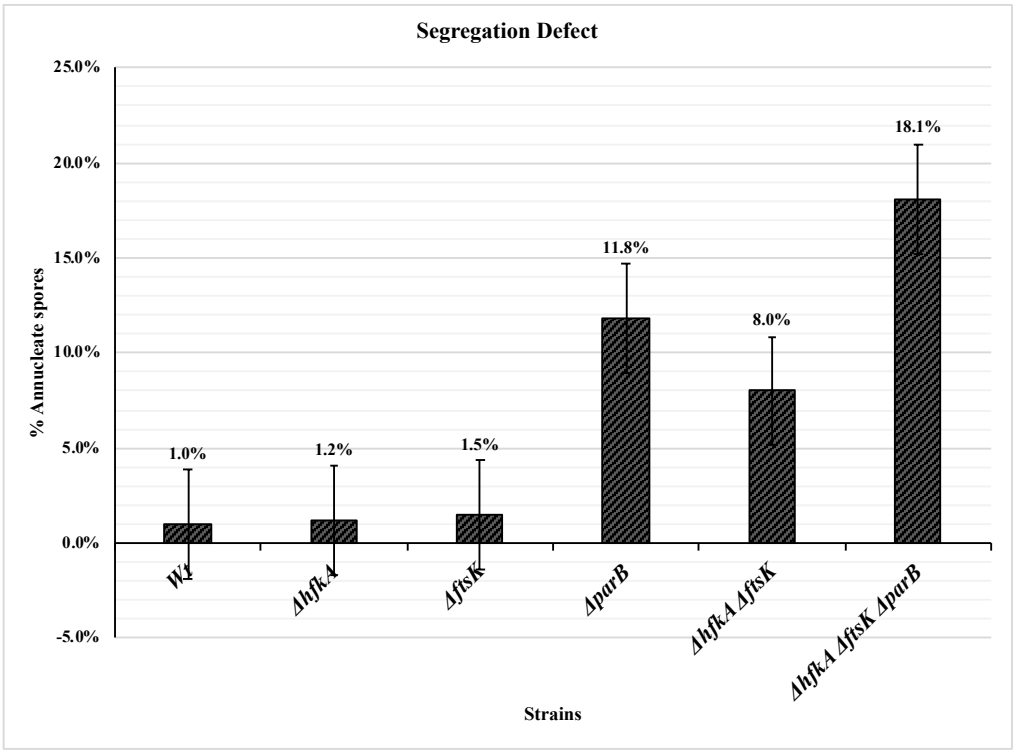

(e.) Δ*hfkA* Δ*ftsK* Δ*smc* Δ*parB*

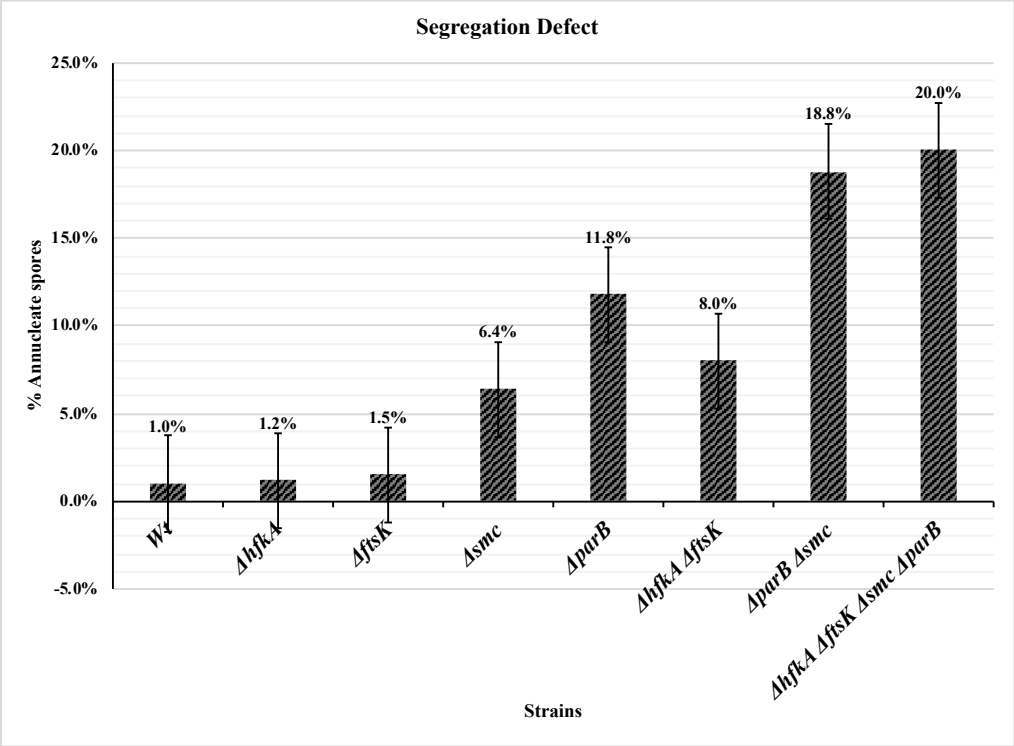

(f.) Δ*hfkA* Δ*ftsK' Δsmc* Δ*parB*

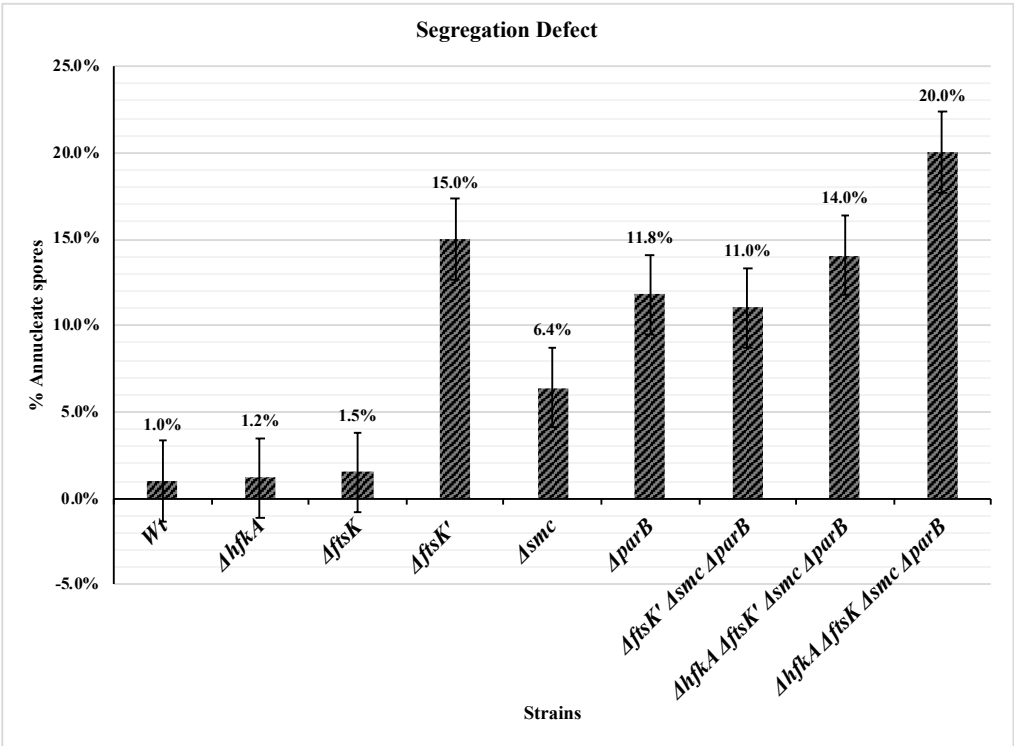

Figure 2.19: Graphical representation of segregation phenotypes of selected *S. coelicolor* strains shows a higher defect in double and triple mutants, but not in quadruple mutants.

Summary data from Figure 2.16-2.18. Different *S. coelicolor* strains have been used to generate graphs of the percent anucleate spores. These percentages were then plotted against the respective strains. **(a.)** Shows the segregation defect of the *hfkA* and *ftsK* single and double mutants. **(b.)** Shows segregation defect of the *parB* and *smc* single and double mutants. **(c.)** Shows the segregation defect of the Δ*hfkA* Δ*ftsK* Δ*smc* triple mutant. **(d.)** Shows the segregation defect of the Δ*hfkA* Δ*ftsK* Δ*parB* triple mutant. (e.) Shows the segregation defect of Δ*hfkA* Δ*ftsK* Δ*smc* Δ*parB* quadruple mutant, along with the single and double mutant. (f.) Shows the segregation defect of the A Δ*hfkA* Δ*ftsK'* Δ*smc* Δ*parB* mutant strain containing a truncated deletion of *ftsK'* had a segregation defect lower than the quadruple mutant with a null deletion of *ftsK*. Overall analysis indicates that the severity of phenotype is caused due to the additive effect of Δ*parB* Δ*smc* deletion.

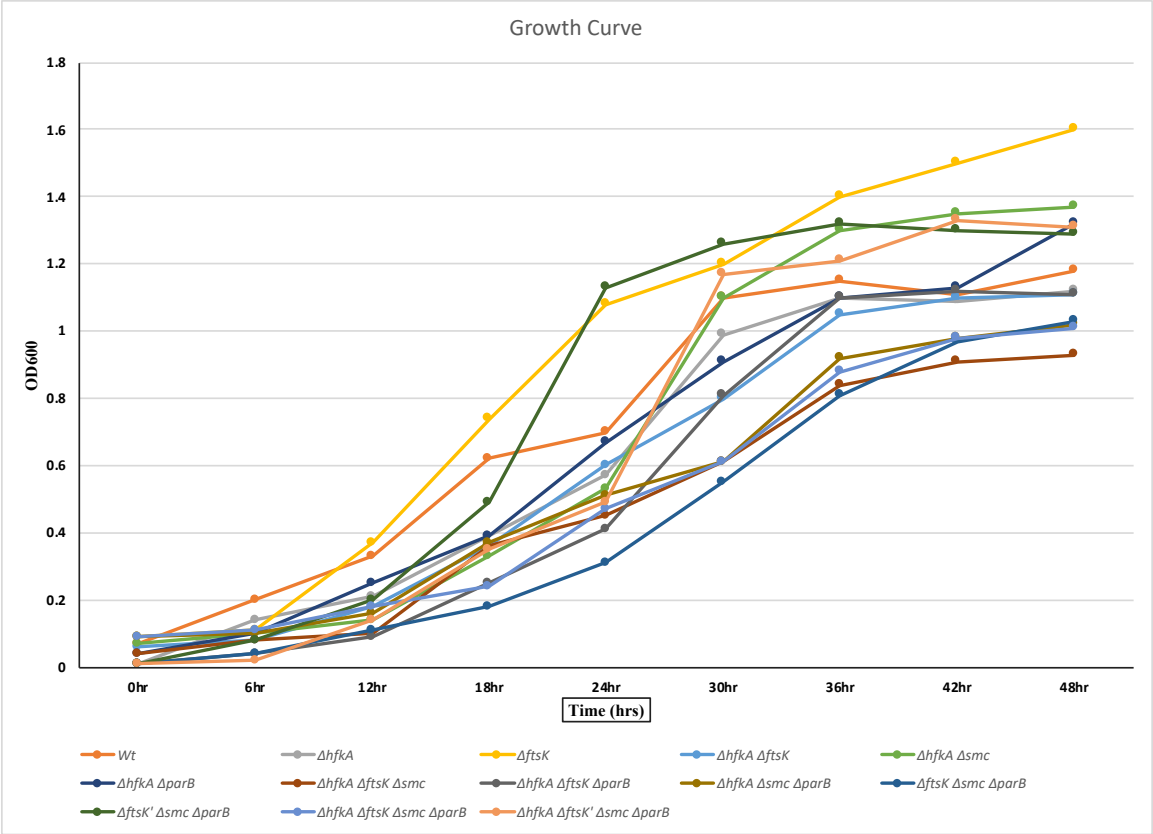

Figure 2.20: Growth curve analysis of selected *S. coelicolor* mutants show slight delay yet no explicit differences in growth.

Absorbance was measured for each strain at the interval of 6 hours for 48 hours during vegetative growth of pregerminated *S. coelicolor* strain spores in liquid ISP2 media. OD600 was measured every 6 hours. Uninoculated media was used as a negative (-) control, and the wild type strain M145 was used as a positive (+) control. For most strains, the log phase was observed between 18 to 30 hours, after that point, the growth began to plateau. The single and double mutants followed a wild type-like growth pattern, whereas the triple and quadruple mutant strains showed a slight delay in reaching the log phase.

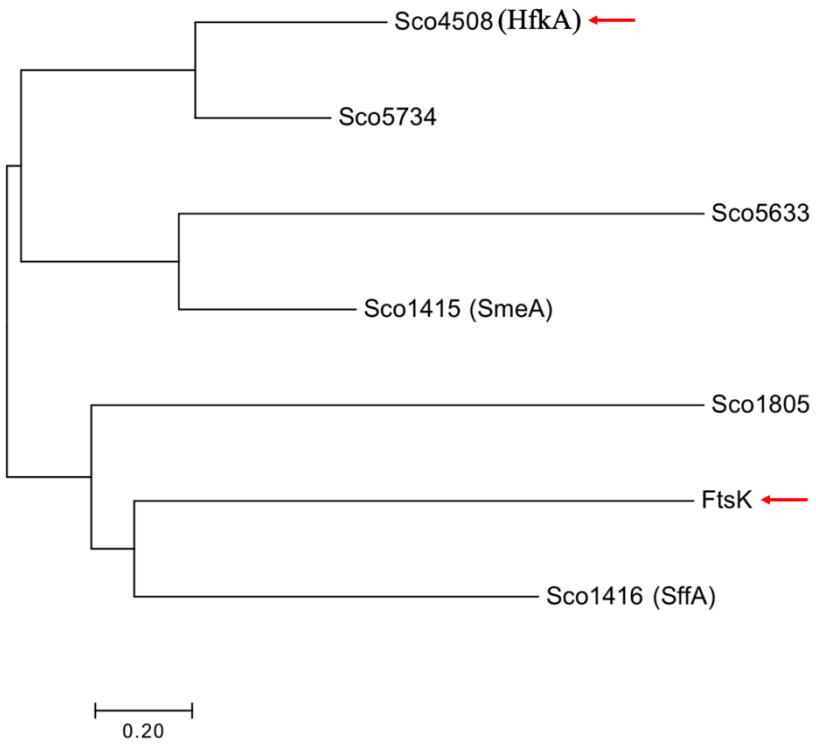

Figure 2.21: Phylogenetic tree of FtsK and FtsK-like proteins in *S. coelicolor* shows the grouping of HfkA with a known potential secretory protein Sco5734.

Shown is a phylogenetic tree generated using the multiple sequence alignment using Mega 7 of known FtsK-like proteins in *S. coelicolor*. FtsK protein (Sco5750) was aligned with the computationally identified FtsK-like proteins Sco4508 (HfkA), Sco5734, Sco5633, Sco1805; and also, experimentally analyzed FtsK/SpoIIIE-like proteins Sco1415 (SmeA)and Sco1416 (SffA). It can be seen that HfkA does not group with FtsK but with Sco5734, which has been previously identified as part of the type VII ESX secretion system (Roman et al., 2010).

```
HfkA        VRLTLTVVDPYGGGSADVVLDADPESTVGDIAEELAKQVGIAGAQVIPIGHQGQAGTGGA   60
Sco5734     ------------------------------------------------------------   0

HfkA        PLVYVDGYAVDPSATVVGSPLREGAVVSLQDPSGCLPGEPTGLVELRVVGGPGAGFVHRL   120
Sco5734     ------------------------------------------------------------   0

HfkA        GVGKYDIGSGPAAYVRIEDPEVDARALTLSVATDGTCKVAVHSDKEGVTLDGESVQERDG   180
Sco5734     ------------------------------------------------------------   0

HfkA        DDWPLGAQIAVGNSLVELARYAPPNAALKWSEDGVGLDYNRPPRLRPAERQTNFRLPSSP   240
Sco5734     ---------------------------------VSQFVIKRPPRTLPPDVPSDELLLEAP   27
                                               :  :****  * :  ::  * .:*

HfkA        RD-YEARPLPWLMALTPLVGAVVAVMVF-G---RWYYLIMAGLS-----PILLFANYFND   290
Sco5734     PELPRGQQEGVLMQVLPTLGMGSSVVFYFASPNAHPFMRIMGVVMLMSTAAMVVAQIVR-   86
             :  ..:    ** : * :*   :*:.: .      :: : *:        ::.*: ..

HfkA        KKHGRKSH-AKQVKEYEEQKARIEKDAQAALVAERDDRRQAIPDPAVVLSVATGPRTRLW   349
Sco5734     YRRGTQGQMADVRRDYLRYLAQTRRRIRRTALRQRDAQLYLHPAPDQLW-AVVAEGSRVW   145
             ::* :.: *.  ::* .  *: .:  : : : :** :    * *  :  ....  :*:*

HfkA        ERRRTDRDHLLLRVGTGQLPSEVVLDDPEQ--DD-----------HRRQVTWKIEDAPVA   396
Sco5734     ERRIGDADFGQVRLGLGPQQLSTPLVAPDTAPVDELEPLCAGAMQRFLAVHGQLDALPVA   205
            ***  * *.  :*:* *    .. *  *:    *           :   *  :::  ***

HfkA        LSLRTLGVVGIAGPGDSARSLGRWAVAQTAALHSPMDVQFYVLSENSAQSEWDWVRWLPH   456
Sco5734     LSLRAFYHVTVSGDPEQARSTARALVAQATTLHSPDDLVVAVVTAPGAVSRWDWSKWLPH   265
            ****::  * ::*  :.*** .*  ***:::**** *: . *::  .* *.*** :****

HfkA        SRPSGGQDVNVLIGTDAETVGARIGELTQILDARKKAAEQKGGGAQGSSFTDPDIVVVWD   516
Sco5734     CQVAGQLDGAG----SRRLFGDDLGELEPLLAAHLDGRPRF-SRDGRPLLDQPHILVVLD   320
            .: :*  *       . . .*  :***  :* *: ..  :  .      : :*.*:** *

HfkA        GSRRLRSLPGVVRLLREGPAVSMFAVCIDAEERFLPGECQAFVV----AEPRAEESGRQQ   572
Sco5734     GGMVP--------------PTSAFAAAEG-----LQGVTVVEVVAGELDQPRGDLS----   357
            *.                  .* **.. .     * *   . **     :**.: *

HfkA        RDAEARPAQQVAGGFPSFQAWHTNAPAEPEQRARAEKLRLRVEEAGVERITGVRPDFVTP   632
Sco5734     --VVVRP----------DRLWLDSG--------------------GGVAYEG-APDVMPL   384
              . .**           : *  ..                    *     *  **.:

HfkA        AWCLRLARSLSALRDISGETEDSALPGSSRLLDVLQLEPPTADAIGARWRMGGQSTM--A   690
Sco5734     PGAEALARQLAPLRMGGGD-DDEPLLANLDFTELLGLGDAASVDVRRTWRPRSTPERLRV   443
              .  ***.*: **  .*: :*. * ..  : ::* *   ::  :   **  .      .

HfkA        VIGESYDG-PFGI-----DMRKDGPHGLIAGTTGSGKSELLQTIVAALAVANTPENMTFV   744
Sco5734     PIGVGEDGRPVMLDLKEAAQDGMGPHGLCVGATGSGKSELLRTLVLGLAVTHSSETLNFV   503
             ** . ** *. :          ***** .*:*********:*:* .***::: *.:.**

HfkA        LVDYKGGSAFKDCVKLPHTVGMVTDLDAH--LVERALESLGAELKRREHILA-AADAKDI   801
Sco5734     LADFKGGATFAGMSQMPHVAAVITNLADDLTLVDRMGDAIRGELQRRQELLRSAGNYANL   563
            *.*:***::* .  ::**...::*:*  .  **:*  ::: .**:**:.:*  *.:  ::

HfkA        EDYQDLVRRDPSHAPVPRLLIVIDEFASMVRDLPDFVTGLVNIAQRGRSLGIHLLLATQR   861
Sco5734     HDYEKARAAGAPLEPLASLVLVIDEFSELLTAKPDFIDMFIQIGRIGRSLGVHLLLASQR   623
            .**:.    .    *:  *::*****:.::   ***:  :::*.: *****:*****:**

HfkA        PSGVVSPEIRANTNLRIALRVTDGGESSDVIDSPEAGHISKNTPGRAYVRLGHSSLVPFQ   921
Sco5734     LEEGRLRGLDTYLSYRVGLRTFSAAESRAALGVPDAYHL-PSVPGSGYLKFGTEEMVRFK   682
             .      : :  . *:.**. ...**  .:. *:* *:  ..** .*:::* ..:* *:
```

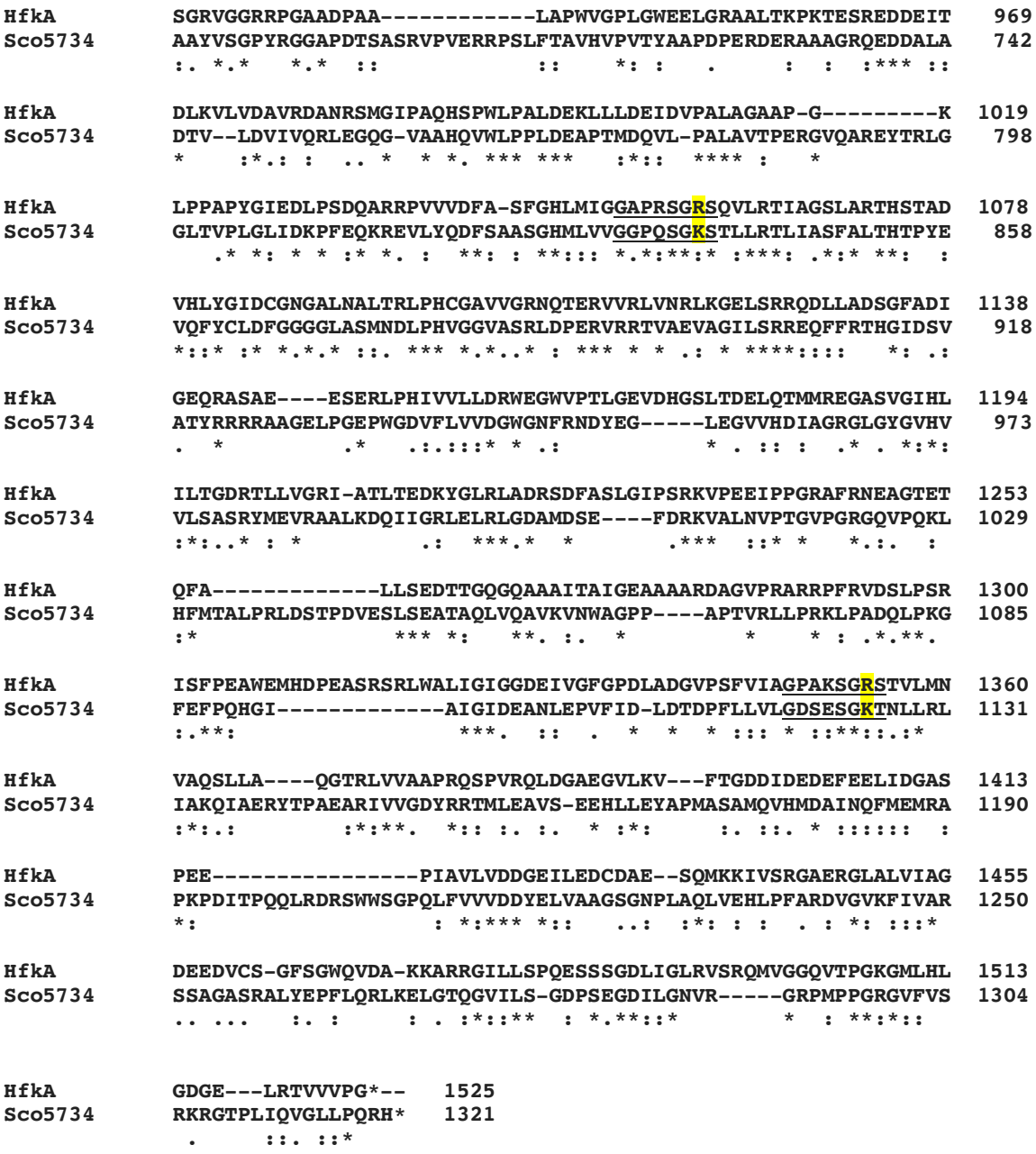

Figure 2.22: The FtsK-like protein HfkA shares conserved regions with the secretory protein Sco5734 in *S. coelicolor*.

A sequence alignment of HfkA and Sco5734 amino acid sequence of *S. coelicolor* using Clustal Omega alignment. The N-terminal and cytoplasmic C-terminal domains are aligned

to show the levels of conserved sequences. An asterisk (*) indicates a conserved residue, colon (:) indicates conservation between groups of strongly similar properties, period (.) indicates conservation between groups of weakly similar properties. Sco5734 is a known type VII secretion system protein. The alignment shows the similarity shared between HfKA and Sco5734. Based on conserved and consensus sequences, the three deviant walker A boxes are identified and underlined in both. It is interesting to note than in the first Walker A box, the "K" is retained in both, in the second and third Walker A box, the "R" was substituted to a "K", which is a unique observation. These are highlighted in yellow. Compared to FtsK, HfkA shares additional homology, however, no DNA binding domain was found in either HfkA or Sco5734.

References

Abdallah, A. M., Gey van Pittius, N. C., Champion, P. A., Cox, J., Luirink, J., Vandenbroucke-Grauls, C. M., Appelmelk, B. J., Bitter, W. (2007). Type VII secretion - mycobacteria show the way. *Nature Rev Microbiol.*, *5*, 883-91.

Ates, L. S., Houben, E. N. G., Bitter, W. (2016). Type VII secretion: a highly versatile secretion system. *Microbiology Spectrum*, *4*, 1-21.

Ausmees, N., Wahlstedt, H., Bagchi, S., Elliot, M. A., Buttner, M. J., Flärdh, K. (2007). SmeA, a small membrane protein with multiple functions in *Streptomyces* sporulation including targeting of a SpoIIIE/FtsK-like protein to cell division septa. *Mol Microbiol.*, *65*, 1458-1473.

Berezuk, A. M., Glavota, S., Roach, E. J., Goodyear, M. C., Krieger, J. R., Khursigara, C. M. (2018). Outer membrane lipoprotein RlpA is a novel periplasmic interaction partner of the cell division protein FtsK in *Escherichia coli*. *Sci Rep.*, *8*, 1-14.

Besprozvannaya, M., Burton, B. M. (2014). Do the same traffic rules apply? Directional chromosome segregation by SpoIIIE and FtsK. *Mol Microbiol.*, *93*, 599-608.

Biller, S. J., Burkholder, W. F. (2009). The *Bacillus subtilis* SftA (YtpS) and SpoIIIE DNA translocases play distinct roles in growing cells to ensure faithful chromosome partitioning. *Mol Microbiol.*, *74*, 790-809.

Bradshaw, E., Saalbach, G., McArthur, M. (2013). Proteomic survey of the *Stretomyces coelicolor* nucleoid. *J Proteomics*, *83*, 37-46.

Burts, M. L., Williams, W. A., DeBord, K., Missiakas, D. M. (2005). EsxA and EsxB are secreted by an ESAT-6-like system that is required for the pathogenesis of *Staphylococcus aureus* infections. *Proc Natl Acad Sci U S A.*, *102*, 1169-1174.

Chandra, G., Chater, K. F. (2008). Evolutionary flux of potentially bldA-dependent *Streptomyces* genes containing the rare leucine codon TTA. *Antonie van Leeuwenhoek*, *94*, 111-126.

Dedrick, R. M., Wildschutte, H., McCormick, J. R. (2009). Genetic interactions of *smc*, *ftsK*, and *parB* genes in *Stretomyces coelicolor* and their developmental genome segregation phenotypes. *J Bacteriol.*, *191*, 320-332.

Ditkowski, B., Troc, P., Ginda, K., Donczew, M., Chater, K. F., Zakrzewska-Czerwinska, J., Jakimowicz, D. (2010). The actinobacterial signature protein ParJ (SCO1662) regulates ParA polymerization and affects chromosome segregation and cell division during *Streptomyces* sporulation. *Mol Microbiol.*, *78*, 1403-1415.

Dubarry, N., Possoz, C., Barre, F. X. (2010). Multiple regions along the *Escherichia coli* FtsK protein are implicated in cell division. *Mol Microbiol.*, *78*, 1088-100.

Easter Jr, J., Gober, J. W. (2002). ParB-stimulated nucleotide exchange regulates a switch in functionally distinct ParA activities. *Mol Cell.*, *10*, 427-434.

Fyans, J. K., Bignell, D., Loria, R., Toth, I., Palmer, T. (2013). The ESX/type VII secretion system modulates development, but not virulence, of the plant pathogen *Streptomyces scabies*. *Molecular Plant Pathology*, *14*, 119-130.

Grainge, I. (2010). FtsK-a bacterial cell division checkpoint?. *Mol Microbiol.*, *78*, 1055-1057.

Hester, C. M., Lutkenhaus, J. (2007). Soj (ParA) DNA binding is mediated by conserved arginines and is essential for plasmid segregation. *Proc Natl Acad Sci U S A.*, *104*, 20326-20331.

Hopwood, D. A. (2007). How do antibiotic-producing bacteria ensure their self-resistance before antibiotic biosynthesis incapacitates them? *Mol Microbiol.*, *63*, 937-940.

Houben, E. N., Korotkov, K. V., Bitter, W. (2014). Take five - type VII secretion systems of *Mycobacteria*. *Biochim Biophys Acta*, *1843*, 1707-1716.

Huppert, L. A., Ramsdell, T. L., Chase, M. R., Sarracino, D. A., Fortune, S. M., Burton, B. M. (2014). The ESX system in *Bacillus subtilis* mediates protein secretion. *PLoS One*, *9*, 1-9.

Jakimowicz, D., Gust, B., Zakrzewska-Czerwinska, J., Chater, K. F. (2005). Developmental-stage-specific assembly of ParB complexes in *Stretomyces coelicolor* hyphae. *J Bacteriol.*, *187*, 3572-3580.

Jakimowicz, D., Zydek, P., Kois, A., Zakrzewska-Czerwinska, J., Chater, K. F. (2007). Alignment of multiple chromosomes along helical ParA scaffolding in sporulating *Streptomyces* hyphae. *Mol Microbiol.*, *65*, 625-641.

Jakimowicz, D., van Wezel, G. P. (2012). Cell division and DNA segregation in *Streptomyces*: how to build a septum in the middle of nowhere? *Mol Microbiol.*, *85*, 393-404.

Jäger, F., Zoltner, M., Kneuper, H., Hunter, W. N., Palmer, T. (2016). Membrane interactions and self-association of components of the Ess/type VII secretion system of *Staphylococcus aureus*. *FEBS Letters*, *590*, 349-357.

Kois, A., Swiatek, M., Jakimowicz, D., Zakrzewska-Czerwinska, J. (2009). SMC protein dependent chromosome condensation during aerial hyphal development in *Streptomyces*. *J Bacteriol.*, *191*, 310-319.

Kim, H. J., Calcutt, M. J., Schmidt, F. J., Chater, K. F. (2000). Partitioning of the linear chromosome during sporulation of *Stretomyces coelicolor* A3(2) involves an *oriC*-linked *parAB* locus. *J Bacteriol.*, *182*, 1313-1320.

Lee, J. Y., Finkelstein, I. J., Arciszewska, L. K., Sherratt, D. J., Greene, E. C. (2014). Single-molecule imaging of FtsK translocation reveals mechanistic features of protein-protein collisions on DNA. *Mol Cell.*, *4*, 832–843.

Liu, G., Draper, G. C., Donachie, W. D. (1998). FtsK is a bifunctional protein involved in cell division and chromosome localization in *Escherichia coli*. *Mol Microbiol.*, *29*, 893–903.

Massey, T. H., Mercogliano, C. P., Yates, J., Sherratt, D. J., Löwe, J. (2006). Double-stranded DNA translocation: structure and mechanism of hexameric FtsK. *Mol Cell.*, *23*, 457-469.

Matsuhashi, M., Tamaki, S., Curtis, S. J., Strominger, J. L. (1979). Mutational evidence for identity of penicillin-binding protein 5 in *Escherichia coli* with the major D-Alanine carboxypeptidase IA activity. *J Bacteriol.*, *137*, 644-647.

McCormick, J. R., Flärdh, K. (2012). Signals and regulators that govern *Streptomyces* development. *FEMS Microbiol Rev.*, *36*, 206-231.

Niu, G., Chater, K. F., Tian, Y., Zhang, J., Tan, H. (2016). Specialised metabolites regulating antibiotic biosynthesis in *Streptomyces* spp. *FEMS Microbiol Rev.*, *40*, 554-573.

Ptacin, J. L., Lee, S. F., Garner, E. C., Toro, E., Eckart, M., Comolli, L. R., Shapiro, L. (2010). A spindle-like apparatus guides bacterial chromosome segregation. *Nature Cell Biol.*, *12*, 791-798.

Ramsdell, T. L., Huppert, L. A., Sysoeva, T. A., Fortune, S. M., Burton, B. M. (2015). Linked domain architectures allow for specialization of function in the FtsK/SpoIIIE ATPases of ESX secretion systems. *J Mol Biol.*, *427*, 1119–1132.

Roman, S. A. S, Facey, P. D, Fernandez-Martinez, L., Rodriguez, C., Vallin, C., Sol, R. D., Dyson, P. A. (2010). Heterodimer of EsxA and EsxB is involved in sporulation and is secreted by a type VII secretion system in *Streptomyces coelicolor*. *Microbiology*, *156*, 1719–1729.

Saleh, O. A., Pérals, C., Barre, F. X., Allemand, J. F. (2004). Fast, DNA-sequence independent translocation by FtsK in a single-molecule experiment. *EMBO J.*, *23*, 2430-2439.

Simeone, R., Bottai, D., Brosch, R. (2009). ESX/type VII secretion systems and their role in host-pathogen interaction. *Curr Opin Microbiol.*, *12*, 4-10.

Sivanathan, V., Allen, M., de Bekker, C., Baker, R., Arciszewska, L. (2006). The FtsK gamma domain directs oriented DNA translocation by interacting with KOPS. *Nat Struct Mol Biol.*, *13*, 965–972.

Unnikrishnan, M., Constantinidou, C., Palmer, T., Pallen, M. J. (2017). The Enigmatic Esx proteins: looking beyond *Mycobacteria*. *Trends Microbiol.*, *25*, 192-204.

Veiga, H., Pinho, M. G. (2017). *Staphylococcus aureus* requires at least one FtsK/SpoIIIE protein for correct chromosome segregation. *Mol Microbiol.*, *103*, 504-517.

Wang, L., Yu, Y., He, X., Zhou, X., Deng, Z., Chater, K. F., Tao, M. (2007). Role of an FtsK-Like protein in genetic stability in *Stretomyces coelicolor* A3(2). *J Bacteriol.*, *189*, 2310–2318.

Wu, L. J., Errington, J. (1994). *Bacillus subtilis* SpoIIIE protein required for DNA segregation during asymmetric cell division. *Science*, *264*, 572-575.

Appendix I

A genealogy table describing the origin of different strains isolated for this study

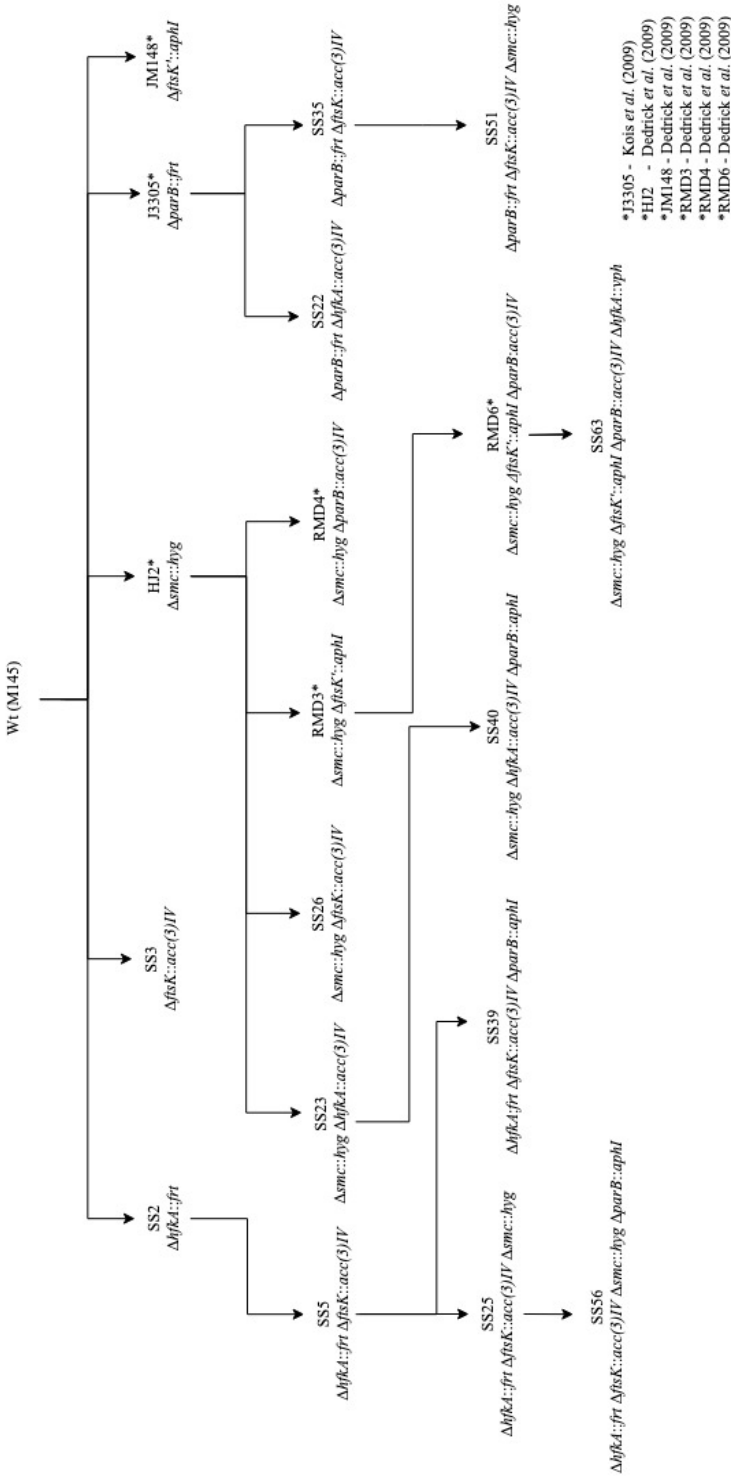

Appendix II

Construction of plasmids expressing fusions to `FtsK for use in a bacterial two-hybrid assay

To use the bacterial adenylate cyclase two-hybrid (BACTH) system for identifying novel interactions with `FtsK, the 3' end of the gene encoding the cytoplasmic domain for FtsK was selected as "bait". The plasmid pAEB228 was digested with *Pvu*II, and a 4.2 kb fragment containing *ftsK* was purified and used as a template for PCR. Specific oligonucleotides (Table 2.4) were designed with added *Kpn*I restriction sites to amplify a 2,036 bp region of *ftsK* and the amplicon was cloned into the TOPO pCR2.1 cloning vector (Life Technologies). The clone pSS5 was verified using restriction digestion and sequencing of the entire cloned fragment.

The verified plasmid was digested with *Kpn*I and the fragment was separately cloned into the four BACTH vectors pUT18, pUT18C, pKT25 and pKNT25 containing the subdomains T18 and T25 subdomains of adenylate cyclase in *E. coli* (Euromedex). The clone candidates for each vector were initially verified using restriction digestion with *Kpn*I, and positive clones were then sequenced at the cloning junctions to verify the reading frame and orientation.

The *`ftsK* BACTH plasmids were individually co-transformed with compatible partners into an *E. coli cyaA* null strain BTH101 (Euromedex) to test for interaction on MacConkey medium containing maltose. Empty vectors were used for a negative control and the positive control were plasmids provided by the BACTH kit (Euromedex). Positively interacting colonies were then subjected to a Beta-galactosidase assay, which was conducted using manufacturer's recommendations on overnight cultures of three

independent isolates of each strain (Euromedex). The activity units were averaged from the 3 determinations (triplicate) for each interaction.

FtsK-interacting proteins as potential targets for segregation

To seek out additional proteins involved in chromosome segregation, known proteins were tested for interaction with FtsK. The transmembrane domain N-terminal of FtsK has been shown to interact with several other cellular divisome proteins in *E. coli* like FtsQ, FtsL, FtsI and FtsZ in a two-hybrid system (Dubarry et al., 2010). This *in vivo* assay to identify interaction of fusion proteins using a cAMP-dependent pathway, turns colonies representing interacting proteins a red color on McConkey agar when supplemented with maltose (Karimova et al., 1998). Several BACTH (Bacterial adenylate cyclase two hybrid system) plasmids available in the laboratory were tested for interaction with *`ftsK* BATCH plasmids. pKT25-zip and pUT18-zip plasmids were used as a positive control, and the negative control was strain BTH101 expressing pKT25 and pT18C empty vectors.

`FtsK expressing protein was found to weakly interact with `Ftsk itself, ParA, and ParJ in this two-hybrid system. The `FtsK-T25 and `FtsK-T18C interaction was consistent with the evidence of oligomerization of FtsK into a hexameric ring (Massey et al., 2006). Interaction of FtsK with ParA and ParJ was a novel finding during this study. Previously published results of interaction between ParA and ParJ have been identified and characterized (Ditkowski et al., 2013) These interactions were quantified using a beta- galactosidase enzymatic activity assay of selected positive interactions (Figure A2.1). Several two-hybrid plasmids expressing cell division and segregation proteins in the laboratory were tested that did not interact with FtsK like FtsZ, SlzA, HaaA, ParB,

and ParH. To discover more FtsK C-terminal interacting proteins, a genomic library could be screened. In *S. coelicolor*, novel proteins ParJ and Scy were found by random library screening using a bacterial two-hybrid system (BTH) as ParA-interacting proteins involved in chromosome segregation (Ditkowski et al., 2010; Ditkowski et al., 2013).

(a.)

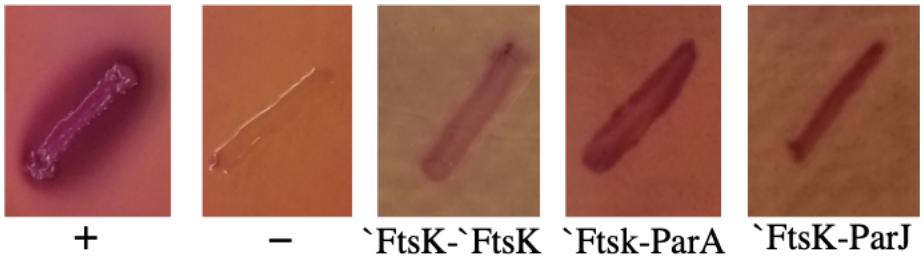

(b.)

Interacting proteins	Enzymatic activity units/mg
`FtsK-`FtsK	105 ± 14
‘FtsK- ParA	224± 24
`FtsK- ParJ	139± 25
+ control	557± 18

- Background activity of 62 ± 11 was subtracted

Figure A2.1: **Representation of `FtsK interacting proteins in a Bacterial Adenylate Cyclase Two-Hybrid (BACTH) system.**

(a.) The positive control with strain BTH101 expressing pT25-zip and pT18-zip, and the negative control was strain BTH101 expressing pKT25 and pT18C. `FtsK-T25 was found to weakly interact with `FtsK-T18C, ParA-T18C, and ParJ-T18C on McConkey media supplemented with maltose. (b.) These interactions were quantified using a beta-galactosidase enzymatic activity assay or selected positive interactions. Each value represents the average of three independent colonies.

References

Ditkowski, B., Troc, P., Ginda, K., Donczew, M., Chater, K. F., Zakrzewska-Czerwinska, J., Jakimowicz, D. (2010). The actinobacterial signature protein ParJ (SCO1662) regulates ParA polymerization and affects chromosome segregation and cell division during *Streptomyces* sporulation. *Mol Microbiol.*, *78*, 1403-1415.

Ditkowski, B., Holmes, N., Rydzak, J., Donczew, M., Bezulska, M., Ginda, K., Kedzierski, P., Zakrzewska-Czerwińska, J., Kelemen, G. H., Jakimowicz, D. (2013). Dynamic interplay of ParA with the polarity protein, Scy, coordinates the growth with chromosome segregation in *Streptomyces coelicolor*. *Open Biology*, *3*, 1-13.

Dubarry, N., Possoz, C., Barre, F. X. (2010). Multiple regions along the *Escherichia coli* FtsK protein are implicated in cell division. *Mol Microbiol.*, *78*, 1088-100.

Karimova, G., Pidoux, J., Ullmann, A., Ladant, D. (1998). A bacterial two-hybrid system based on a reconstituted signal transduction pathway. *Proc Natl Acad Sci U S A.*, *95*, 5752-5756.